Phylogenetic and molecular biological study of nitrogen transporters in Bangiales (Rhodophyta)

(原始紅藻類における窒素トランスポーター系統的および分子生物学的研究)

北海道大学大学院水産科学院

海洋応用生命科学専攻

Graduate School of Fisheries Sciences

Division of Marine Life Science

李　成澤

Chengze Li

2019 年

Contents

Chapter 1

General introduction

Nitrogen is macronutrients indispensable for plant growth in most terrestrial and aquatic ecosystems (Edward and Richard, 2001, Witte, 2011). It exists as organic forms like urea, amino acids, free peptides and proteins, and as inorganic forms of ion nitrate (NO_3^-), nitrite (NO_2^-) and ammonium (NH_4^+), which are main nitrogen sources in soil and seawater (Hurd et al., 2014, Okumoto and Versaw, 2017). Incorporation of these nitrogen sources into cells is mediated by transporters differently recognizing inorganic and organic nitrogen source (Gazzarrini et al., 1999, Ludewig et al., 2007, Pinton et al., 2015). As shown in Figure 1, influx of extracellular NH_4^+ into cells is performed by ammonium transporters (AMTs, D'Apuzzo, 2004), while urea uptakes into cell by urea transporter (DUR3s, Wang et al., 2008a) and then reduced to NH_4^+ by urease (Imamura et al., 2010). In addition, NO_3^- is imported into cells by nitrate transporter (NRTs) that form a large family with many members and distinct functions (Bai et al., 2013). Incorporated NO_3^- is reduced to NO_2^- by nitrate reductase (NR), and then further reduced to NH_4^+ by nitrite reductase (NiR) (Figure 1, Imamura et al., 2010). Since the nitrogen assimilation in cells is predominantly performed by the glutamine synthetase (GS)-glutamate synthase (GOGAT) cycle (Suzuki and Knaff, 2005), cellular NH_4^+ derived from extracellular nitrogen sources is the obvious substrates for the assimilatory reaction (Suzuki and Knaff, 2005), by which NH_4^+ is assimilated into Glu and Gln by GS and GOGAT, respectively (Figure 1). Nitrogen atoms in NH_4^+ are then

further incorporated into other nitrogen-containing molecules like amino acids and nucleotides (Okumoto and Versaw, 2017), indicating the vital importance of influx and assimilation of nitrogen sources in survival of terrestrial plants and algae.

NH_4^+ serves as an major nitrogen source for many organisms, including higher plants and algae (Couturier et al., 2007, Gonza´lez-Ballester et al., 2005, Nicolaus von Wirén et al., 2000) and is used in the biosynthesis of nitrogen-containing compounds after incorporated into cells via AMTs (Gazzarrini et al., 1999, Ludewig et al., 2007). In plants, AMTs are encoded by a multigene family comprising the AMT1 and AMT2 subfamilies (Couturier et al., 2007, Wittgenstein et al., 2014). AMT1s are known to be responsible for high-affinity NH_4^+ transport in rice (*Oryza sativa*), wheat (*Triticum aestivum*) and many other plant species (Li et al., 2016, Li et al., 2017,Ludewig et al., 2007, Wittgenstein et al., 2014, Zhang et al., 2018). Genes encoding AMT1s show different expression patterns. For instance, in *Arabidopsis thaliana*, *AtAMT1;1* is expressed in the roots and leaves (Gazzarrini et al., 1999) and the expression of *AtAMT1;2/1;3* and *AtAMT1;5* are mostly restricted to roots (Yuan et al., 2007), while *AMT1;4* shows pollen-specific expression (Yuan et al., 2009). In addition, *AtAMT1;1* and *AtAMT1;3* are induced by nitrogen starvation, whereas *AtAMT1;2* expression is insensitive to nitrogen deficiency (Loque et al., 2006). A recent study showed that the protein encoded by *AtAMT2;1* transfers NH_4^+ from roots to shoots (Giehl et al., 2017), but the physiological functions of AMT2s are less understood than those of AMT1s.

NO_3^- is also the main nitrogen source for plants and algae (Bouguyon et al., 2012, Krapp et al., 2014, Krouk et al., 2010). Among land plants such as *A. thaliana*, *O. sativa*,

Sorghum bicolor, *Zea mays* and *Populus trichocarpa*, three different families of nitrate transporters NRT1, NRT2 and NRT3 have been identified (Plett et al., 2010). These transporters symport NO_3^- and proton with low or high affinity to NO_3^- (Pinton et al., 2015). The *A. thaliana* genome contains 53 NRT1 family genes (Tsay et al., 2007). However, only eight members (AtNRT1.1 to AtNRT1.8) have been functionally analyzed as low-affinity NO_3^- transporters (Plett et al., 2010). The *NRT2* family consists of high-affinity NO_3^- transporters containing NO_3^--inducible and constitutively expressed members (Tsay et al., 2007). The *NRT3* genes in *A. thaliana* play a role in NO_3^- transport through regulating the activity of *NRT2* genes without transporter activity (Okamoto et al., 2006, Orsel et al., 2006). In contrast to terrestrial plants carrying above three types of NRTs, only NRT2 members are present in algae. Genome of the green alga *Chlamydomonas reinhardtii* contains six NRT2 members, while the red algae *Pyropia yezoensis* and *Porphyra umbilicalis* have only one *NRT2* gene (Brawley et al., 2017, Kakinuma et al., 2008). In *P. yezoensis*, NRT2 comprehensively expresses both in gametophyte and sporophyte and does not show inducible expression patterns under nitrogen deficient conditions (Kakinuma et al., 2008).

Since urea is a small, neutral and polar molecule and presents ubiquitously in nature, it is a rapidly available nitrogen source for the growth of various organisms including bacteria, fungi, plants and algae (Wang et al., 2008a). Urea has to be moved across different biological membranes, for which transport-proteins specific for urea are required (Wang et al., 2008a). Unlike a large number of NRTs existing in land plants, a single gene coding for a DUR3 has been identified and characterized in genomes of

vascular *A. thaliana*, *Z. mays*, *O. sativa* and many other species (Kojima et al., 2007, Liu et al., 2014, Pinton et al., 2015, Wang et al., 2012). Of these DUR3s, it has been confirmed that transcriptional upregulation of both *A. thaliana* urea transporter (*AtDUR3*) and *O. sativa* urea transporter (*OsDUR3*) in the roots is triggered by nitrogen deficiency (Kojima et al., 2007, Wang et al., 2012). In contrast, the moss *Physcomitrella patterns* possesses two DUR3 homologs, showing 85% identity in amino acid sequences (De Michele et al., 2012). Similarly, algae have two or more DUR3 members: three in green alga *Chl. reinhardtii* named *CrDUR3A, CrDUR3B, and CrDUR3C* that are closely related to each other (about 80% identity), three in red alga *Po. umbilicalis* and three in red alga *P. yezoensis* named *PyDUR3.1, PyDUR3.2* and *PyDUR3.3* exhibiting different life cycles-specific expression (Kakinuma et al., 2008, Kakinuma et al., 2015).

It is well known that nitrogen-deficiency results in leaf senescence in land plants (Aguera et al., 2010, Meng et al., 2016). Since nitrogen is reused to support plant growth and reproduction by relocating from aging leaves to younger tissues (Li et al., 2016, Li et al., 2017), nitrogen deficiency tends to induce senescence in older tissues (Gregersen et al., 2008), indicating the importance of nutrient recycling between tissues during senescence (Meng et al., 2016). Thus, re-localization of nitrogen is essential for leaf senescence (Aguera et al., 2010, Edward and Richard, 2001). During these processes, nitrogen transporter regulates nitrogen homeostasis and remobilizes nitrogen from sources to sink tissues via phloem transport in *Arabidopsis* in response to N limitation (Kiba et al., 2012). Similarly, nitrogen deficiency induces discoloration (“iro-ochi”) in

thalli of *P. yezoensis*, which decreases its quality as a food (Sakaguchi et al., 2002). However, the discolored thalli can be recovered by increasing nitrogen sources in the medium, where NH_4^+ was thought to be highly efficient (Sakaguchi et al., 2002, Kakinuma et al., 2017). During this process, nitrogen transporters play crucial roles, since expression of genes encoding nitrogen transporters such as PyAMT1, PyDUR3.1 and PyDUR3.3 is strongly induced under nitrogen-deficient conditions (Kakinuma et al., 2008, Kakinuma et al., 2015, Kakinuma et al., 2017), which stimulates influx of nitrogen sources from environments.

Based on these background, the aims in this study are three fold: (1) identification on AMT genes in *P. yezoensis*, (2) identification and characterization of nitrogen transporters in *Bangia* species with comprehensive analyses of the phylogenetic relationships of nitrogen transporters among land plants and red algae, and (3) expression analysis of nitrogen transporters in different life cycle stages and under nitrogen-deficient conditions. Accordingly, identification and phylogenetic and expression analyses of multiple *AMT* gene family members were performed in *P. yezoensis* in the Chapter 2, whereas identification and phylogenetic classification of nitrogen transporters in the *Bangia* species were performed in the Chapter 3. Moreover, in the Chapter 4, identification of suitable reference genes and gene expression analysis of nitrogen transporter genes under nitrogen-deficient, desiccation, high salinity, and temperature changes were performed in the *Bangia* species. Finally, the Chapter 5 represents a discussion integrated all the results on the nitrogen transporters in *Pyropia* and *Bangia* species.

Chapter 2

Difference in nitrogen starvation-inducible expression patterns among phylogenetically diverse ammonium transporter genes in the red seaweed *Pyropia yezoensis*

2.1 Introduction

In the red seaweed *P. yezoensis*, nitrogen limitation induces severe discoloration in the gametophytic thallus (Kakinuma et al., 2017) due to a 20–50% reduction of the pigment content, which decreases its quality as a food (Amano and Noda, 1987, Kim et al., 2007, Sakaguchi et al., 2002). This discoloration can be rescued by increasing the nitrogen concentration in the medium (Amano and Noda, 1987, Kakinuma et al., 2017). Of nitrogen sources, NH_4^+ is preferentially used over NO_3^-, urea and other organic nitrogen sources in *P. yezoensis* (Amano and Noda, 1987, Kakinuma et al., 2017), suggesting the importance of AMTs for nitrogen homeostasis in this species. Genomic and transcriptomic analyses have identified several AMT genes in algae, including the green algae *Chl. reinhardtii* (Gonza´lez-Ballester et al., 2005, Merchant et al., 2007) and *Volvox carteri* (Prochnik et al., 2010), the red algae *Galdieria sulphuraria* (Schonknecht et al., 2013) and *Po. umbilicalis* (Brawley et al., 2017), and the diatom *Cylindrotheca fusiformis* (Hildebrand, 2005). However, the knowledge of AMT genes in *P. yezoensis* is currently restricted to *PyAMT1*, whose expression is induced under nitrogen-deficient conditions (Kakinuma et al., 2017).

The *P. yezoensis* life cycle has been recognized as a diphasic consisting of gametophyte and sporophyte generations (Adams et al., 2017, Takahashi and Mikami, 2017). In *P. yezoensis*, the nitrate transporter gene *PyNRT2* shows gametophyte-specific expression (Kakinuma et al., 2008), whereas the urea transporter gene *PyDUR3.3* exhibits sporophyte-specific and nutrient deficiency-independent expression, although nutrient deficiency-inducible expression was observed for other urea transporter genes like ubiquitously expressed *PyDUR3.1* and gametophyte-specific *PyDUR3.2* (Kakinuma et al., 2008, 2015). The expression of *PyAMT1* is gametophyte-specific and regulated both temporally and nitrogen deficient-dependently (Kakinuma et al., 2017). Notably, nitrogen deficiency-inducible expression of *PyAMT1* is strongly suppressed by addition of NH_4^+ compared to urea and other amino acid compounds (Kakinuma et al., 2017).

These findings led us to hypothesize the presence of an *AMT* gene family in *P. yezoensis* and expression patterns of each member are regulated differently during the life cycle and under nutrient deficient conditions. Recently, the life cycle of *P. yezoensis* was revised to be a triphasic consisting of gametophyte, sporophyte and conchosporophyte (Mikami et al., 2019), indicating that gene expression patterns during the life cycle should be re-analyzed among three different generations. Thus, I here represent the presence and phylogenetic analysis of multiple *AMT1* genes and differences in the regulation of these *AMT1* genes during the life cycle and under nitrogen-deficient conditions in *P. yezoensis.*

2.2 Materials and methods

2.2.1 Algal samples and culture conditions

Gametophytes, conchosporophytes and sporophytes of *P. yezoensis* (strain U-51) were maintained in SEALIFE (Marinetech, Tokyo, Japan)-based enriched sterilized seawater (ESS_2, Kitade et al., 1996) containing $NaNO_3$ as a nitrogen source, vitamins, and trace metal elements. The algae were grown under 60 μmol photons · m^{-2} · s^{-1} light in a short-day photoperiod (10 h light/14 h dark) at 15°C with air filtered through a 0.22-μm filter (Whatman; Maidstone, UK). The culture medium was changed weekly.

For nitrogen starvation experiments, gametophytes, conchosporophytes and sporophytes were treated with artificial seawater without ESS_2 (free of a nitrogen source) for a week. Algal materials were sampled daily after starting the starvation treatment to measure discoloration and gene expression.

2.2.2 Quantification of photosynthetic pigments

Gametophytes and sporophytes were treated with N-free (ESS_2-free) seawater for 3, 5 or 7 days to observe discoloration. For recovery from discoloration, gametophytes and sporophytes discolored for a week were transferred into seawater supplied with 500 μM of NH_4Cl, $NaNO_3$, or urea and then cultured for a further week. Discolored and recovered samples (0.1g fresh weight per sample) were used to calculate chlorophyll *a*

(Chl *a*) contents according to Seely et al. (1972) and phycoerythrin (PE) and phycocyanin (PC) contents as described by Beer and Eshel (1985).

2.2.3 Identification and characterization of AMTs

Unigenes annotated as putative *AMTs* were selected from the transcriptome analyses of *P. yezoensis* (Mikami et al., 2019). Predicted amino acid sequences of translation products of these unigenes were compared with those of already known AMTs by a BLAST search (https://blast.ncbi.nlm.nih.gov/Blast.cgi) after determination of full-length open reading frames (ORFs) with the ORF finder (https://www.ncbi.nlm.nih.gov/orffinder/). The ProtParam tool (https://web.expasy.org/protparam/) was used to predict the molecular weights, theoretical isoelectric point (pI), and grand average of hydropathicity (GRAVY). The location of the ammonium transporter domain was determined with Pfam (http://pfam.xfam.org/search#tabview=tab0) and transmembrane helices in the conserved AMT domain were predicted using a SMART search (http://smart.embl-heidelberg.de).

2.2.4 Phylogenetic analysis

AMTs used for the phylogenetic analysis were obtained from GenBank, genome and EST databases and the unpublished transcriptome analyses, which are listed in Table 1

and with their accession numbers and gene IDs. These included AMTs from Streptophyta (*A. thaliana*, https://www.arabidopsis.org; *Physcomitrella patens*, https://genome.jgi.doe.gov/Phypa1_1/Phypa1_1.home.html), Rhodophyta (*Po. umbilicalis*, https://phytozome.jgi.doe.gov/pz/portal.html; *Po. purpurea*, https://www.ncbi.nlm.nih.gov/sar/SRX100230; *Porphyridium purpureum*, http://cyanophora.rutgers.edu/porphyridium/; *Cyanidioschyzon merolae*, http://merolae.biol.s.u-tokyo.ac.jp; *G. sulphuraria*, http://plants.ensembl.org/Galdieria_sulphuraria/Info/Index), Chlorophyta (*Chl. reinhardtii*, https://genome.jgi.doe.gov/Chlre4/Chlre4.home.html; *V. carteri f. nagariensis*, https://www.uniprot.org/proteomes/UP000001058), and Heterokontophyta (*Phaeodactylum tricornutum*, https://genome.jgi.doe.gov/Phatr2/Phatr2.home.html; *C. fusiformis*, https://www.uniprot.org/uniprot/?query=cylindrotheca+fusiformis&sort=score). A neighbor-joining phylogenetic tree was constructed with MEGA 7 software (https://www.megasoftware.net) using ClustalW to align the AMT amino acid sequences.

2.2.5 Total RNA extraction and cDNA synthesis

Total RNA was separately extracted from gametophyte, conchosporophyte, and sporophyte tissues using the RNeasy Plant Mini Kit (Qiagen, Hilden, Germany) and then treated with DNase (TURBO DNA-free TM kit, Invitrogen, Carlsbad, USA) to

remove genomic DNA contamination. Then, first-stand complementary DNA (cDNA) was synthesized from 300 ng of total RNA with the PrimeScript 1st strand cDNA Synthesis Kit (TaKaRa Bio, Kusatsu, Japan) according to the manufacturer's instructions. Before being used as a template in quantitative PCR (qPCR) analyses, the quality of the cDNA was evaluated by amplification of the *P. yezoensis 18S* rRNA gene with its gene primer set (Kakinuma et al., 2015) via PCR reactions with Phusion high-fidelity DNA polymerase with GC buffer (New England Biolabs, Ipswich, USA) according to the manufacturer's instructions.

2.2.6 Gene expression analysis

Primers for qPCR were designed using Primer premier 5 software (http://www.premierbiosoft.com) and are listed in Table 2. To confirm the sizes of amplified products and applicability of primers, a mixture of three cDNA samples was used with all primer sets for PCR with Phusion high-fidelity DNA polymerase and GC buffer according to the manufacturer's instructions. PCR products were checked by agarose gel electrophoresis. Primer sets that amplified DNA bands with expected sizes were employed for the qPCR. qPCR was carried out in a total volume of 20 µl containing 10 µl of 2×SYBR Premix Ex Taq GC, 0.4 µl of ROX Reference Dye, 2 µl of cDNA template, and 0.4 µl (10 µM) of each primer, using the SYBR Premix Ex Taq GC kit (TaKaRa Bio, Kusatsu, Japan). The thermal cycling parameters consisted of 95°C for 5 min and 40 cycles of 94°C for 30 s, 60°C for 30 s, and 72°C for 20 s. The

dissociation curve was generated by heating from 60 to 95°C to check for specificity of amplification using an Applied Biosystems 7300 real-time PCR system (Life Technologies, Carlsbad, USA). All statistical analyses were performed using SPSS software. Data were analyzed using Student's t-test. *P* value less than 0.05 was considered statistically significant.

2.3 Results

2.3.1 A multiplicity of *P. yezoensis AMT* genes

Based on the functional annotation in *P. yezoensis* transcriptome analysis (Mikami et al., 2019), I identified seven unigenes (Unigene10902, CL1839, CL3739, Unigene15210, CL1882. Contig5, CL1882. Contig6, and Unigene24155) as candidate *P. yezoensis AMT* (*PyAMT*) genes, among of which Unigene10902 is identical to the known *PyAMT1* (Kakinuma et al., 2017). The six novel unigenes of AMT candidates contained predicted open reading frames (ORFs) encoding 484, 654, 589, 616, 690, and 522 amino acid products (Figure 2) with molecular masses of 51.2, 67.8, 58.67, 63.68, 72.06, and 53.78 kDa, respectively, and all contained the conserved AMT domain (Table 3). In addition, CL1839, CL3739, Unigene15210, CL1882. Contig5, CL1882. Contig6, and Unigene24155 showed 55.04%, 32.42%, 38.07%, 27.77%, 25.36%, and 16.88% identity to PyAMT1, respectively. Based on these findings, I concluded that all of the candidates are likely to be AMTs. However, in contrast to the products of the

other candidate genes which had 11 TM helixes (Figure 3, Table 4), the product of Unigene24155 had 12 predicted transmembrane (TM) helixes (Figure 4), suggesting a structural difference in Unigene24155 from the other genes. Other structural characteristics of these gene products, including total number of atoms and theoretical pI, are listed in Table 3.

The crystal structure of the ammonium transporter protein in *Escherichia coli* (AmtB) revealed that two phenylalanine residues, Phe107 and Phe215, block the hydrophobic NH_4^+ conduction pore and two highly conserved histidine residues, His168 and His318, maintain the shape of the central pore involved in NH_4^+ transport (Soupene et al., 2002a, Zheng et al., 2004). As shown in Figure 2, these four sites were highly conserved in *P. yezoensis* AMTs, suggesting that they have NH_4^+ transport activity. Moreover, consistent with Kakinuma et al. (2017), a tripeptide sequence, Phe-Gly-Phe (Tyr/Asn), indicating AMT identity, was found in all of the PyAMTs (Figure 2). Moreover, three-dimensional structures predicted *in silico* for all of *P. yezoensis* AMT domain-containing proteins were similar to those of known AMTs. Indeed, crystal structures of 5 PyAMTs (PyAMT1, CL1839, Unigene15210, CL1882. Contig5, CL1882. Contig6) structurally resembled to that of the AMT template c5aexB (*Saccharomyces cerevisiae* MEP2), while CL3739 was quite similar to the other AMT template c5aezA (*Candida albicans* MEP2) (Figure 5). Moreover, three-dimensional structures of Unigene24155 was closely related to that of the template c3hd6A (human rhesus protein, Rh, structurally related to AMT) (Figure 5). The confidence values of all the prediction are 100%. Taken together with characteristics in primary sequences

(Figure 2), these findings highly suggested functional NH_4^+-transport and Rh activities of AMT domain-containing proteins from *P. yezoensis.*

2.3.2 Phylogenetic classification of *P. yezoensis* AMTs into AMT1 and Rhesus protein subfamilies

To explore what type(s) of AMTs these unigenes encode, I performed a phylogenetic analysis with other full-length amino acid sequences of known AMTs from algae, plants, animals, and bacteria. Results indicated that all of the *P. yezoensis* sequences except for Unigene24155 were placed in the plant AMT subfamily 1 clade. Therefore, I considered these unigenes to encode AMT1s and designated them as *PyAMT1.2* (CL1839), *PyAMT1.3* (CL3739), *PyAMT1.4* (Unigene15210), *PyAMT1.5* (CL1882. Contig5), and *PyAMT1.6* (CL1882. Contig6). Unigene24155 shared 27.56% and 24.70% identity with CrRh1 and CrRh2 from the green alga *Chl. reinhardtii*, respectively, but only 16.88% with PyAMT1. The analysis placed this protein in the Rh clade, which is phylogenetically divergent from both AMT1 and AMT2 clades (Figure 6). Rh proteins are homologues of AMT proteins that were first identified in human erythroid cells (Huang and Peng, 2005, Marini et al., 1997). The predicted 12 transmembrane helixes of the Unigene24155 protein are in accordance with Rh proteins of other organisms (Nakhoul and Hamm, 2004, Soupene et al., 2002b). Thus, I designated Unigene24155 as *PyRh*.

The phylogenetic analysis also indicated that algal AMTs were mostly classified

into the AMT1 subfamily, which is distantly related to the AMT2 subfamily clade. In addition, AMT1s from red algae, green algae, diatoms and land plants formed independent clades. Thus, an ancient algal AMT1 may have existed prior to the divergence of red and green algae, although the origin of AMT2s is unclear.

The six PyAMT1s were subdivided into three different Rhodophyta clades, each of which contained pairs of PyAMT1s: PyAMT1 and PyAMT1.2, PyAMT1.3 and PyAMT1.4, and PyAMT1.5 and PyAMT1.6 (Figure 6). In addition, the three Rhodophyta clades also contained pairs of AMT1s from the red seaweed *Po. umbilicalis* (Brawley et al, 2017): the PyAMT1/1.2 clade with Pum0126s0003.1 (OSX77964.1), Pum1775s0001.1 (OSX69172.1), Pum0463s0020.1 (OSX72158.1), and Pum0165s0019.1 (OSX77025.2); the PyAMT1.3/1.4 clade with Pum0027s0002.1 (OSX80976.1) and Pum1656s0001.1 (OSX69292.1); and the PyAMT1.5/1.6 clade with Pum0022s0083.1 (OSX81363.1) (Figure 6). Moreover, AMT1s from Chlorophyta were separated into three different clades, independent from each other and from the three clades of Rhodophyta. Thus, expansion and divergence of the ancient algal *AMT1* gene into three groups occurred independently in red and green algae after their establishment.

2.3.3 Differences in temporal expression patterns of *PyAMT1* genes and *PyRh* during the life cycle of *P. yezoensis*

Figure 7 shows the relative transcript abundance of *PyAMT1* genes in the gametophytes,

conchosporophytes and sporophytes under normal growth conditions. When life cycle specificity of gene expression was compared between the gene pairs found in the three phylogenetic clades, *PyAMT1* was specifically expressed in the gametophytes, while the expression of *PyAMT1.2* was found in both the sporophytes and conchosporophytes. By contrast, *PyAMT1.3* and *PyAMT1.4* exhibited the same sporophyte-dominant expression pattern. *PyAMT1.6* was expressed constitutively, whereas transcripts of *PyAMT1.5* were not detectable at any stage. Thus, two of the gene pairs in the same clade did not share the same expression pattern. I did not find evidence of *PyRh* expression at any point in the life cycle (data not shown).

2.3.4 Induction of and recovery from discoloration

Gametophyte and sporophyte tissues maintained in the ESS_2-containing seawater were transferred to seawater without ESS_2 and cultivated for an additional 3, 5 or 7 days. As results, discoloration was initially observed after 3 days and gradually strengthen until 7 days in both gametophytes and sporophytes (Figure 8). Correspondingly, the contents of photosynthetic pigments Chl *a*, PE and PC were decreased respectively in gametophytes from 1.37 to 0.40, 6.42 to 3.18, and 1.27 to 0.35 mg g^{-1} FW and in sporophyte from 1.49 to 0.58, 5.24 to 1.99, and 0.48 to 0.18 mg g^{-1} FW (Figure 9). To examine recovery from discoloration, 7-day-discolored gametophytes and sporophytes were treated with nutrition-deficient medium containing 500 μM NH_4Cl, $NaNO_3$, or urea for a week. As shown in Figure 8, discoloration was recovered visibly, which was

supported by the increase in the contents of Chl *a*, PE and PC to the levels corresponding to those in non-discolored gametophytes and sporophytes (Figure 9). In this case, NH_4Cl revealed the strongest effects than $NaNO_3$ and urea (Figures 8 and 9), suggesting essential roles of the AMT activity for recovery from discoloration in *P. yezoensis*.

2.3.5 Diversity in the nutrition starvation-inducible expression pattern of *PyAMT1* genes during the life cycle

I examined the nitrogen deficiency-inducible expression of the *PyAMT1* genes. As shown in Figure 10, all *PyAMT1* genes displayed nitrogen deficiency-inducible expression without alterations in their life cycle stage specificity. However, the expression patterns differed among the genes. For instance, transient induction in gametophytes was observed for *PyAMT1*, *PyAMT1.2*, and *PyAMT1.3*, whereas expression of *PyAMT1.2* and *PyAMT1.4* gradually increased in both conchosporophytes and sporophytes. Moreover, the *PyAMT6* expression gradually increased in gametophyte tissue, and transient expression of *PyAMT6* was observed in conchosporophytes and sporophytes. Transcripts of *PyAMT1.5* and *PyRh* remained undetectable in all tissues evaluated, even under nitrogen-deficient conditions (data not shown).

I further examined the expression of the *PyAMT1* genes to determine the effects of nitrogen recovery on their expression. For these experiments, I selected *PyAMT1.2* and

PyAMT1.4, whose expression continually increased in sporophytes under nitrogen deficiency. When discolored sporophytes produced by 7-day culture in the ESS_2-less medium were transferred to ESS_2-less medium containing 500 μM NH_4Cl and further cultured for 3 days, the expression of the two genes was strongly down-regulated within 24 h (Figure 11). In addition, the same effect was observed by addition of 500 μM $NaNO_3$ or 500 μM urea to the ESS_2-less medium (Figure 11). These results were consistent with the previous observation indicating down regulation of *PyAMT1* gene expression by addition of inorganic and organic nitrogen sources (Kakinuma et al., 2017).

2.4 Discussion

The phylogenetic analysis demonstrated the diversity of the AMT1 subfamily in *P. yezoensis*, consisting of independent phylum-specific clades (Figure 6). Land plants have their own AMT1 subfamilies containing five genes in *Arabidopsis* (Gazzarrini et al., 1999, Loque et al., 2006, Yuan et al., 2007, Yuan et al., 2009), at least 10 genes in rice (Li et al., 2016) and 23 genes in wheat (Li et al., 2017). Although AMT1s from land plants formed a single clade, it was separated from the algal AMT1 subfamily in which the unicellular green algae *Chl. reinhardtii* and the red seaweed *Po. umbilicalis* have 11 and 7 *AMT1* genes, respectively (Brawley et al., 2017, Merchant et al., 2007), in addition to the 6 *PyAMT1* genes. AMTs in *Po. umbilicalis* have been annotated as AMT1, AMT2, and AMT3 by Brawley et al (2017). Despite these names, the

phylogenetic analysis indicated that all of the AMTs in *Po. umbilicalis* are AMT1 subfamily members (PuAMT1s) as are other algal genes (Figure 6). Moreover, the six PyAMT1s and seven PuAMT1s were subdivided into three groups (Figure 6). The existence of multiple independent AMT1 clades in *P. yezoensis* and *Po. umbilicalis* is the distinguishing characteristic of AMT1s from Bangiales, since AMT1s from land plants formed a single clade (Figure 6). These findings imply that an ancient red algal *AMT* gene may have diversified into three genes prior to the separation of *Pyropia* and *Porphyra*, and then further diversification occurred independently for each of the three genes in these species.

Similar to Rhodophyta, AMT1s of Chlorophyta were divided into three groups, although their phylogenetic positions were different from the Rhodophyta clades (Figure 6). This result is in agreement with the report that three subfamilies of CrAMT1s have been established in *Chl. reinhardtii* (Gonza´lez-Ballester et al., 2005). Therefore, a two-step diversification of algal AMT1s has been proposed: an early expansion of the ancient algal gene into three variants prior to the divergence of Chlorophyta and Rhodophyta and a late duplication of each of the three variants after the divergence of the green and red lineages.

The multiplicity of *AMT1* genes in Chlorophyta and Rhodophyta points to functional divergence of these genes in seaweeds. This hypothesis is supported by the gene expression analyses indicating differences in temporal and nitrogen stress-inducible expression patterns for the *PyAMT1* genes (Figures 7 and 10). *PyAMT1*, *PyAMT1.3*, and *PyAMT1.4* commonly exhibited a transient increase in their expression

under nitrogen-deficient conditions, although differences were observed in their life cycle stage-specific expression. Thus, it seems that functional divergence in PyAMT1s might allow for functional specialization over a range of NH_4^+ concentrations, which would enable *P. yezoensis* to react appropriately to a wide range of NH_4^+ concentrations in the environment. In the future, functional analysis of each PyAMT1 focused on NH_4^+ uptake under nitrogen deficiency conditions should help us to understand their transport capacity and how *P. yezoensis* responds and adapts to nitrogen deficiency stress during its life cycle.

Nitrogen deficiency results in leaf senescence in land plants (Aguera et al., 2010, Meng et al., 2016). Since nitrogen is reused to support plant growth and reproduction by reallocating from aging leaves to younger tissues (Li et al., 2016, Li et al., 2017), nitrogen deficiency tends to induce senescence in older tissues (Gregersen et al., 2008). Thus, nitrogen plays an essential role during leaf senescence (Aguera et al., 2010, Edward and Richard, 2001), indicating the importance of nutrient recycling between tissues during senescence (Meng et al., 2016). As leaf senescence progresses, nitrogen deficiency induces discoloration in tissues of *P. yezoensis* (Figure 8). Given the simple architecture of the thallus and conchocelis, and the fact that discoloration was observed throughout the entire organism (Figure 8), I conclude that reallocation of nitrogen is not responsible for the discoloration in *P. yezoensis*, suggesting that the mechanism behind the discoloration caused by nitrogen starvation is different from that in land plants. The discoloration in *P. yezoensis* thalli was rescued and the mRNA level of *PyAMT1* was down regulated by an increase in the concentrations of not only inorganic

but also organic nitrogen sources (Kakinuma et al., 2017). Similarly, nitrogen deficiency-inducible discoloration and the expression of *PyAMT1.2* or *PyAMT1.4* in the sporophyte were also strongly repressed after addition of NH_4Cl, $NaNO_3$, and urea in the culture medium (Figure 11). Since inorganic and organic nitrogen sources are metabolized into NH_4^+ to assimilate the nitrogen into cellular components (Imamura et al., 2010, Xu et al., 2012), $NaNO_3$ and urea might increase the intracellular NH_4^+ contents and similarly affect the expression of *PyAMT1* genes. These findings indicated that discoloration in *P. yezoensis* during nitrogen starvation is induced by the decreased extracellular nitrogen content, although leaf senescence in land plants occurs as a result of nitrogen reallocation between different tissues (Diaz et al., 2008, Gregersen et al., 2008).

Another distinguishing characteristic of algal NH_4^+ transporters is the presence of Rh proteins, such as PyRh in *P. yezoensis* and contig2015.11 in *Por. purpureum* (Figure 6), which contain the conserved AMT domain but are distantly related to the AMT1 and AMT2 subfamilies (Nakhoul and Hamm, 2004, Peng and Huang, 2006). *Rh* split from *AMT* in archaeal species and coexists in microbes and invertebrates, but not in fungi, vascular plants, and vertebrates (Peng and Huang, 2006). To date, *Rh* has not been reported in algae except for CrRh1 and CrRh2 from the green alga *Chl. reinhardtii* (Soupene et al., 2002b, Soupene et al., 2004); the findings reveal the presence of *Rh* in red algae (Figure 6). Although the expression of *CrRh1* and *CrRh2* is regulated by CO_2 (Soupene et al., 2002b, Soupene et al., 2004), the expression of *PyRh* was not detected during the life cycle in *P. yezoensis* nor under the nitrogen-deficient conditions (data

not shown). Thus, little is known about the physiological functions of Rh proteins in algae.

By this study, it was found that algal NH_4^+ transporters are divided into the AMT1 and Rh subfamilies. The AMT1 subfamily of *P. yezoensis* consists of three groups containing genes whose expression patterns differ temporally and nitrogen deficiency-dependently during the life cycle, providing novel information about red algal NH_4^+ transporters. The future work should elucidate the functions of each member of the AMT1 and Rh subfamilies, which could help clarify the unique algal strategies of response and acclimation to nitrogen deficiency stress by phylogenetically independent and diverse AMT1s and Rhs during the life cycle.

Chapter 3

Characterization and phylogenetic analyses of ammonium, nitrate and urea transporters in the red seaweed '*Bangia*' sp. ESS1

3.1 Introduction

Members of the order Bangiales live in the intertidal zone where organisms periodically experience abiotic stresses such as aberrant temperature, nutrient deficiency, salinity fluctuation, and long periods of desiccation (Broom et al., 2004, Karsten and West, 2000, Thompson et al., 2004, Wang et al., 2008b, Zou and Gao, 2002). Compared to the recent progress of molecular biological studies on abiotic stress responses in the genus *Pyropia* (Gao et al., 2018, Gao et al., 2019, Kakinuma et al., 2017, Li et al., 2018, Luo et al., 2014, Uji et al., 2012), the study of abiotic stress responses in the genus *Bangia* is not as advanced. However, given its simple body architecture of gametophytic thalli and ease of a laboratory culture, I recently employed *Bangia* species for physiological and molecular biological research to elucidate the regulatory mechanisms of the response and acclimation to abiotic stresses in Bangiales. Promotion of the asexual life cycle, a strategy to increase the number of gametophytic clones by producing asexual spores endowed with the gametophyte identity (Takahashi and Mikami, 2017), by high-temperature stress was confirmed in *Bangia fuscopurpurea* (Mikami and Kishimoto, 2018). Similar results have been obtained from experiments using *B. fuscopurpurea* collected from different sites (Notoya and Iijima, 2003, Wang

et al., 2008b). In addition, I have successfully expressed foreign reporter genes transiently in gametophytes of *B. fuscopurpurea* using a particle bombardment system (Hirata et al., 2011). Analyses of abiotic-stress-inducible gene expression have also been performed in several laboratories (Cao et al., 2017a, Cao et al., 2017b, Wang et al., 2011, Yokono et al., 2012). Thus, *Bangia* species have potential as model red seaweeds for biological research.

Reconstruction of phylogenetic relationships in the genus *Bangia* has been established recently (Sutherland et al., 2011). For the past few decades, all members of the genus *Bangia* have been classified into only three species: *B. atropurpurea*, *B. fuscopurpurea*, and *B. gloiopeltidicola*. However, extensive phylogenetic analysis using sequence information of nuclear small subunit ribosomal RNA (*SSU rRNA*) and plastid Rubisco large subunit (*rbcL*) genes from many representatives of *Bangia* species revealed that the genus *Bangia* could be divided into four groups: *Bangia*, '*Bangia*' 1, '*Bangia*' 2, and '*Bangia*' 3. *B. atropurpurea* and *B. gloiopeltidicola* fall into groups *Bangia* and '*Bangia*' 3, respectively, while *B. fuscopurpurea*, used in numerous previous studies and thought to represent a single species, is classified into '*Bangia*' 1 and '*Bangia*' 2 groups. These findings indicate that specimens previously classified as *B. fuscopurpurea* are a mixture of phylogenetically close but distinct species. Thus, it is necessary to classify the materials collected at Esashi on the northern Hokkaido Island of Japan, which were described as *B. fuscopurpurea* in previous reports (Hirata et al., 2011, Kishimoto et al., 2019, Mikami and Kishimoto, 2018).

Despite recent progress of biological researches in *Bangia*, little is known about

discoloration and nitrogen transporters of *Bangia* species. To understand the regulatory mechanisms of response to nitrogen-deficiency in Bangiales, identification of nitrogen transporters in *Bangia* species and comparison with those in *Pyropia* and *Porphyra* species are necessary.

Accordingly, I classified the *Bangia* species using in the study and then the identification and phylogenetic analyses of nitrogen transporters in this species were performed.

3.2 Materials and methods

3.2.1 Phylogenetic analysis of *Bangia* species

The *rbcL* gene encoded in the plastid genome of the *Bangia* material was partly amplified with gene-specific primers (5′-AAGTGAACGTTACGAATCTGG-3′ and 5′-GATGCTTTATTTACACCCT-3′) (Ohnishi et al., 2013) using Ex Taq polymerase and sequenced on an ABI Model 3130 Genetic Analyzer (Life Technologies, Carlsbad, USA). The nucleotide sequence of the amplified DNA fragment was deposited in DDBJ/EMBL/GenBank with the accession number MN052802. Specimens and accession numbers of *rbcL* gene sequences employed in phylogenetic analysis are listed in Table 5. A neighbor-joining phylogenetic tree was reconstructed with MEGA 7 software (https://www.megasoftware.net), using ClustalW to align the *rbcL* nucleotide sequences.

3.2.2 Identification and characterization of nitrogen transporters in *Bangia*

Unigenes annotated as putative *AMT*s, *NRT* and *DUR3*s were selected from the transcriptome analyses of the *Bangia* species, and their amino acid sequences were compared with those of known AMTs, NRTs and DUR3s by a BLAST search (https://blast.ncbi.nlm.nih.gov/Blast.cgi) after determination of full-length ORFs with the ORF finder (https://www.ncbi.nlm.nih.gov/orffinder/). The ProtParam tool (https://web.expasy.org/protparam/) was used to predict the molecular weights, pI, and GRAVY. The location of the ammonium transporter domain was determined with Pfam (http://pfam.xfam.org/search#tabview=tab0), and transmembrane helices in the conserved domain were predicted using a SMART search (http://smart.embl-heidelberg.de).

3.2.3 Multiple alignment of nitrogen transporters from *Pyropia*, *Porphyra* and *Bangia* species

Multiple alignments based on amino acid sequences of AMT, NRT2 and DUR3 from the *Bangia* and other red algal species (including *P. yezoensis* and *Po. umbilicalis*) were performed using DNAMAN 8 software. In addition, three-dimensional structures of AMTs, NRT2 and DUR3s of the *Bangia* species were predicted with the Phyre2 Server (http://www.sbg.bio.ic.ac.uk/phyre2/html/).

3.2.4 Phylogenetic analyses of nitrogen transporters in plants and algae

To examine the evolutionary relationships each of AMT, NRT and DUR3 with those from other plants and algae, neighbor-joining phylogenetic trees was constructed with MEGA 7 software (https://www.megasoftware.net). AMTs, NRTs and DUR3s used for the phylogenetic analysis were obtained from GenBank, genome and EST databases, which are listed in Table 1, Table 6, Table 7 and Table 8 with their accession numbers and gene IDs. These included sequences from Streptophyta (*A. thaliana*, https://www.arabidopsis.org; *Ph. patens*, https://genome.jgi.doe.gov/Phypa1_1/Phypa1_1.home.html), Rhodophyta (*Po. umbilicalis*, https://phytozome.jgi.doe.gov/pz/portal.html#; *Pophyra purpurea*, https://www.ncbi.nlm.nih.gov/sar/SRX100230; *Por. purpureum*, http://cyanophora.rutgers.edu/porphyridium/; *Cy. merolae*, http://merolae.biol.s.u-tokyo.ac.jp; *G. sulphuraria*, http://plants.ensembl.org/Galdieria_sulphuraria/Info/Index), Chlorophyta (*Chl. reinhardtii*, https://genome.jgi.doe.gov/Chlre4/Chlre4.home.html; *V. carteri f. nagariensis*, https://www.uniprot.org/proteomes/UP000001058), and Heterokontophyta (*Pha. tricornutum*, https://genome.jgi.doe.gov/Phatr2/Phatr2.home.html; *C. fusiformis*, https://www.uniprot.org/uniprot/?query=cylindrotheca+fusiformis&sort=score).

3.3 Results

3.3.1 Phylogenetic classification of the specimen used in this study

A DNA fragment corresponding to the *rbcL* gene was amplified from the *Bangia* material, sequenced, and used for phylogenetic analysis. Results indicated that the sample was classified into the '*Bangia*' 2 group established by Sutherland et al. (2011), with the closest relationship to '*B. fuscopurpurea*' CMNH UM BF1 collected at Banda, Tateyama, Chiba, Japan (Figure 12). I designated the experimental material '*Bangia*' sp. ESS1 (ESS was derived from Esashi).

3.3.2 Phylogenetic classification of nitrogen transporters in '*Bangia*' sp. ESS1

Based on the functional annotation in the unpublished '*Bangia*' sp. ESS1 transcriptome analysis, I identified six unigenes (CL2278, CL2683, CL232, CL2570, CL337 and Unigene24217) as candidate '*Bangia*' sp. ESS1 *AMT* (*BE1AMT*) genes, one unigene (Unigene22285) as candidate '*Bangia*' sp. ESS1 *NRT2* (*BE1NRT2*) gene and two unigenes (CL2421 and Unigene31059) as candidate '*Bangia*' sp. ESS1 *DUR3* (*BE1DUR3*) genes. To explore what type(s) of nitrogen transporters these unigenes encoded, I performed the phylogenetic analyses of BE1AMTs, BE1NRT and BE1DUR3s with other amino acid sequences of known AMTs, NRTs and DUR3s from algae and plants.

Similar to results of phylogenetic analysis in Chapter 2 (Figure 6), all of the '*Bangia*' sp. ESS1 unigene sequences except for Unigene24217 were placed in the plant AMT subfamily 1 clade. Therefore, I considered these unigenes to encode AMT1s and designated them as *BE1AMT1.1* (CL2278), *BE1AMT1.3* (CL2683), *BE1AMT1.4* (CL232), *BE1AMT1.5* (CL2570), and *BE1AMT1.6* (CL337). The five BE1AMT1s were subdivided into three different Rhodophyta clades, each of which contained BE1AMT1, and pairs of BE1AMT1.3 and BE1AMT1.4 and BE1AMT1.5 and BE1AMT1.6 (Figure 13). In addition, the three BE1AMT1 clades were identical to the three PyAMT1 clades: that is, the BE1AMT1 clade with PyAMT1 and PyAMT1.2, the BE1AMT1.3 and BE1AMT 1.4 clade with PyAMT1.3 and PyAMT1.4 and the BE1AMT1.5 and BE1AMT1.6 clade with PyAMT1.5 and PyAMT1.6 (Figure 13).

Unigene24217 shared 30.65% identity with PyRh from *P. yezoensis*, but only 17.39% with BE1AMT1. The analysis placed this protein in the Rh clade, which is phylogenetically divergent from both AMT1 and AMT2 clades (Figure 13). The predicted 12 transmembrane helixes of the Unigene24155 protein is in accordance with Rh proteins of other organisms (Nakhoul and Hamm, 2004, Soupene et al., 2002b). Thus, I designated Unigene24217 as *BE1Rh*.

The putative NRT2 (Unigene22285) formed one clade with other four NTR2s from *Chondrus crispus*, *Gracilariopsis chorda*, *Po. umbilicalis and P. yezoensis*. In addition, all of these species respectively contained only one single NRT2 (Figure 14). Moreover, BE1NRT2 shared relatively high identities that 87.73% and 86.46% with NRT2 in *P. yezoensis* and *Po. umbilicalis*, respectively, which showed fewer divergency in NRT2

members of red algae. Therefore, Unigene22285 was designated BE1NRT2.

DUR3s from green and red algae, formed a single green and two red algal clades (Rhodophyta I and II), respectively, each of which contained one or two DUR3 members from other red algae like *Cho. crispus*, *G. chorda*, *P. yezoensis*, *Po. umbilicalis* and '*Bangia*' sp. ESS1. Since CL2421 was included in Rhodophyta I with PyDUR3.1 and Unigene31059 belonged to Rhodophyta II with PyDUR3.2 and PyDUR3.3 (Figure 15), CL2421 and Unigene31059 were designated BE1DUR3.1 and BE1DUR3.2, respectively.

3.3.3 Structural characteristics of AMT1s/Rh, NRT2 and DUR3s of '*Bangia*' sp. ESS1

The six BE1AMT/Rh genes contained predicted ORFs encoding 490, 616, 566, 463, 576, and 458 amino acid products (Figure 16) with molecular masses of 51.3, 63.6, 59.5, 47.5, 62.3, and 49.8 kDa, respectively, and all contained the conserved AMT domain and 11 or 12 TMs (Table 6, Figures 3 and 17). In addition, CL2278, CL2683, CL232, CL2570, CL337 and Unigene24217 shared 35.99% identities with each other. In addition, similar to the crystal structures of PyAMTs predicted in chapter 2, all the BE1AMT1s structurally resembled to that of the AMT template c5aexB (*S. cerevisiae* MEP2) (Figure 18). Same with structure of PyRh, BE1Rh was closely related to that of the template c3hd6A (human rhesus protein, Rh, structurally related to AMT) (Figure 18). Based on these findings, I predicted that all of unigenes are functional.

The cDNA length of putative *BE1NRT2* was 2,395 bp including an ORF encoding a polypeptide of 479 amino acid residues with 12 TM helixes and contained a NRT2 family-specific motif from 51 to 412 amino acid position (Table 6, Figure 19). The amino acids of putative *BE1NRT2* showed 87.73% and 86.46% identities with NRT2s from *P. yezoensis* and *Po. umbilicalis*, respectively (Figure 19). Multiple amino acid sequence alignment revealed that NRT2s of red algae all contain a conserved consensus motif (A-G-W-G-N-L-G) that is proposed to determine substrate specificity (Amarasinghe et al., 1998, Pao et al., 1998). However, a conserved protein kinase C recognition motif (S-X-R) in the loop between 10th and 11th TMs is not observed in any red algal NRT2s (Figure 19). As *in silico* prediction of three-dimensional structures, PyNRT2 and BE1NRT2 were quite similar to the template d1pw4a (*E. coli* glycerol-3-phosphate transporter) (Figure 20). The confidence value of the prediction is 100%. These findings strongly suggested the functionality of BE1NRT2.

DUR3s are known to belong to the SSS superfamily, which includes more than one hundred members of prokaryotic and eukaryotic origin (Liu et al., 2003, Wang et al., 2012). Similar to members of the SSS superfamily containing 11-15 putative TMs, all of red algal DUR3s contained 15 TMs (Figure 21). Indeed, two *BE1DUR3.1* and *BE1DUR3.2* genes had predicted ORFs encoding 752 and 680 amino acid products (Figure 21) with molecular masses of 79.6 and 71.2 kDa containing the conserved DUR3 domain 15 TM helixes (Table 6, Figure 21). Other structural characteristics of these gene products, including total number of atoms and theoretical pI, are listed in Table 6. Functionality of DUR3s in '*Bangia*' sp. ESS1 was supported by the predicted

three-dimensional structures, which indicated that the structures of DUR3s in *P. yezoensis* and '*Bangia*' sp. ESS1 were closely related to the template c2xq2A (sodium/glucose cotransporter) with DUR3 activity (Figure 22). The confidence values of all the prediction are 100%.

3.4 Discussion

I classified the material '*Bangia*' sp. ESS1 used in this study as a member of the '*Bangia*' 2 group based on phylogenetic analysis (Figure 12). Recently, the plastid genome of a member of the '*Bangia*' 2 group, designated '*Bangia*' sp. OUCPT-01 and collected at Putian, Fujian, China, was recently sequenced completely (Cao et al., 2018); however, '*Bangia*' sp. OUCPT-01 is different from '*Bangia*' sp. ESS because it forms a clade with '*Bangia*' sp. BGA collected at Gentle Annie, Westland, New Zealand, while '*Bangia*' sp. ESS1 and '*B. fuscopurpurea*' CMNH UM BF1 form a distinct sister clade (Figure 12). These findings make the results of biological studies using *Bangia* species highly confusing because experimental results are partially derived from different *Bangia* species; thus, it is difficult to obtain a unified view of physiological regulations in a certain species or among species. Therefore, physiological and molecular biological research in *Bangia* must be performed using several specimens classified phylogenetically and maintained in laboratories to examine biological characteristics of each and among the four '*Bangia*' groups. This in turn will provide evidence for the current phylogenetic classification of *Bangia* species.

Main goal of this study was to identify and characterize ammonium, nitrate and urea transporters in '*Bangia*' sp. ESS1 and assess their phylogenetic relationships with other known algal and plant transporters. As results, AMT1s, NRT2 and DUR3s were identified in '*Bangia*' sp. ESS1 and characterized structurally and phylogenetically in this study.

As described in the Discussion of chapter 2, unlike the land plants possessing with AMT1 and AMT2 subfamilies, the AMT domain-containing proteins from micro- and macro-algae belonged to either the AMT1 or Rh subfamily, indicating the absence of AMT2 in algae. The phylogenetic analysis indicated that five AMT1 gene family members of '*Bangia*' sp. ESS1 also diverged into three clades containing counterparts from *P. yezoensis* and *Po. umbilicalis*, which implied that an ancient red algal *AMT* gene may have diversified into three genes prior to the separation of *Pyropia*, *Porphyra*, and *Bangia*, and then furtherly diversified independently for each of the three genes in each of these species. Additionally, Rh protein in '*Bangia*' sp. ESS1 fall into the clade containing PyRh, which strengthens the presence of Rh protein in red algae (Figure 13).

Vascular plants have only a single copy gene encoding a putative H^+/urea symporter DUR3, whereas multiple DUR3 genes were found in fungi and algae (Wang et al., 2008a). Indeed, green algae *Chl. reinhardtii* and *V. carteri* have 3 and 2 DUR3 genes, respectively, forming a single Chlorophyta clade (Figure 15). Similarly, red algae like *G. chorda*, *Cho. crispus*, *Po. umbilicalis*, *P. yezoensis* and '*Bangia*' sp. ESS1 have 2 or 3 DUR3 members, which belonged either Rhodophyta I or Rhodophyta II clade (Figure 15). These results suggest the diversification of *Chlamydomonas* and

Volvox occurred prior to the duplication of the ancient DUR3 genes, although the ancestral DUR3 gene may duplicated prior to the separation of red algae *Pyropia*, *Porphyra* and *Bangia* and then further diversified independently in these algae. In this study, a homolog of PyDUR3.3 was not identified. Since PyDUR3.3 expresses sporophyte-specifically, molecular cloning of a gene encoding DUR3 is necessary using the data of transcriptome analysis for sporophyte, which could provide an opportunity for complete comparison of DUR3s among *Pyropia*, *Porphyra* and *Bangia* species.

As summary, the *Bangia* material previously called *B. fuscopurpurea* was classified into the '*Bangia*' 2 group and designated '*Bangia*' sp. ESS1. '*Bangia*' sp. ESS1 has a gene family of AMT consisting of five AMT1s, which were diversified into three independent phylogenetic clades with corresponding AMT1s from other red algae, and one Rh. In contrast, '*Bangia*' sp. ESS1 has only single copy gene of NRT2 as other red algae. In addition, there is a gene family of DUR3 in '*Bangia*' sp. ESS1. To understand functional diversification among these transporters, expression analysis of genes encoding AMT1s, NRT2 and DUR3s should be performed under nutrition-deficient conditions in '*Bangia*' sp. ESS1.

Chapter 4

Analysis of nitrogen-deficiency inducible expression of nitrogen transporter genes by normalization with newly identified reference genes in '*Bangia*' sp. ESS1

4.1 Introduction

Regulation of genes involved in acquisition of stress tolerance is fundamental for intertidal seaweeds to have normal development and growth under strict living conditions (Mikami, 2018). Thus, gene expression analysis is important for understanding the mechanisms of response to environmental stress in intertidal seaweeds.

Real-time quantitative reverse transcription polymerase chain reaction (qRT-PCR) allows monitoring of relative changes in gene expression (Panina et al., 2018) using a normalization strategy that relies on comparison of the target gene with an endogenous control (reference gene). At present, housekeeping genes such as *actin*, *tubulin*, and *glyceraldehyde-3-phosphate dehydrogenase* (*GAPDH*) as well as ribosomal RNA genes are commonly used as reference genes. These genes are thought to be universally required for basic cellular functions and to be constitutively and stably expressed under different experimental conditions in land plants (Czechowski, 2005, Pabuayon et al., 2016, Tenea et al., 2011,); fungi (Chen et al., 2016, Kothe et al., 2014, Llanos et al., 2015); the green algae *V. carteri* (Kianianmomeni and Hallmann, 2013), *Ulva linza*

(Dong et al., 2012), and *Chlamydomonas* sp. ICE-L (Liu et al., 2012); the brown alga *Ectocarpus siliculosus* (Le Bail et al., 2008); and the red algae *P. yezoensis* (Bhattacharya et al., 2013, Gao et al., 2018, Kong et al., 2014), *P. haitanensis* (Luo et al., 2014), and *G. lemaneiformis* (Ding et al., 2014). Indeed, these housekeeping genes have been employed as reference genes in *Chlamydomonas*, *Volvox*, *Pyropia*, and *Porphyra* species. However, little is known about appropriate reference genes in *Bangia* species to date. Therefore, I first identify reference genes suitable for gene expression analysis under various abiotic stresses in *Bangia* species. In addition, further validation of the selected reference genes was performed with a cold-stress-inducible gene encoding delta12-fatty acid desaturase (Des12) in *B. fuscopurpurea* (Cao et al., 2017a).

As mentioned in chapter 2, AMT1s, NRT2 and DUR3s in *P. yezoensis* displayed different generation-dependent expression specialties and nitrogen-deficiency inducibilities. *PyNRT2* shows gametophyte-specific expression (Kakinuma et al., 2008). *PyDUR3.3* exhibits sporophyte-specific expression that is nutrient deficiency independent; however, nutrient deficiency-inducible expression was observed for *PyDUR3.1* and *PyDUR3.2*, although they are expressed generation independently and gametophyte specifically, respectively (Kakinuma et al., 2008, 2015). The expression of *PyAMT1* is gametophyte specific and is regulated both temporally and by nitrogen deficiency stress (Kakinuma et al., 2017). Thus, another goal in this chapter is to investigate the gene expression patterns of nitrogen transporters in gametophytes of '*Bangia*' sp. ESS1 under nitrogen-deficient conditions to compare those in *P. yezoensis*. To this end, I employed reference genes identified in this Chapter for normalization of

expression levels of all of nitrogen transporter genes.

4.2 Materials and methods

4.2.1 Algal strain and culture conditions

Thalli of '*Bangia*' sp. ESS1 were originally collected at Esashi, Hokkaido, Japan, on May 17, 2010 and maintained clonally in the laboratory as an experimental line. Filamentous gametophytes were cultured in sterilized artificial seawater (SEALIFE; Marinetech, Tokyo, Japan) containing ESS_2 with $NaNO_3$ as a nitrogen source, vitamins, and trace metal elements (Takahashi et al., 2010) under 60 μmol photons·m^{-2}·s^{-1} in a short-day photoperiod (10 h light/14 h dark) at 15°C with air filtered through a 0.22-μm filter (Whatman; Maidstone, UK). The culture medium was changed weekly.

Nutrient deficiency, high salinity, desiccation, cold, and heat were selected as abiotic stresses (Table 9). For nutrient deficiency treatment, 0.1 g of thalli was treated with ESS_2-less seawater for 24, 48, 72, 96, 120, 144, and 168 h. For high-salinity stress, thalli were incubated in medium containing 25, 50, or 100 mM NaCl for 24, 48, and 72 h. For desiccation stress, 0.1 g of thalli were desiccated in a clean bench until the weight of samples reached 75, 50, or 25% of the initial weight (W_i). To examine recovery from desiccation, thalli weighing 25% of W_i were incubated in normal seawater medium for 1 h. For temperature treatment, 0.1 g of thalli were exposed to 5 or 30°C for 24, 48, and 72 h. All samples were immersed in liquid nitrogen and stored at -80°C prior to RNA

extraction.

4.2.2 Total RNA extraction and cDNA synthesis

Total RNA was separately extracted from each sample using RNeasy Plant Mini kit (Qiagen, Hilden, Germany) and then treated with DNase (TURBO DNA-free TM kit, Invitrogen, Carlsbad, USA) to remove genomic DNA contamination. Purity and concentration of RNA samples were calculated using a GeneQuant pro spectrophotometer (UK), and the integrity of RNA samples was checked using agarose gel electrophoresis. RNA samples of good quality with A_{260}/A_{280} ratios ranging from 1.9 to 2.1 were used. First-strand complementary DNA (cDNA) was synthesized from 300 ng of total RNA in a volume of 20 µl using a PrimeScript 1st strand cDNA synthesis kit according to the manufacturer's instructions. The cDNA was diluted 20 times before use as template in qRT-PCR.

4.2.3 Design and evaluation of primers for candidate reference genes

Six housekeeping genes encoding 18S rRNA, 60S rRNA, GAPDH, EF1, actin, and *α*-tubulin were selected as candidates for reference genes. Primers for qRT-PCR of *18S rRNA* and *GAPDH* genes were available from previous studies (Cao et al., 2017a, Wang et al., 2011). Nucleotide sequences of the other four candidate genes were obtained from the unpublished transcriptome analysis: *EF1* (Unigene64544), *actin* (CL1634.

Contig3), *α-tubulin* (CL70. Contig4), and *60S rRNA* (Unigene3570). Primers for these genes were designed using Primer Premier 5 software (http://www.premierbiosoft.com) with the following conditions: annealing temperature of 60°C, DNA G+C content of 40 to 60%, and amplicon length of 80 to 200 bp (Table 10). The specificity of primer pairs for each candidate gene to produce PCR fragments of a single expected size was validated by agarose gel electrophoresis of products from PCR reactions performed using Phusion high-fidelity DNA polymerase and GC buffer according to the manufacturer's instructions. A standard curve for each gene was generated using a 5-fold dilution series of one sample over six dilution points measured in three technical replicates, and PCR amplification efficiency was also calculated.

4.2.4 Quantitative gene expression analysis

Reactions of qRT-PCR were carried out in a total volume of 20 µl containing 10 µl of 2× SYBR Premix Ex Taq GC, 0.4 µl of ROX Reference Dye, 2 µl of cDNA template, and 0.4 µl (10 µM) of each primer, using the SYBR Premix Ex Taq GC kit. The thermal cycling parameters consisted of 95°C for 5 min and 40 cycles of 94°C for 30 s, 60°C for 30 s, and 72°C for 20 s. A dissociation curve was generated by heating from 60 to 95°C to check for specificity of amplification using an Applied Biosystems 7300 real-time PCR system (Life Technologies, Carlsbad, USA). Each reaction was triplicated, and the data were analyzed using Student's t-test. *P* value less than 0.05 was considered statistically significant.

4.2.5 Evaluation of gene expression stability and its validation using *Des12*

Two software packages, geNorm (Vandesompele et al., 2002) and NormFinder (Andersen et al., 2004), were used to assess the stability of the expression level of each reference gene under different experimental treatment conditions. geNorm ranks the candidate reference genes according to calculation of an expression stability value (*M*). A lower *M* value reflects higher stability of gene expression. geNorm also determines the optimal number of reference genes required for accurate normalization of target gene expression by a pairwise variation ($V_{n/n+1}$). Generally, a $V_{n/n+1}$ value less than 0.15 indicates no need for an additional reference gene for normalization. NormFinder produces expression stability values (SVs) to evaluate candidate reference genes in a given experimental design and considers intra- and intergroup variations, enabling an estimate of candidate gene stability values for normalization without any influence of coregulated candidate genes. Low SV indicates high stability in normalization.

For validation of these evaluations, the expression of the *Des12* gene was normalized using the reference genes evaluated as suitable by geNorm combined with NormFinder under different abiotic stresses. The primer sequence of *Des12* (Cao et al., 2017a) is indicated in Table 10.

4.2.6 Gene expression analyses of nitrogen transporters in '*Bangia*' sp. ESS1 under nitrogen-deficient conditions

Gene expression analyses of nitrogen transporters in '*Bangia*' sp. ESS1 under nitrogen-deficient conditions have been performed after the determination of the suitable reference genes identified in this Chapter. Primers for nitrogen transporter genes were designed for gene expression analyses under the nutrient-deficient conditions (Table 11). Thalli (0.1 g) was cultured in ESS_2-less seawater for 24, 48, 72, 96, 120, 144, and 168 h. Total RNA was extracted from these samples for synthesis of cDNA and subsequent qRT-PCR using an Applied Biosystems 7300 real-time PCR system (Life Technologies, Carlsbad, USA). The experiments were repeated for three times and these data were examined with Student's t-test. *P* value less than 0.05 was considered statistically significant.

4.3 Results

4.3.1 Amplification efficiency and cycle threshold values of PCR reactions using candidate reference genes

Based on the unpublished transcriptome data and information from previous studies (Cao et al., 2017a, Wang et al., 2011), the six housekeeping genes *18S rRNA*, *GAPDH*, *EF1*, *60S rRNA*, *actin*, and *α-tubulin* were chosen as candidates for reference genes to

evaluate their applicability in quantitative gene expression analysis. All the primer pairs for these candidate genes amplified single fragments of the expected size (Table 10) that gave rise to one single peak in the melting curve (data not shown). These primer pairs were therefore considered specific and used for evaluation of gene expression levels by qRT-PCR. In addition, the correlation coefficient (R^2) and PCR efficiency of each gene were analyzed using standard curves. The R^2 value and efficiency ranged from 0.991 to 0.994 and 91.1% to 105.0%, respectively (Table 10), both of which were within the acceptable range (0.9910 to 0.9998 for R^2 and 90 - 105% for PCR efficiency), indicating the suitability of all primer sets for further gene expression analysis by qRT-PCR.

Cycle threshold (Ct) values represent relative expression levels; low and high values indicate high and low levels of gene expression, respectively. The Ct values of the six candidate reference genes from four different treatments across all samples in '*Bangia*' sp. ESS1 were calculated as shown in Figure 23. The Ct values of the reference genes varied from 11.5 to 30.7, with the majority between 18 and 28. The *18S rRNA* gene showed the highest expression level with Ct values ranging from 11.5 to 13.0, while *GAPDH* displayed the lowest expression level with Ct values ranging from 26.1 to 30.7. Based on the comparative ranges of Ct values for each reference gene, *18S rRNA* showed the most stable gene expression, while *60S rRNA* had the most obvious expression variation.

However, a simple evaluation of the raw Ct values could not provide sufficient information to determine expression stability of the candidate reference genes. I

therefore used geNorm and NormFinder to provide more information on expression stability.

4.3.2 Expression stability of candidate reference genes

The expression stability values (*M*) produced by geNorm software allow ranking of the expression stability of each reference gene. Figure 24 ranks the reference genes for effectiveness under each stress treatment based on *M*, with the least and most stable genes plotted at the left and right, respectively. Other points represent genes with intermediate expression stabilities compared to those of the least and most stable genes. All *M* values were lower than 1.5, indicating that the expression levels of these genes were relatively stable under all experimental conditions. Among the genes, *60S rRNA* and *actin* were the most stable under nutrient deficiency, salinity, or temperature treatment, whereas *EF1* and *α-tubulin* showed the best stability under desiccation treatment and conditions combining all treatments (total in Figures 24 and 25).

To provide an independent assessment, the expression stabilities of reference genes were also ranked by NormFinder. Table 12 shows that *α-tubulin* and *60S rRNA* were the most stable genes under desiccation and temperature treatments, respectively, while *GAPDH* was highly stable under nutrient deficiency and salinity conditions. *GAPDH*, *α-tubulin*, and *EF1* were the most stable genes under conditions combining all treatments.

The geNorm software also produced information on pairwise variation value

($V_{n/n+1}$), which was used to assess the optimal number of reference genes for accurate normalization. In this analysis, a $V_{n/n+1}$ value below 0.15 indicates that an additional reference gene is not required. The $V_{2/3}$ for each single treatment was below 0.15, implying that use of two stable reference genes is acceptable for normalizing gene expression within each single treatment (Figure 25). In addition, $V_{2/3}$ and $V_{3/4}$ were above 0.15 and below 0.15, respectively, under treatment combining all conditions, revealing that three reference genes are required for gene expression analysis under combined stress conditions (Table 13).

These findings, presented in Figures 24 and 25 and Tables 12 and 13, indicated that use of two or three reference genes ranked as the top two or three in Table 13 is suitable for normalization of stress-inducible gene expression in '*Bangia*' sp. ESS1. For example, *EF1* and *α-tubulin* are suitable for desiccation treatment, whereas nutrient deficiency and salinity treatments require use of *60S rRNA*, *actin*, and *GAPDH*. Combination of all treatments requires *EF1*, *α-tubulin*, and *GAPDH* as reference genes.

4.3.3 Validation of reference gene suitability by quantification of expression levels of *Des12* from '*Bangia*' sp. ESS1 under different stress conditions

To evaluate the suitability of reference genes selected by the analyses, I quantified the expression levels of *BE1Des12* under normal (15°C), cold stress (5°C), and heat stress (30°C) conditions for 24, 48, and 72 h by qRT-PCR using the most stable (*60S rRNA* and *actin*) and least stable (*18S rRNA*) reference genes. When *60S rRNA*, *actin*, and the

combination of both were used as reference genes for normalization, expression levels of *Des12* from '*Bangia*' sp. ESS1 (*BE1Des12*) were increased by exposure to cold stress, reaching the highest level at 72 h, while expression levels were not changed under heat stress (Figure 26). By contrast, when the *18S rRNA* gene was used as the reference gene, normalized expression levels of *BE1Des12* under both cold and heat stress were not significantly different from those under normal conditions (Figure 26). These experiments confirmed the suitability of *actin* and *60S rRNA* as reference genes for examination of cold-inducible *BE1Des12* expression in '*Bangia*' sp. ESS1.

These findings also indicated the suitability of the two top-ranked genes in Table 13 as reference genes under the corresponding stress conditions. As *BE1Des12* induction by stresses other than cold has not been examined to date, I quantified *BE1Des12* expression levels under various stress conditions by normalization with the most suitable reference genes shown in Table 13. Desiccation, nutrient deficiency, and high salinity induced expression of *BE1Des12*, although the kinetics of induction varied among these stresses (Figure 21), suggesting that modifications of membrane fatty acid composition probably occurred following *BE1Des12* expression in response to various stresses in '*Bangia*' sp. ESS1.

4.3.4 Effects of nitrogen-deficiency on expression patterns of *AMT1/Rh*, *NRT2* and *DUR3* genes in '*Bangia*' sp. ESS1

As mentioned above, the combination of *60s rRNA* and *actin* were optimally used to

normalize the gene expression under nutrient-deficient conditions. Thus, expression patterns of nitrogen transporter genes found in '*Bangia*' sp. ESS1 were analyzed quantitatively by normalization with these two reference genes. Figure 28 shows the relative transcript abundance of *BE1AMT1*/*Rh* genes in gametophytes of '*Bangia*' sp. ESS1. When algal materials maintained in the ESS_2-containing seawater medium were transferred to seawater without ESS_2 and cultivated for an additional 7 days, *BE1AMT1.1* was induced at the first two days and then the expression gradually decreased as *PyAMT1*, an ortholog of *BE1AMT1.1,* whereas *BE1AMT1.3* showed the transient induction followed with a slight and gradual declination as its ortholog *PyAMT1.3* (Figure 28, compare with Figure 10). In addition, *BE1AMT1.4* showed a transient induction pattern with at peak at third day although phylogenetic partner *PyAMT1.4* was no expressed in gametophyte of *P. yezoensis*. Moreover, *BE1AMT1.5*, *BE1AMT1.6* and *PyAMT1.6* belonging to the same clade displayed a same continually induction pattern (Figure 28, compare with Figure 10); however, the expression of *PyAMT1.5*, an ortholog of *BE1AMT1.5,* was undetectable under any conditions (data not shown). Expression of *BE1Rh* also remained undetectable as *PyRh* in *P. yezoensis* (data not shown).

Unlike the nitrogen deficiency-inducible expression patterns in *BE1AMT1*s, transcripts of *BE1NRT2* were not induced or repressed by nitrogen deficiency (Figure 28), which is similar to *PyNRT2* that does not response to nitrogen-deficient conditions (Kakinuma et al., 2008). In contrast, genes encoding two urea transporters *BE1DUR3.1* and *BE1DUR3.2* commonly showed transient inducible pattern under nitrogen-

deficient conditions (Figure 28), which is similar to respective orthologs *PyDUR3.1* and *PyDUR3.2* inducible by nitrogen-deficient stress (Kakinuma et al., 2008, 2015).

4.4 Discussion

4.4.1 Requirement of differential use of reference genes suitable for appropriate stress conditions

The aim here was to identify reference genes suitable for qRT-PCR analysis in studies on the regulation of stress response and tolerance in '*Bangia*' sp. ESS1. I thus evaluated six candidate reference genes under cold, heat, nutrition deficiency, desiccation, and high salinity, the most common environmental factors influencing growth and development of algae. Stability of candidate gene expression was assessed using two widely used analysis programs, geNorm and NormFinder (Figures 24 and 25; Tables 12 and 13). These programs determined the order of candidate genes in terms of suitability as reference genes under each stress condition and the numbers of reference genes required for accurate normalization. As shown in Tables 12 and 13, *GAPDH* is a suitable reference gene for gene expression analysis under nutrient deficiency and salinity treatments, whereas normalization of gene expression levels under desiccation stress requires *ELF1*. *GAPDH* and *ELF1* are necessary for normalization under stress conditions combining all treatments. In addition, *actin* is a suitable reference for examination of gene expression under nutrient deficiency, temperature changes, and

high salinity, while *α-tubulin* is a highly stable reference gene under desiccation and combined-stress conditions. Moreover, *60S rRNA* is suitable for normalization of gene expression under temperature changes, nutritional deficiency, and high salinity. The suitability of *60S rRNA* and *actin* was indeed validated by quantitative gene expression analysis of low-temperature-inducible expression of *BE1Des12* (Figure 26), although Cao et al. (2017a) employed *tubulin* and *GAPDH* genes were employed as references. Therefore, I conclude that there is no perfect reference gene suitable for gene expression analysis under a variety of stress conditions; thus, selection of reference genes appropriate for the desired stress conditions is necessary for performing accurate qRT-PCR analyses in '*Bangia*' sp. ESS1.

These findings are in part consistent with previous knowledge. For instance, *GAPDH* has been established as a suitable reference gene for gene expression studies in the green alga *Chlamydomonas* sp. ICE-L under different light intensities (Mou et al., 2015) and in the red alga *G. lemaneiformis* under temperature stress and at different life cycle stages (Ding et al., 2014). *EF1* is also recognized as a highly suitable reference gene, showing stable expression, for instance, under the diurnal cycle, high light, high salinity, and UV-B irradiation in the green alga *Chlamydomonas* sp. ICE-L (Mou et al., 2015) and under certain stress conditions and at different developmental stages in the red alga *P. yezoensis* (Kong et al., 2014). In addition, the *actin* gene is useful for studying gene expression responses to temperature changes in *G. lemaneiformis* (Ding et al., 2014); however, it is suitable as a reference gene for studying responses to abiotic stress in *P. yezoensis* but not gene expression changes at

different life cycle stages (Kong et al., 2014). The *tubulin* gene is generally used as a reference gene in the brown alga *E. siliculosus*, the dinoflagellate *Prorocentrum minimum*, the green alga *U. linza*, and the red alga *P. yezoensis* (Dong et al., 2012, Guo and Ki, 2012, Kong et al., 2014, Le Bail et al., 2008). Moreover, ribosomal protein genes have been reported as reference genes in the green algae *Chlamydomonas* sp. ICE-L (Liu et al., 2012) and *V. carteri* (Zhang et al., 2018) as well as the diatom *Pha. tricornutum* (Siaut et al., 2007). It is not known how these reference genes were selected in these reports, so I suggest reconfirming the suitability of these reference genes to allow more accurate quantification of stress-inducible gene expression in these algae.

It is notable that *18S rRNA* was not suitable as a reference gene for analysis of stress-inducible gene expression in '*Bangia'* sp. ESS1. The *18S rRNA* gene is commonly used as a reference gene in algae (Coyne, 2010, Fischer et al., 2007). For instance, *18S rRNA* showed outstanding stability under different light intensities (Dong et al., 2012) and among life cycle stages (Kianianmomeni and Hallmann, 2013) in green algae and has been used extensively to normalize gene expression during development and under temperature changes and nutrient deficiency in red algae (Luo et al., 2014, Wang et al., 2011,). However, *18S rRNA* showed moderate stability across all the treatments I examined in this study. The median Ct value of 12.3 for *18S rRNA* was much lower than those for the other reference genes (Figure 23), meaning that the abundance of *18S rRNA* mRNA transcripts was much higher. The high abundance of *18S rRNA* makes it difficult to reliably subtract the background baseline value when normalizing the mRNA transcripts of target genes. In addition, *18S rRNA* did not rank

among the three most stable reference genes in any treatment (Table 13). These findings suggest that experiments using *18S rRNA* as a reference gene should be revised by identifying more suitable reference genes in algae. For instance, *18S rRNA* has been employed as a reference gene for gene expression analyses in the red alga *P. yezoensis* (Kakinuma et al., 2008, 2017, Uji et al., 2012); however, it is necessary to find more suitable reference genes for studies of stress-inducible and life cycle generation-dependent gene expression in this organism.

4.4.2 Diversity in expression patterns of nitrogen transporters under nitrogen-deficient conditions in '*Bangia*' sp. ESS1

Both in land plants and algae, transcription levels of *AMT1*s change due to the nitrogen nutritional status. As mentioned in the Chapter 2, the expression patterns of *PyAMT1*s differ temporally and are nitrogen deficient-dependently during the life cycle. Except for *BE1AMT1.4* and *PyAMT1.4* showing opposite expression patterns, each *BE1AMT1s/Rh* displayed nitrogen deficient-dependent expression pattern similar to its corresponding ortholog in the *PyAMT1*s/*Rh* family (Figures 28 and 10), suggesting the highly conservation of nitrogen deficiency-inducibility in the AMT1s/Rh families of *P. yezoensis* and '*Bangia*' sp. ESS1.

In higher plants, NRT2 is generally encoded by multigene families, which every member carries its own specific function (Bouguyon et al., 2012, Plett et al., 2010, Zanin et al., 2015). In *A. thaliana* roots, expression of seven *NRT2* genes are

differently regulated by nitrate, where *AtNRT2.1/2.2* is nitrate-inducible, but other *NRT2* genes are nitrate-repressible or -insensitive (Orsel et al., 2006, Vidal et al., 2015). Since expression of the sole *NRT2* gene in red algae *P. yezoensis and* '*Bangia*' sp. ESS1 is insensitive to nitrate deficiency, suggesting the differences in the regulation of the *NRT2* gene expression between red algae and land plants. It is necessary to elucidate whether there is a relationship between these structural characteristics mentioned in the previous Chapter and insensitivity of the gene expression to nitrogen deficiency of red algal NRT2s.

Expression of *BE1DUR3.1* and *BE1DUR3.2* is up-regulated when '*Bangia*' sp. ESS1 was exposed to nitrogen-deficient conditions (Figure 28). In *P. yezoensis,* ubiquitously expressed *PyDUR3.1* and the gametophyte-specific *PyDUR3.2* also represented nitrogen starvation-inducible expression (Kakinuma et al., 2008, 2015). These findings suggest that DUR3s play essential roles in the uptake of urea as a nitrogen source under nitrogen-deficient conditions in both *Pyropia* and *Bangia* species. In the present study, an ortholog of *PyDUR3.3* showing sporophyte-specific expression in *P. yezoensis* was not identified because of the lack of gene information from sporophytes of '*Bangia*' sp. ESS1. Thus, identification and expression analyses of the *PyDUR3.3* ortholog in '*Bangia*' sp. ESS1 are necessary to elucidation of mechanisms involving regulation of *DUR3* genes under nitrogen deficiency-inducibility in Bangiales.

Taken together, '*Bangia*' sp. ESS1 can response to the nitrogen deficient stress by modulation of expression of nitrate transporter genes as found in the other red

seaweed *P. yezoensis*. Since kinetics of expression patterns of these nitrogen transporter genes is basically similar between orthologs from '*Bangia*' sp. ESS1 and *P. yezoensis*, nitrogen-dependent regulatory mechanisms of gene expression are proposed to be conserved between these two species belonging to different genus of red algae. Therefore, it is highly important to identify *cis*-acting promoter elements and *trans*-acting transcription factors involved in nitrogen-dependent gene expression in red seaweeds, which improves the understanding about stress-dependent gene expression systems in Bangiales.

Chapter 5

General discussion

Absorption of inorganic and organic nitrogen compounds, like ammonium-nitrogen, nitrate-nitrogen and urea-nitrogen, into cells from environments are essential for growth and development in photosynthetic eukaryotes including plants and algae (He et al., 2008, Kant et al., 2010, Verkroost and Wassen, 2005, Wang et al., 2014, Xu et al., 2012). It has been established that ammonium, nitrate and urea are transported through AMT, NRT and DUR3, respectively, in terrestrial plants (Kojima et al., 2007, Loque et al., 2006, Okamoto et al., 2006); however, knowledge about these transporters is not so much accumulated in seaweeds to date. Accordingly, the present study focused on identification, structural characterization and phylogenetic and nitrogen deficiency-inducible gene expression analyses of the *AMT*, *NRT2* and *DUR3* genes in *P. yezoensis* and '*Bangia*' sp. ESS1.

In brief, we first performed identification and phylogenetic and expression analyses of multiple *AMT* gene family members in *P. yezoensis*. It was found that algal NH_4^+ transporters are divided into the AMT1 and Rh subfamilies. The AMT1 subfamily of *P. yezoensis* consists of three groups containing genes whose expression patterns differ temporally and nitrogen deficiency-dependently during the life cycle, providing novel information about red algal NH_4^+ transporters.

We also performed identification and phylogenetic classification of nitrogen transporters in the *Bangia* species. The *Bangia* material previously called *B.*

fuscopurpurea was classified into the '*Bangia*' 2 group and designated '*Bangia*' sp. ESS1. This species has a gene family of AMT consisting of five AMT1s diversified into three independent phylogenetic groups with corresponding AMT1s from other red algae and one Rh. In addition, '*Bangia*' sp. ESS1 has only single copy gene of NRT2 as other red algae and a gene family of DUR3.

Finally, identification of suitable reference genes and gene expression analysis of nitrogen transporter genes under nitrogen-deficient conditions were performed in the *Bangia* species in comparison with those in *P. yezoensis*. The results showed that the *60S rRNA* and *actin* genes were most suitable for gene expression analyses in response to nutrient deficiency, high salinity, and temperature stress, whereas normalization of desiccation-inducible expression required use of the *EF1* and *tubulin* genes. Similar with the expression patterns of *AMT1*s genes from *Pyropia, AMT1*s genes from *Bangia* also displayed nitrogen deficient-inducible expression pattern, suggesting the highly conservation of nitrogen deficiency-inducibility in the AMT1 families of two genera. However, the expression of *Rh* genes was not observed in both *Pyropia* and *Bangia*. Unlike nitrogen deficiency-inducible expression of NRTs in land plants, expression of the sole *NRT2* gene in red algae *P. yezoensis and* '*Bangia*' sp. ESS1 is insensitive to nitrate deficiency, suggesting the differences in the regulation of the *NRT2* gene expression between red algae and land plants. Since expression of *DUR3*s is up-regulated when '*Bangia*' sp. ESS1 was exposed to nitrogen-deficient conditions as observed in *P. yezoensis*, DUR3s might play essential roles in the uptake of urea under nitrogen-deficient conditions in Bangiales.

These above findings provide the novel findings about nitrogen receptors in Bangiales. As the next step, therefore, it is important to address functional significance of divergence of the *AMT1* and *DUR3* gene families and the presence of the *Rh* gene to understand the biological meaning of these structural and gene expression characteristics elucidated in the present study. However, functional analysis of genes is currently impossible because of the lack of reverse-genetic experimental systems for disruption or artificially activation of desired genes in seaweeds (Mikami, 2014, Mikami, 2018), although it is possible to perform confirmation of their transporting activities using heterologous expression systems like yeast and *Xenopus* oocytes at present. Therefore, study in near future should be focused on the establishment of reverse-genetic experimental systems to elucidate the biological significance of the nitrogen deficiency-dependent expression of nitrate transporter genes during the life cycle in *P. yezoensis* and '*Bangia*' sp. ESS1. These studies could provide important knowledge useful for taking measures to recover the reduced productivity caused by discoloration in seaweed mariculture.

Acknowledgments

I would like to give my deepest gratitude to my academic supervisor Dr. Koji Mikami, Faculty of Fisheries Sciences, Hokkaido University, for his scholastic guidance, advice and support for this study and really appreciated his great efforts and helpful comments in scrutinizing reviewing this thesis. I do my great pleasure to express my special thanks and gratitude to Drs. Hideki Kishimura, Masashi Hosokawa and Akira Inoue, Faculty of Fisheries Sciences, Hokkaido University, for their valuable advices and constructive criticism to improve this thesis. I express my gratitude to all the members of graduated and undergraduate students in Dr. Mikami's laboratory from 2015 to 2019 for their constant spiritual and technical support throughout my whole PhD study. In addition, I sincerely acknowledge the Japan Ministry of Education, Culture, Sports, Science and Technology (MEXT) and China Scholarship Council (CSC) for providing me the scholarship.

I also want to extend my deepest sense of gratitude to my beloved parents, my parents-in-law, my elder brother's family for their encouragement, continuous support. Especially, I want to thank my husband Hongdi Wang for his support during staining in Japan and dedicate this work to all my families.

Reference

Adams, E., Mikami, K. & Shin, R. 2017. Selection and functional analysis of a *Pyropia yezoensis* ammonium transporter PyAMT1 in potassium deficiency. *Journal of Applied Phycology* 29:2617-26.

Aguera, E., Cabello, P. & Haba, P. 2010. Induction of leaf senescence by low nitrogen nutrition in sunflower (*Helianthus annuus*) plants. *Physiologia Plantarum* 138:256-67.

Amano, H. & Noda, H. 1987. Effect of nitrogenous fertilizers on the recovery of discoloured fronds of *Porphyra yezoensis*. *Botanica Marina* 30:467-73.

Amarasinghe, B. H. R. R., Bruxelles, G. L. d., Braddon, M., Onyeocha, I., Forde, B. G. & Udvardi, M. K. 1998. Regulation of GmNRT2 expression and nitrate transport activity in roots of soybean (*Glycine max*). *Planta* 206:44-52.

Andersen, C. L., Jensen, J. L. & Orntoft, T. F. 2004. Normalization of real-time quantitative reverse transcription-PCR data: a model-based variance estimation approach to identify genes suited for normalization, applied to bladder and colon cancer data sets. *Cancer Research* 64:5245-50.

Bai, H., Euring, D., Volmer, K., Janz, D. & Polle, A. 2013. The Nitrate transporter (NRT) gene family in poplar. *Plos One* 8.

Bhattacharya, D., Wu, X., Huang, A., Xu, M., Wang, C., Jia, Z., Wang, G. & Niu, J. 2013. Variation of expression levels of seven housekeeping genes at different life-history stages in *Porphyra yezoensis*. *Plos One* 8.

Bouguyon, E., Gojon, A. & Nacry, P. 2012. Nitrate sensing and signaling in plants.

Seminars in Cell & Developmental Biology 23:648-54.

Brawley, S. H., Blouin, N. A., Ficko-Blean, E., Wheeler, G. L., Lohr, M., Goodson, H. V., Jenkins, J. W., Blaby-Haas, C. E., Helliwell, K. E., Chan, C. X., Marriage, T. N., Bhattacharya, D., Klein, A. S., Badis, Y., Brodie, J., Cao, Y. Y., Collen, J., Dittami, S. M., Gachon, C. M. M., Green, B. R., Karpowicz, S. J., Kim, J. W., Kudahl, U. J., Lin, S. J., Michel, G., Mittag, M., Olson, B. J. S. C., Pangilinan, J. L., Peng, Y., Qiu, H., Shu, S. Q., Singer, J. T., Smith, A. G., Sprecher, B. N., Wagner, V., Wang, W. F., Wang, Z. Y., Yan, J. Y., Yarish, C., Zauner-Riek, S., Zhuang, Y. Y., Zou, Y., Lindquist, E. A., Grimwood, J., Barry, K. W., Rokhsar, D. S., Schmutz, J., Stiller, J. W., Grossman, A. R. & Prochnik, S. E. 2017. Insights into the red algae and eukaryotic evolution from the genome of *Porphyra umbilicalis* (Bangiophyceae, Rhodophyta). *PNAS* 114: 6361-E70.

Broom, J. E., Farr, T. J. & Nelson, W. A. 2004. Phylogeny of the Bangia flora of New Zealand suggests a southern origin for *Porphyra* and *Bangia* (Bangiales, Rhodophyta). *Molecular Phylogenetics & Evolution* 31:1197-207.

Cao, M., Bi, G., Mao, Y., Li, G. & Kong, F. 2018. The first plastid genome of a filamentous taxon '*Bangia*' sp. OUCPT-01 in the Bangiales. *Scientific Reports* 8.

Cao, M., Wang, D., Mao, Y., Kong, F., Bi, G., Xing, Q. & Weng, Z. 2017a. Integrating transcriptomics and metabolomics to characterize the regulation of EPA biosynthesis in response to cold stress in seaweed *Bangia fuscopurpurea*. *Plos One* 12: e0186986.

Cao, T. J., Huang, X. Q., Qu, Y. Y., Zhuang, Z., Deng, Y. Y. & Lu, S. 2017b. Cloning and functional characterization of a lycopene beta-cyclase from macrophytic red alga *Bangia fuscopurpurea*. *Marine Drugs* 15.

Chen, C., Xie, T., Ye, S., Jensen, A. B. & Eilenberg, J. 2016. Selection of reference genes for expression analysis in the entomophthoralean fungus *Pandora neoaphidis*. *Brazilian Journal of Microbiology* 47:259-65.

Couturier, J., Montanini, B., Martin, F., Brun, A., Blaudez, D. & Chalot, M. 2007. The expanded family of ammonium transporters in the perennial poplar plant. *New Phytologist* 174:137-50.

Coyne, K. J. 2010. Nitrate reductase (Nr1) sequence and expression in the harmful alga *Heterosigma Akashiwo* (Raphidophyceae). *Journal of Phycology* 46:135-42.

Czechowski, T. 2005. Genome-wide identification and testing of superior reference genes for transcript normalization in *Arabidopsis*. *Plant Physiology* 139:5-17.

D'Apuzzo, E. 2004. Characterization of three functional high-affinity ammonium transporters in lotus japonicus with differential transcriptional regulation and spatial expression. *Plant Physiology* 134:1763-74.

De Michele, R., Loque, D., Lalonde, S. & Frommer, W. B. 2012. Ammonium and urea transporter inventory of the *Selaginella* and *Physcomitrella* genomes. *Frontiers in Plant Science* 3:62.

Diaz, C., Lemaitre, T., Christ, A., Azzopardi, M., Kato, Y., Sato, F., Morot-Gaudry, J. F., Le Dily, F. & Masclaux-Daubresse, C. 2008. Nitrogen recycling and remobilization are differentially controlled by leaf senescence and development

stage in *Arabidopsis* under low nitrogen nutrition. *Plant Physiology* 147:1437-49.

Ding, Y., Sun, H., Zhang, R., Yang, Q., Liu, Y., Zang, X. & Zhang, X. 2014. Selection of reference gene from *Gracilaria lemaneiformis* under temperature stress. *Journal of Applied Phycology* 27:1365-72.

Dong, M., Zhang, X., Chi, X., Mou, S., Xu, J., Xu, D., Wang, W. & Ye, N. 2012. The validity of a reference gene is highly dependent on the experimental conditions in green alga *Ulva linza*. *Current Genetics* 58:13-20.

Edward, H. & Richard, M. A. 2001. Nutrients mobilized from leaves of *Arabidopsis thaliana* during leaf senescence. *Journal of Plant Physiology* 158:1317-23.

Fischer, B. B., Krieger-Liszkay, A., Hideg, E., Snyrychova, I., Wiesendanger, M. & Eggen, R. I. 2007. Role of singlet oxygen in chloroplast to nucleus retrograde signaling in *Chlamydomonas reinhardtii*. *FEBS Letters* 581:5555-60.

Gao, D., Kong, F., Sun, P., Bi, G. & Mao, Y. 2018. Transcriptome-wide identification of optimal reference genes for expression analysis of *Pyropia yezoensis* responses to abiotic stress. *BMC Genomics* 19:251.

Gao, G., Gao, Q., Bao, M., Xu, J. & Li, X. 2019. Nitrogen availability modulates the effects of ocean acidification on biomass yield and food quality of a marine crop *Pyropia yezoensis*. *Food Chemistry* 271:623-29.

Gazzarrini, S., Lejay, L., Gojon, A., Ninnemann, O., Frommer, W. B. & Wiréna, N. v. 1999. Three functional transporters for constitutive, diurnally regulated, and starvation-induced uptake of ammonium into *Arabidopsis* roots. *The Plant Cell*

11:937-47.

Giehl, R. F. H., Laginha, A. M., Duan, F., Rentsch, D., Yuan, L. & von Wiren, N. 2017. A critical role of AMT2;1 in root-to-shoot translocation of ammonium in *Arabidopsis*. *Molecular Plant* 10:1449-60.

Gonza´lez-Ballester, D., Camargo, A. & Ferna´ndez, E. 2005. Ammonium transporter genes in *Chlamydomonas*: the nitrate-specific regulatory gene Nit2 is involved in Amt1;1 expression. *Plant Molecular Biology* 56:863-78.

Gregersen, P. L., Holm, P. B. & Krupinska, K. 2008. Leaf senescence and nutrient remobilisation in barley and wheat. *Plant Biology* 1:37-49.

Guo, R. & Ki, J.-S. 2012. Evaluation and validation of internal control genes for studying gene expression in the dinoflagellate *Prorocentrum minimum* using real-time PCR. *European Journal of Protistology* 48:199-206.

He, P., Xu, S., Zhang, H., Wen, S., Dai, Y., Lin, S. & Yarish, C. 2008. Bioremediation efficiency in the removal of dissolved inorganic nutrients by the red seaweed, *Porphyra yezoensis*, cultivated in the open sea. *Water Research* 42:1281-89.

Hildebrand, M. 2005. Cloning and functional characterization of ammonium transporters from the marine diatom *Cylindrotheca fusiformis* (Bacillariophyceae). *Journal of Phycology* 41:105-13.

Hirata, R., Takahashi, M., Saga, N. & Mikami, K. 2011. Transient gene expression system established in *Porphyra yezoensis* is widely applicable in Bangiophycean algae. *Marine Biotechnology (NY)* 13:1038-47.

Huang, C. H. & Peng, J. 2005. Evolutionary conservation and diversification of Rh

family genes and proteins. *PNAS* 102:15512-17.

Hurd, C., Harrison, P. J., Bischof, K. & Lobban, C. S. 2014. *Seaweed Ecology and Physiology.* Cambridge University Press.

Imamura, S., Terashita, M., Ohnuma, M., Maruyama, S., Minoda, A., Weber, A. P. M., Inouye, T., Sekine, Y., Fujita, Y., Omata, T. & Tanaka, K. 2010. Nitrate assimilatory genes and their transcriptional regulation in a unicellular red alga *Cyanidioschyzon merolae*: genetic evidence for nitrite reduction by a sulfite reductase-like enzyme. *Plant and Cell Physiology* 51:707-17.

Kakinuma, M., Coury, D. A., Nakamoto, C., Sakaguchi, K. & Amano, H. 2008. Molecular analysis of physiological responses to changes in nitrogen in a marine macroalga, *Porphyra yezoensis* (Rhodophyta). *Cell Biology and Toxicology* 24:629-39.

Kakinuma, M., Suzuki, K., Iwata, S., Coury, D. A., Iwade, S. & Mikami, K. 2015. Isolation and characterization of a new DUR3-like gene, *PyDUR3.3*, from the marine macroalga *Pyropia yezoensis* (Rhodophyta). *Fisheries Science* 82:171-84.

Kakinuma, M., Nakamoto, C., Kishi, K., Coury, D. A. & Amano, H. 2017. Isolation and functional characterization of an ammonium transporter gene, *PyAMT1*, related to nitrogen assimilation in the marine macroalga *Pyropia yezoensis* (Rhodophyta). *Marine Environmental Research* 128:76-87.

Kant, S., Bi, Y. M. & Rothstein, S. J. 2010. Understanding plant response to nitrogen limitation for the improvement of crop nitrogen use efficiency. *Journal of*

Experimental Botany 62:1499-509.

Karsten, U. & West, J. A. 2000. Living in the intertidal zone - seasonal effects on heterosides and sun-screen compounds in the red alga *Bangia atropurpurea* (Bangiales). *Journal of Experimental Marine Biology and Ecology* 254:221-34.

Kianianmomeni, A. & Hallmann, A. 2013. Validation of reference genes for quantitative gene expression studies in *Volvox carteri* using real-time RT-PCR. *Molecular Biology Reports* 40:6691-9.

Kiba, T., Feria-Bourrellier, A. B., Lafouge, F., Lezhneva, L., Boutet-Mercey, S., Orsel, M., Brehaut, V., Miller, A., Daniel-Vedele, F., Sakakibara, H. & Krapp, A. 2012. The *Arabidopsis* nitrate transporter *NRT2.4* plays a double role in roots and shoots of nitrogen-starved plants. *The Plant Cell* 24:245-58.

Kim, J. K., Kraemer, G. P., Neefus, C. D., Chung, I. K. & Yarish, C. 2007. Effects of temperature and ammonium on growth, pigment production and nitrogen uptake by four species of *Porphyra* (Bangiales, Rhodophyta) native to the New England coast. *Journal of Applied Phycology* 19:431-40.

Kishimoto, I., Ariga, I., Itabashi, Y. & Mikami, K. 2019. Heat-stress memory is responsible for acquired thermotolerance in *Bangia fuscopurpurea*. *Journal of Phycology*, DOI: 10.1111/jpy.12895

Kojima, S., Bohner, A., Gassert, B., Yuan, L. & von Wiren, N. 2007. AtDUR3 represents the major transporter for high-affinity urea transport across the plasma membrane of nitrogen-deficient *Arabidopsis* roots. *The Plant Journal* 52:30-40.

Kong, F., Cao, M., Sun, P., Liu, W. & Mao, Y. 2014. Selection of reference genes for gene expression normalization in *Pyropia yezoensis* using quantitative real-time PCR. *Journal of Applied Phycology* 27:1003-10.

Kothe, E., Cusick, K. D., Fitzgerald, L. A., Pirlo, R. K., Cockrell, A. L., Petersen, E. R. & Biffinger, J. C. 2014. Selection and evaluation of reference genes for expression studies with quantitative PCR in the model fungus neurospora crassa under different environmental conditions in continuous culture. *Plos One* 9.

Krapp, A., David, L. C., Chardin, C., Girin, T., Marmagne, A., Leprince, A. S., Chaillou, S., Ferrario-Mery, S., Meyer, C. & Daniel-Vedele, F. 2014. Nitrate transport and signalling in *Arabidopsis*. *Journal of Experimental Botany* 65:789-98.

Krouk, G., Crawford, N. M., Coruzzi, G. M. & Tsay, Y.-F. 2010. Nitrate signaling: adaptation to fluctuating environments. *Current Opinion in Plant Biology* 13:265-72.

Le Bail, A., Dittami, S. M., de Franco, P. O., Rousvoal, S., Cock, M. J., Tonon, T. & Charrier, B. 2008. Normalisation genes for expression analyses in the brown alga model *Ectocarpus siliculosus*. *BMC Molecular Biology* 9:75.

Li, C., Kong, F., Sun, P., Bi, G., Li, N., Mao, Y. & Sun, M. 2018. Genome-wide identification and expression pattern analysis under abiotic stress of mitogen-activated protein kinase genes in *Pyropia yezoensis*. *Journal of Applied Phycology* 30:2561-72.

Li, C., Tang, Z., Wei, J., Qu, H., Xie, Y. & Xu, G. 2016. The *OsAMT1.1* gene functions in ammonium uptake and ammonium-potassium homeostasis over low and high

ammonium concentration ranges. *Journal of Genetics and Genomics* 43:639-49.

Li, T., Liao, K., Xu, X., Gao, Y., Wang, Z., Zhu, X., Jia, B. & Xuan, Y. 2017. Wheat ammonium transporter (AMT) gene family: diversity and possible role in host-pathogen interaction with stem rust. *Frontiers in Plant Science* 8.

Liu, C., Wu, G., Huang, X., Liu, S. & Cong, B. 2012. Validation of housekeeping genes for gene expression studies in an ice alga *Chlamydomonas* during freezing acclimation. *Extremophiles* 16:419-25.

Liu, G. W., Sun, A. L., Li, D. Q., Athman, A., Gilliham, M. & Liu, L. H. 2014. Molecular identification and functional analysis of a maize (*Zea mays*) DUR3 homolog that transports urea with high affinity. *Planta* 241:861-74.

Liu, L. H., Ludewig, U., Frommer, W. B. & von Wiren, N. 2003. AtDUR3 encodes a new type of high-affinity urea/H^+ symporter in *Arabidopsis*. *Plant Cell* 15:790-800.

Llanos, A., Francois, J. M. & Parrou, J. L. 2015. Tracking the best reference genes for RT-qPCR data normalization in filamentous fungi. *BMC Genomics* 16:71.

Loque, D., Yuan, L., Kojima, S., Gojon, A., Wirth, J., Gazzarrini, S., Ishiyama, K., Takahashi, H. & von Wiren, N. 2006. Additive contribution of AMT1;1 and AMT1;3 to high-affinity ammonium uptake across the plasma membrane of nitrogen-deficient *Arabidopsis* roots. *The Plant Journal* 48:522-34.

Ludewig, U., Neuhauser, B. & Dynowski, M. 2007. Molecular mechanisms of ammonium transport and accumulation in plants. *FEBS Letters* 581:2301-8.

Luo, Q., Zhu, Z., Zhu, Z., Yang, R., Qian, F., Chen, H. & Yan, X. 2014. Different

responses to heat shock stress revealed heteromorphic adaptation strategy of *Pyropia haitanensis* (Bangiales, Rhodophyta). *Plos One* 9:e94354.

Marini, A.-M., Urrestarazu, A., Beauwens, R. & André, B. 1997. The Rh (Rhesus) blood group polypeptides are related to NH_4^+ transporters. *Trends in Biochemical Sciences* 22:460-61.

Meng, S., Peng, J. S., He, Y. N., Zhang, G. B., Yi, H. Y., Fu, Y. L. & Gong, J. M. 2016. *Arabidopsis* NRT1.5 mediates the suppression of nitrate starvation-induced leaf senescence by modulating foliar potassium level. *Molecular Plant* 9:461-70.

Merchant, S. S., Prochnik, S. E., Vallon, O., Harris, E. H., Karpowicz, S. J., Witman, G. B., et al. 2007. The *Chlamydomonas* genome reveals the evolution of key animal and plant functions. *Science* 318:245-51.

Mikami, K. 2014. A technical breakthrough close at hand: feasible approaches toward establishing a gene-targeting genetic transformation system in seaweeds. *Frontiers in Plant Science* 5:498.

Mikami, K. 2018. Recent developments in nuclear reverse-genetic manipulation that advance seaweed biology in the genomic era. *Journal of Aquatic Research and Marine Sciences* 1:1-4.

Mikami, K. & Kishimoto, I. 2018. Temperature promoting the asexual life cycle program in *Bangia fuscopurpurea* (Bangiales, Rhodophyta) from Esashi in the Hokkaido island, Japan. *Algal Resources* 11:25-32.

Mikami, K., Li, C., Irie, R. & Hama, Y. 2019. A unique life cycle transition in the red seaweed *Pyropia yezoensis* depends on apospory. *Communications Biology* 2:

299, DOI: 10.1038/s42003-019-0549-5

Mou, S. L., Zhang, X. W., Miao, J. L., Zheng, Z., Xu, D. & Ye, N. H. 2015. Reference genes for gene expression normalization in *Chlamydomonas* sp ICE-L by quantitative real-time RT-PCR. *Journal of Plant Biochemistry and Biotechnology* 24:276-82.

Nakhoul, N. L. & Hamm, L. L. 2004. Non-erythroid Rh glycoproteins: a putative new family of mammalian ammonium transporters. *Pflugers Archiv-European Journal of Physiology* 447:807-12.

Nicolaus von Wirén, Sonia Gazzarrini, Alain Gojon & Frommer, W. B. 2000. The molecular physiology of ammonium uptake and retrieval. *Current Opinion in Plant Biology 2000* 3:254-61.

Notoya, M. & Iijima, N. 2003. Life history and sexuality of archeospore and apogamy of *Bangia atropurpurea* (Roth) Lyngbye (Bangiales, Rhodophyta) from Fukaura and Enoshima, Japan. *Fisheries Science* 69:779-805.

O'Brien, J. A., Vega, A., Bouguyon, E., Krouk, G., Gojon, A., Coruzzi, G. & Gutierrez, R. A. 2016. Nitrate transport, sensing, and responses in plants. *Molecular Plant* 9:837-56.

Ohnishi, M., Kikuchi, N., Iwasaki, T., Kawaguchi, R. & Shimada, S. 2013. Population genomic structures of endangered species (CR+EN), *Pyropia tenera* (Bangiales, Rhodophyta). *The Japanese Journal of Phycology (Sôrui)* 61:87-96.

Okamoto, M., Kumar, A., Li, W., Wang, Y., Siddiqi, M. Y., Crawford, N. M. & Glass, A. D. 2006. High-affinity nitrate transport in roots of *Arabidopsis* depends on

expression of the NAR2-like gene AtNRT3.1. *Plant Physiology* 140:1036-46.

Okumoto, S. & Versaw, W. 2017. Genetically encoded sensors for monitoring the transport and concentration of nitrogen-containing and phosphorus-containing molecules in plants. *Current Opinion in Plant Biology* 39:129-35.

Orsel, M., Chopin, F., Leleu, O., Smith, S. J., Krapp, A., Daniel-Vedele, F. & Miller, A. J. 2006. Characterization of a two-component high-affinity nitrate uptake system in *Arabidopsis*. Physiology and protein-protein interaction. *Plant Physiology* 142:1304-17.

Pabuayon, I. M., Yamamoto, N., Trinidad, J. L., Longkumer, T., Raorane, M. L. & Kohli, A. 2016. Reference genes for accurate gene expression analyses across different tissues, developmental stages and genotypes in rice for drought tolerance. *Rice* 9:32.

Panina, Y., Germond, A., Masui, S. & Watanabe, T. M. 2018. Validation of common housekeeping genes as reference for qPCR gene expression analysis during iPS reprogramming process. *Scientific Reports* 8: 8716, DOI: 10.1038/s41598-018-26707-8.

Pao, S. S., Paulsen, I. T. & Saier, M. H. 1998. Major facilitator superfamily. *Microbiology and Molecular Biology Reviews* 62:1-34.

Peng, J. & Huang, C. H. 2006. Rh proteins vs Amt proteins: an organismal and phylogenetic perspective on CO_2 and NH_3 gas channels. *Transfusion Clinique et Biologique* 13:85-94.

Pinton, R., Tomasi, N. & Zanin, L. 2015. Molecular and physiological interactions of

urea and nitrate uptake in plants. *Plant Signaling & Behavior* 11.

Plett, D., Toubia, J., Garnett, T., Tester, M., Kaiser, B. N. & Baumann, U. 2010. Dichotomy in the NRT gene families of dicots and grass species. *Plos One* 5:e15289.

Prochnik, S. E., Umen, J., Nedelcu, A. M., Hallmann, A., Miller, S. M., Nishii, I., Ferris, et al. 2010. Genomic analysis of organismal complexity in the multicellular green alga *Volvox carteri*. *Science* 329:223-26.

Sakaguchi, K., Ochiai, N., Park, C. S., Kakinuma, M. & Amano, H. 2002. Evaluation of discoloration in harvested laver *Porphyra yezoensis* and recovery after treatment with ammonium sulfate enriched seawater. *Nippon Suisan Gakkaishi* 69:399-404.

Schonknecht, G., Chen, W. H., Ternes, C. M., Barbier, G. G., Shrestha, R. P., Stanke, M., Brautigam, A., Baker, B. J., Banfield, J. F., Garavito, R. M., Carr, K., Wilkerson, C., Rensing, S. A., Gagneul, D., Dickenson, N. E., Oesterhelt, C., Lercher, M. J. & Weber, A. P. 2013. Gene transfer from bacteria and archaea facilitated evolution of an extremophilic eukaryote. *Science* 339:1207-10.

Siaut, M., Heijde, M., Mangogna, M., Montsant, A., Coesel, S., Allen, A., Manfredonia, A., Falciatore, A. & Bowler, C. 2007. Molecular toolbox for studying diatom biology in *Phaeodactylum tricornutum*. *Gene* 406:23-35.

Soupene, E., Chu, T., Corbin, R. W., Hunt, D. F. & Kustu, S. 2002a. Gas channels for NH_3: proteins from hyperthermophiles complement an *Escherichia coli* mutant. *Journal of Bacteriology* 184:3396-400.

Soupene, E., Inwood, W. & Kustu, S. 2004. Lack of the Rhesus protein Rh1 impairs growth of the green alga *Chlamydomonas reinhardtii* at high CO_2. *PNAS* 101:7787-92.

Soupene, E., King, N., Feild, E., Liu, P., Niyogi, K. K., Huang, C. H. & Kustu, S. 2002b. Rhesus expression in a green alga is regulated by CO_2. *PNAS* 99:7769-73.

Sutherland, J. E., Lindstrom, S. C., Nelson, W. A., Brodie, J., Lynch, M. D. J., Hwang, M. S., Choi, H.-G., Miyata, M., Kikuchi, N., Oliveira, M. C., Farr, T., Neefus, C., Mols-Mortensen, A., Milstein, D. & Müller, K. M. 2011. A new look at an ancient order: generic revision of the Bangiales (Rhodophyta). *Journal of Phycology* 47:1131-51.

Suzuki, A. & Knaff, D. B. 2005. Glutamate synthase: structural, mechanistic and regulatory properties, and role in the amino acid metabolism. *Photosynthesis Research* 83:191-217.

Takahashi, M. & Mikami, K. 2017. Oxidative stress promotes asexual reproduction and apogamy in the red seaweed *Pyropia yezoensis*. *Frontiers in Plant Science* 8:62.

Takahashi, M., Saga, N. & Mikami, K. 2010. Photosynthesis-dependent extracellular Ca_2^+ influx triggers an asexual reproductive cycle in the marine red macroalga *Porphyra yezoensis*. *American Journal of Plant Sciences* 1:1-11.

Tenea, G. N., Peres Bota, A., Cordeiro Raposo, F. & Maquet, A. 2011. Reference genes for gene expression studies in wheat flag leaves grown under different farming conditions. *BMC Research Notes* 4:373.

Thompson, R. C., Norton, T. A. & Hawkins, S. J. 2004. Physical stress and biological

control regulate the producer-consumer balance in intertidal biofilms. *Ecology* 85:1372-82.

Tsay, Y. F., Chiu, C. C., Tsai, C. B., Ho, C. H. & Hsu, P. K. 2007. Nitrate transporters and peptide transporters. *FEBS Letters* 581:2290-300.

Uji, T., Hirata, R., Mikami, K., Mizuta, H. & Saga, N. 2012. Molecular characterization and expression analysis of sodium pump genes in the marine red alga *Porphyra yezoensis*. *Molecular Biology Reports* 39:7973-80.

Vandesompele, J., De Preter, K., Pattyn, F., Poppe, B., Van Roy, N., De Paepe, A. & Speleman, F. 2002. Accurate normalization of real-time quantitative RT-PCR data by geometric averaging of multiple internal control genes. *Genome Biology* 3:34.

Verkroost, A. W. M. & Wassen, M. J. 2005. A simple model for nitrogen-limited plant growth and nitrogen allocation. *Annals of Botany* 96:871-76.

Vidal, E. A., Alvarez, J. M., Moyano, T. C. & Gutierrez, R. A. 2015. Transcriptional networks in the nitrate response of *Arabidopsis thaliana*. *Current Opinion in Plant Biology* 27:125-32.

Wang, C., Fan, X., Wang, G., Niu, J. & Zhou, B. 2011. Differential expression of rubisco in sporophytes and gametophytes of some marine macroalgae. *Plos One* 6:e16351.

Wang, N. X., Huang, B., Xu, S., Wei, Z. B., Miao, A. J., Ji, R. & Yang, L. Y. 2014. Effects of nitrogen and phosphorus on arsenite accumulation, oxidation, and toxicity in *Chlamydomonas reinhardtii*. *Aquatic Toxicology* 157:167-74.

Wang, W., Köhler, B., Cao, F., Liu, G., Gong, Y., Sheng, S., Song, Q., Cheng, X., Garnett, T., Okamoto, M., Qin, R., Mueller-Roeber, B., Tester, M. & Liu, L.-H. 2012. Rice DUR3 mediates high-affinity urea transport and plays an effective role in improvement of urea acquisition and utilization when expressed in *Arabidopsis*. *New Phytologist* 193:432-44.

Wang, W., Köhler, B., Cao, F. & Liu, L. 2008a. Molecular and physiological aspects of urea transport in higher plants. *Plant Science* 175:467-77.

Wang, W., Zhu, J., Xu, P., Xu, J., Lin, X., Huang, C., Song, W., Peng, G. & Wang, G. 2008b. Characterization of the life history of *Bangia fuscopurpurea* (Bangiaceae, Rhodophyta) in connection with its cultivation in China. *Aquaculture* 278:101-09.

Witte, C. P. 2011. Urea metabolism in plants. *Plant Science* 180:431-8.

Wittgenstein, N. J. v., Le, C. H., Hawkins, B. J. & Ehlting, J. r. 2014. Evolutionary classification of ammonium, nitrate, and peptide transporters in land plants. *BMC Evolutionary Biology* 14:1-17.

Xu, G., Fan, X. & Miller, A. J. 2012. Plant nitrogen assimilation and use efficiency. *Annual Review of Plant Biology* 63:153-82.

Yokono, M., Uchida, H., Suzawa, Y., Akiomoto, S. & Murakami, A. 2012. Stabilization and modulation of the phycobilisome by calcium in the calciphilic freshwater red alga *Bangia atropurpurea*. *Biochimica et Biophysica Acta* 1817:306-11.

Yuan, L., Graff, L., Loqué, D., Kojima, S., Tsuchiya, Y. N., Takahashi, H. & von Wirén, N. 2009. AtAMT1;4, a pollen-specific high-affinity ammonium transporter of

the plasma membrane in *Arabidopsis*. *Plant and Cell Physiology* 50:13-25.

Yuan, L., Loque, D., Kojima, S., Rauch, S., Ishiyama, K., Inoue, E., Takahashi, H. & von Wiren, N. 2007. The organization of high-affinity ammonium uptake in *Arabidopsis* roots depends on the spatial arrangement and biochemical properties of AMT1-type transporters. *The Plant Cell Online* 19:2636-52.

Zanin, L., Zamboni, A., Monte, R., Tomasi, N., Varanini, Z., Cesco, S. & Pinton, R. 2015. Transcriptomic analysis highlights reciprocal interactions of urea and nitrate for nitrogen acquisition by Maize roots. *Plant and Cell Physiology* 56:532-48.

Zhang, F., Liu, Y., Wang, L., Bai, P., Ruan, L., Zhang, C., Wei, K. & Cheng, H. 2018. Molecular cloning and expression analysis of ammonium transporters in tea plants (*Camellia sinensis* (L.) O. Kuntze) under different nitrogen treatments. *Gene* 658:136-45.

Zheng, L., Kostrewa, D., Berneche, S., Winkler, F. K. & Li, X. D. 2004. The mechanism of ammonia transport based on the crystal structure of AmtB of *Escherichia coli*. *PNAS* 101:17090-95.

Zou, D. & Gao, K. 2002. Effects of desiccation and CO_2 concentrations on emersed photosynthesis in *Porphyra haitanensis* (Bangiales, Rhodophyta), a species farmed in China. *European Journal of Phycology* 37:587-92.

Figure legends

Figure 1. Schematic representation of the nitrogen assimilation pathway in algae.

AMT, ammonium transporter; NRT, nitrate transporter; DUR, urea transporter; NR, nitrate reductase; NiR, nitrite transporter; GS, glutamine synthase; 2-OG, 2-oxoglutarate; GOGAT, glutamin:2-OG aminotransferase; Gln, glutamine; Glu, glutamic acid.

Figure 2. Multiple amino acid sequence alignment of AMTs in *Pyropia yezoensis*.

Amino acid residues conserved in all seven proteins, in six proteins and in five proteins are highlighted by black (with white characters), purple and blue backgrounds, respectively. The boxes indicate the Phe-Gly-Phe (Tyr/Asn) triplet conserved in AMTs, as well as and phenylalanine and histidine residues corresponding to residues involved in NH_4^+ binding and transport in *Escherichia coli* EcAmtB. The amino acid numbers are indicated on the right.

Figure 3. Localization of transmembrane helices in AMT candidates in *Pyropia yezoensis*.

TMs are indicated by red lines with black numbers. Amino acid residues conserved in all six proteins, in five proteins and in four or three proteins are highlighted by black (with white characters), purple and blue backgrounds, respectively.

Figure 4. Localization of transmembrane helices in algal Rh proteins.

Rh proteins from *Pyropia yezoensis* and *Chlamydomonas reinhardtii* were compared. TMs are indicated by red lines with black numbers. Amino acid residues conserved in all four proteins, in three proteins and in three or two proteins are highlighted by black (with white characters), purple and blue backgrounds, respectively.

Figure 5. Three-dimensional structures of AMT domain-containing proteins.

Templates c5aexB and c5aezA indicate three-dimensional structures of AMTs (MEP2s) from *Saccharomyces cerevisiae* and *Candida albicans*, respectively, while c3hd6A represents a three-dimensional structure of the human Rh protein. The confidence values of all the prediction are 100%. “Cov” means the coverage percent of AMT domain-containing proteins to the corresponding templates.

Figure 6. Neighbor joining-based phylogenetic tree of AMTs from terrestrial plants and algae.

Boxes indicate AMTs and Rh from *Pyropia yezoensis*. The bootstrap values with 1000 replicates over 70% are indicated at the nodes of the tree. The DDBJ/EMBL/GenBank accession numbers of AMTs and Rhs used in the phylogenetic analysis are listed in Table 1.

Figure 7. Differences in temporal expression patterns of *PyAMTs* in the life cycle of *Pyropia yezoensis.*

The relative mRNA levels of *PyAMT1s* were normalized with the reference gene *18S rRNA*. Error bars indicate the standard deviation of triplicate experiments (n=3), and bars with different letters indicate significant differences at $P < 0.05$. G, gametophyte; C, conchosporophyte; S, sporophyte.

Figure 8. Artificial induction of and recovery from discoloration in *Pyropia yezoensis*. Gametophytes (left) and sporophytes (right) were treated with N-free (ESS_2-free) seawater for a week, and sampling was performed at 3, 5 and 7 days to observe discoloration. Control indicates samples cultured in ESS_2-enriched seawater. Discolored gametophyte and sporophytes produced in N-free seawater for 7 days were transferred into ESS2-less seawater supplied with 500 μM of NH_4Cl, $NaNO_3$, or urea and then cultured for an additional 7 days to examine the recovery from discoloration. Scale bars in left and right panels indicate 1 cm and 50 μm in gametophytes and 1 cm and 500 μm in sporophytes.

Figure 9. Changes in the contents of chlorophyll a, phycoerythrin and phycocyanin in discolored and recovered *Pyropia yezoensis*.
Culture conditions were identical to those in Figure 5. “C” means control samples. Error bars indicate the standard deviation of triplicate experiments (n=3), and different letters on bars indicate significant differences at $P < 0.05$.

Figure 10. Differences in nitrogen starvation-induced expression patterns among *PyAMT1* genes.

Samples of gametophytes, conchosporophytes, and sporophytes treated with ESS_2-free seawater were collected every day for 7 days to examine the expression of the *PyAMT1* genes by RT-qPCR. The relative mRNA levels were normalized with the reference gene *18S rRNA*. Error bars indicate the standard deviation of triplicate experiments (n=3), and bars with different letters indicate significant differences at $P < 0.05$. G, gametophyte; C, conchosporophyte; S, sporophyte. The numbers on the X axis indicate the duration of culture under nitrogen-deficient conditions (days).

Figure 11. Suppression of the nitrogen starvation-induced expression of *PyAMT1* genes via recovery with different nitrogen sources.

Sporophyte samples grown in ESS_2-less seawater for 7 days (ΔN) were treated with seawater containing 500 μM of NH_4Cl, $NaNO_3$, or urea for 3 days. Sporophytes cultured in nitrogen-supplied seawater were collected every day for 3 days, and the expression of *PyAMT1.2* and *PyAMT1.4* was examined by RT-qPCR (upper and lower, respectively). The relative mRNA levels were normalized with the reference gene *18S rRNA*. Error bars indicate the standard deviation of triplicate experiments (n=3), and bars with different letters indicate significant differences at $P < 0.05$. S, sporophytes cultured in ESS_2-containing seawater. The numbers on the X axis indicate the duration of culture under nitrogen-deficient conditions (days).

Figure 12. Phylogenetic classification of the *Bangia* species used in the study. Neighbor joining-based phylogenetic tree was reconstructed using sequences of *rbcL* genes from different specimens from the genus *Bangia*. DDBJ/EMBL/GenBank accession numbers of *rbcL* genes are listed in Table 5. The specimen used in this study is boxed. Bootstrap values over 50% from 1,000 replicates are indicated at nodes. Bar, 0.01 substitutions per site.

Figure 13. Neighbor joining-based phylogenetic tree of AMTs from '*Bangia*' sp. ESS1 with terrestrial plants and other algae.
Boxes indicate BE1AMTs and BE1Rh. The bootstrap values with 1,000 replicates over 70% are indicated at the nodes of the tree. The DDBJ/EMBL/GenBank accession numbers of AMTs and Rhs used in the phylogenetic analysis are listed in Table 1 and Table 6.

Figure 14. Neighbor joining-based phylogenetic tree of NRTs from '*Bangia*' sp. ESS1 with terrestrial plants and other algae.
Boxes indicate NRT2 of '*Bangia*' sp. ESS1. The bootstrap values with 1,000 replicates over 70% are indicated at the nodes of the tree. The DDBJ/EMBL/GenBank accession numbers of NRTs used in the phylogenetic analysis are listed in Table 7.

Figure 15. Neighbor joining-based phylogenetic tree of DUR3s from '*Bangia*' sp. ESS1 with terrestrial plants and other algae.

Boxes indicate DUR3 of '*Bangia*' sp. ESS1. The bootstrap values with 1,000 replicates over 60% are indicated at the nodes of the tree. The DDBJ/EMBL/GenBank accession numbers of DUR3s used in the phylogenetic analysis are listed in Table 8.

Figure 16. Conservation of AMT identity among five BE1AMT1s and BE1Rh. Amino acid sequences of AMT1 and Rh proteins from '*Bangia*' sp. ESS1 and PyAMT1 from *Pyropia yezoensis* are aligned. Amino acid residues conserved in all seven proteins, in six proteins and in five proteins are highlighted by black (with white characters), purple and blue backgrounds, respectively. The boxes indicate the Phe-Gly-Phe (Tyr/Asn) triplet conserved in AMTs, as well as and phenylalanine and histidine residues corresponding to residues involved in NH_4^+ binding and transport in *Escherichia coli* EcAmtB. The amino acid numbers are indicated on the right.

Figure 17. Localization of transmembrane helices in in PyAMT1 and BE1AMT1s. TMs are indicated by red lines with black numbers. Amino acid residues conserved in all six proteins, in five proteins and in four or three proteins are highlighted by black (with white characters), purple and blue backgrounds, respectively.

Figure 18. Three-dimensional structures of BE1AMTs and known AMTs. Templates c5aexB indicates three-dimensional structures of AMTs (MEP2s) from *Saccharomyces cerevisiae*, while c3hd6A represents a three-dimensional structure of the human rhesus protein (Rh). The confidence values of all the prediction are 100%. "Cov" means the

coverage percent of AMT domain-containing proteins to the corresponding templates.

Figure 19. Multiple amino acid alignment of PyNRT2, PouNRT2 and BE1NRT2. Amino acid residues conserved in all 3 proteins and in 2 proteins are highlighted by black (with white characters) and blue backgrounds, respectively. The lightly yellow shade box indicates the conserved consensus motif (AGWGNLG). The amino acid numbers are indicated on the right. Information of transmembrane (TM) helices in red algal NRT2s. TMs numbering was indicated by black numbers and red lines.

Figure 20. Three-dimensional structures of BE1NRT2s and known NRT2s. Templates d1pw4a indicates three-dimensional structures of *Escherichia coli* glycerol-3-phosphate transporter. The confidence value of the prediction is 100%. “Cov” means the coverage percent of NRT2 domain-containing proteins to the corresponding templates.

Figure 21. Multiple amino acid alignment of PyDUR3s, PouDUR3s and BE1DUR3s. Amino acid residues conserved in all eight proteins, in seven proteins and in six proteins are highlighted by black (with white characters), purple and blue backgrounds, respectively. The amino acid numbers are indicated on the right. TMs are indicated by red lines with black numbers.

Figure 22. Three-dimensional structures of BE1DUR3s and known DUR3s.

Templates c2xq2A indicates three-dimensional structures of sodium / glucose cotransporter. The confidence values of all the prediction are 100%. “Cov” means the coverage percent of DUR3 domain-containing proteins to the corresponding templates.

Figure 23. Cycle threshold (Ct) values of candidate reference genes across conditions tested.

Boxes show the median values (central lines), Q1 (lower outline), and Q3 (upper outline), and whiskers. The whiskers are set at 1.5 times interquartile range (IQR) above Q3 and 1.5 times IQR below Q1. Data were derived from 27 culture samples and repeated for 3 times.

Figure 24. Gene expression stability values (*M*) and ranking of six reference genes in all samples under different treatments calculated using geNorm software.

Average expression stability value (*M*) was calculated by stepwise exclusion of the least stable gene compared across different desiccation, nutrient deficiency, salinity, and temperature conditions, and the combination of all conditions (Total). In each plot, the least stable gene is on the left, and the most stable gene is on the right. Data were derived from 27 culture samples and repeated for 3 times.

Figure 25. Determination of the optimal number of reference genes for normalizing gene expression data.

Pairwise variation ($V_{n/n+1}$, where n represents number of genes) was analyzed between normalization factors (NFn and NFn+1) by geNorm software for all different conditions examined (desiccation, nutrient deficiency, salinity, temperature, and all these factors combined). The dotted line at 0.15 is a cutoff value, below which an additional reference gene is not needed. Data were derived from 27 culture samples and repeated for 3 times.

Figure 26. Gene expression patterns of *delta12-fatty acid desaturase* (*BE1Des12*) under temperature stress.

The data of qRT-PCR was normalized by the two most stable reference genes, *60S rRNA* and *actin*, and the least stable reference gene, *18S rRNA*. Relative expression values shown are mean fold changes compared to samples at 15°C (Control samples, C), with error bars representing standard deviation. Data are from triplicate samples, each with triple technical replicates for qRT-PCR. Different letters above the bars indicate significant differences from the control at 15°C ($P < 0.05$).

Figure 27. Gene expression patterns of *delta12-fatty acid desaturase* (*BE1Des12*) under desiccation, nutrient deficiency, and high salinity.

The data of qRT-PCR was normalized using the two most stable reference genes for each treatment. Relative expression values are mean fold changes compared to control (C) samples, with error bars representing standard deviation. Data are from triplicate samples, each with triple technical replicates for qRT-PCR. Different letters above the

bars indicate significant differences from the control at 15°C ($P < 0.05$). NaCl was used for the high salinity treatment. The label of "25%→1h" in desiccation experiments means that thalli weighing 25% of the initial weight were incubated in normal seawater medium for 1 h.

Figure 28. Differences in nitrogen starvation-induced expression patterns among nitrogen transporter genes in gametophytes of '*Bangia*' sp. ESS1.
Samples of gametophytes treated with ESS_2-free seawater were collected every day for 7 days to examine the expression of the *BE1AMT1, BE1NRT2 and BE1DUR3* genes by qRT-PCR. The relative mRNA levels were normalized with the reference genes *60S rRNA* and *actin*. Error bars indicate the standard deviation of triplicate experiments (n=3), and bars with different letters indicate significant differences at $P < 0.05$. The numbers on the X axis indicate the duration of culture under nitrogen-deficient conditions (days). "C" means control samples.

Tables

Table 1. AMTs and Rhs from land plant and algae used for the phylogenetic analysis

Species	Gene symbol/Annotation	Accession No.	Division	AAs
Aquilegia coerulea		PIA32185.1	Streptophyta	468
Aquilegia coerulea		PIA65513.1	Streptophyta	475
Aquilegia coerulea		PIA59506.1	Streptophyta	489
Aquilegia coerulea		PIA35542.1	Streptophyta	479
Aquilegia coerulea		PIA31609.1	Streptophyta	477
Aquilegia coerulea		PIA31140.1	Streptophyta	485
Aquilegia coerulea		PIA45105.1	Streptophyta	481
Arabidopsis thaliana	*AMT1.1*	AEE83287.1	Streptophyta	501
Arabidopsis thaliana	*AMT1.2*	AAD38253.1	Streptophyta	514
Arabidopsis thaliana	*AMT1.3*	AEE76886.1	Streptophyta	498
Arabidopsis thaliana	*AMT1.4*	AEE85527.1	Streptophyta	504
Arabidopsis thaliana	*AMT1.5*	AEE76885.1	Streptophyta	496
Arabidopsis thaliana	*AMT2*	AEC09519.1	Streptophyta	475
'Bangia' sp ESS1	*AMT1.1*	MN337339	Rhodophyta	490
'Bangia' sp ESS1	*AMT1.3*	MN337340	Rhodophyta	616
'Bangia' sp ESS1	*AMT1.4*	MN337341	Rhodophyta	567
'Bangia' sp ESS1	*AMT1.5*	MN337342	Rhodophyta	463
'Bangia' sp ESS1	*AMT1.6*	MN337343	Rhodophyta	576
'Bangia' sp ESS1	*Rh*	MN337344	Rhodophyta	458
Chlamydomonas reinhardtii	ammonium transporter	XP_001702082.1	Chlorophyta	432
Chlamydomonas reinhardtii	ammonium transporter	XP_001692671.1	Chlorophyta	542
Chlamydomonas reinhardtii	ammonium transporter	XP_001693464.1	Chlorophyta	499
Chlamydomonas reinhardtii	ammonium transporter	XP_001697504.1	Chlorophyta	539
Chlamydomonas reinhardtii	ammonium transporter	AAS90602.1	Chlorophyta	579
Chlamydomonas reinhardtii	ammonium transporter	XP_001695208.1	Chlorophyta	610
Chlamydomonas reinhardtii	ammonium transporter	XP_001692923.1	Chlorophyta	481
Chlamydomonas reinhardtii	*AMT1.2*	AAM94623.2	Chlorophyta	542
Chlamydomonas reinhardtii	*Rh1*	XP_001695464.1	Chlorophyta	574
Chlamydomonas reinhardtii	*Rh2*	AAM19664.1	Chlorophyta	638
Chondrus crispus	unnamed protein product	XP_005710198.1	Rhodophyta	458
Cyanidioschyzon merolae	ammonium transporter	XP_005536541.1	Rhodophyta	373
Cylindrotheca fusiformis	*AMT1*	AAV70489.1	Heterokontophyta	511
Cylindrotheca fusiformis	*AMT-like*	AAV70490.1	Heterokontophyta	511
Ectocarpus siliculosus	ammonium transporter	CBN77717.1	Heterokontophyta	494
Emiliania huxleyi	ammonium transporter	XP_005785348.1	Heterokontophyta	462
Galdieria sulphuraria	ammonium transporter	EME32138.1	Rhodophyta	502

Galdieria sulphuraria	ammonium transporter	EME30100.1	Rhodophyta	604
Homo sapiens	*Rh (CE)*	NP_065231.3	Mammalia	417
Homo sapiens	*Rh (D)*	NP_001269800.1	Mammalia	493
Phaeodactylum tricornutum	ammonium transporter	XP_002176480.1	Heterokontophyta	540
Phalaenopsis equestris	ammonium transporter 1 member 2-like	XP_020575103.1	Magnoliophyta	514
Physcomitrella patens	ammonium transporter	XP_001758600.1	Bryophyta	504
Physcomitrella patens	ammonium transporter	XP_001758599.1	Bryophyta	503
Physcomitrella patens	ammonium transporter	PNR26034.1	Bryophyta	440
Physcomitrella patens	ammonium transporter	XP_001758603.1	Bryophyta	505
Physcomitrella patens	ammonium transporter	XP_001786055.1	Bryophyta	495
Physcomitrella patens	ammonium transporter	XP_001785500.1	Bryophyta	505
Physcomitrella patens	ammonium transporter	XP_001758611.1	Bryophyta	511
Physcomitrella patens	ammonium transporter	XP_001778521.1	Streptophyta	563
Physcomitrella patens	ammonium transporter	XP_001770054.1	Streptophyta	498
Physcomitrella patens	ammonium transporter	XP_001762803.1	Streptophyta	475
Physcomitrella patens	ammonium transporter	XP_001754238.1	Streptophyta	493
Physcomitrella patens	ammonium transporter	XP_001752514.1	Streptophyta	490
Physcomitrella patens	ammonium transporter	XP_001781204.1	Streptophyta	495
Physcomitrella patens	ammonium transporter	XP_001754816.1	Streptophyta	494
Porphyra purpurea	Contig05572		Rhodophyta	455
Porphyra purpurea	Contig8812		Rhodophyta	487
Porphyra purpurea	Contig05687		Rhodophyta	489
Porphyra purpurea	Contig2135		Rhodophyta	485
Porphyra umbilicalis	Pum0027s0002.1 (*AMT2.2*)	OSX80976.1	Rhodophyta	411
Porphyra umbilicalis	Pum0165s0019.1 (*AMT2.1*)	OSX69292.1	Rhodophyta	644
Porphyra umbilicalis	Pum0463s0020.1 (*AMT1.2*)	OSX72158.1	Rhodophyta	545
Porphyra umbilicalis	Pum0126s0003.1 (*AMT1.4*)	OSX77964.1	Rhodophyta	480
Porphyra umbilicalis	Pum0165s0019.1 (*AMT1.1*)	OSX77025.1	Rhodophyta	485
Porphyra umbilicalis	Pum1775s0001.1 (*AMT1.3*)	OSX69172.1	Rhodophyta	428
Porphyra umbilicalis	Pum0022s0083.1 (*AMT3*)	OSX81363.1	Rhodophyta	616
Porphyridium purpureum	contig3836.1		Rhodophyta	562
Porphyridium purpureum	contig2277.5		Rhodophyta	517
Porphyridium purpureum	contig2333.1		Rhodophyta	492
Porphyridium purpureum	contig2015.11		Rhodophyta	444
Pyropia yezoensis	*AMT1*	BAV55983.1	Rhodophyta	483
Pyropia yezoensis	*AMT1.2*	MK537329	Rhodophyta	484
Pyropia yezoensis	*AMT1.3*	MK537330	Rhodophyta	654
Pyropia yezoensis	*AMT1.4*	MK537331	Rhodophyta	589
Pyropia yezoensis	*AMT1.5*	MK537332	Rhodophyta	616
Pyropia yezoensis	*AMT1.6*	MK537333	Rhodophyta	690
Pyropia yezoensis	*Rh*	MK537334	Rhodophyta	522
Sus scrofa	*Rh*	BAB84562.1	Mammalia	423

Volvox carteri f. nagariensis	EFJ48363.1	Chlorophyta	426
Volvox carteri f. nagariensis	EFJ41931.1	Chlorophyta	518
Volvox carteri f. nagariensis	EFJ47696.1	Chlorophyta	496
Volvox carteri f. nagariensis	EFJ41931.1	Chlorophyta	518
Volvox carteri f. nagariensis	EFJ40601.1	Chlorophyta	570
Volvox carteri f. nagariensis	EFJ43712.1	Chlorophyta	639
Volvox carteri f. nagariensis	EFJ47052.1	Chlorophyta	463
Volvox carteri f. nagariensis	EFJ51468.1	Chlorophyta	453

Table 2. Primer sequences used for quantitative PCR analyses

Primer name	Sequence (5'-3')	Product size (bp)
Q-Py18S-F	CGACCGTTTACTGTGAAG	160
Q-Py18S-R	GACAATGAAATACGAATGCC	
Q-PyAMT1-F	TGTGGTTTGGGTGGTACGG	169
Q-PyAMT1-R	GCAGCTTGATGACAATGAGGG	
Q-PyAMT1.2-F	GTGGCCGAGGAAGGGATT	132
Q-PyAMT1.2-R	AGCGTGCGGACAAAGAAC	
Q-PyAMT1.3-F	TCCAATCCTTGCTTTTCA	98
Q-PyAMT1.3-R	GTTCCCGCTTGCTCCATA	
Q-PyAMT1.4-F	GGGCGGGTTTATCTTGTG	162
Q-PyAMT1.4-R	GTCTGCTGGACGGTGAGG	
Q-PyAMT1.5-F	CCGAGTATGGGTGGTTGG	152
Q-PyAMT1.5-R	GGTGGGTAGGCGGTGAAG	
Q-PyAMT1.6-F	GCGGGCATGGAAGGACAG	145
Q-PyAMT1.6-R	AAGGCGGGGAAGGAGGGA	
Q-PyRh-F	AAGCGAGAAGACGGAGCA	194
Q-PyRh-R	TGGAAGACATTCAGAACG	

Table 3. Physical and chemical characteristics of PyAMTs and PyRh

Name	Amino acids numbers	Molecular weight	Total number of atoms	Isoelectric point (pI)	Grand average of hydropathicity (GRAVY)	Ammonium transporter domain location[a]	Accession number
PyAMT1	483	50.98	7,164	4.80	0.637	40-449	BAV55983.1
PyAMT1.2	484	51.20	7,202	4.79	0.555	38-448	MK537329
PyAMT1.3	654	67.80	9,576	6.16	0.518	75-505	MK537330
PyAMT1.4	589	58.67	8,227	5.98	0.543	53-486	MK537331
PyAMT1.5	616	63.68	8,934	5.08	0.501	51-473	MK537332
PyAMT1.6	690	72.06	10,149	9.21	0.390	52-474	MK537333
PyRh	522	53.78	7,540	5.50	0.543	30-431	MK537334

Table 4. Locations of transmembrane (TM) helices in PyAMT1s and PyRh[a]

TM helices	PyAMT1	PyAMT1.2	PyAMT1.3	PyAMT1.4	PyAMT1.5	PyAMT1.6	PyRh
1	41-63	40-62	7-29	5-27	29-47	34-48	21-43
2	76-98	75-97	77-99	52-74	51-73	52-74	63-85
3	118-140	117-139	120-142	86-108	85-107	86-108	92-114
4	147-169	146-168	157-176	132-154	140-162	140-162	129-151
5	184-206	183-205	183-204	159-181	167-189	169-191	158-180
6	218-240	217-239	224-246	201-223	215-226	214-236	190-207
7	262-284	261-283	267-289	244-263	255-277	249-271	227-244
8	296-318	290-309	324-343	306-328	290-312	291-313	259-281
9	322-344	319-341	350-372	341-374	327-349	325-347	294-311
10	351-373	346-368	377-394	389-411	370-392	375-397	315-337
11	402-424	401-423	452-474	414-430	424-446	421-443	349-371
12							399-412

[a] The number indicating positions of TM helices is based on assignment of the start methionine residue as 1 in PyAMTs and PyRh.

Table 5. Species and GenBank accession numbers of their *rbcL* gene sequences used for the phylogenetic analysis

Taxon	**Collection location**	**Accession No.**
'Bangia fuscopurpurea' BB Bf 1	Bolinas Bay, CA, USA	EU289018
'Bangia fuscopurpurea' CMNH UM BF1	Banda, Tateyama, Chiba, Japan	HQ687502
'Bangia fuscopurpurea' France	Nice, France	AF168659
'Bangia fuscopurpurea' Taiwan	Taiwan	AF168654
'Bangia fuscopurpurea' WA	Fisherman's Bay, WA, USA	AF169329
'Bangia' maxima	Bolinas Bay, CA, USA	EU289020
'Bangia' sp. BC Can	Ogden Point, Victoria, BC, Canada	AF043376
'Bangia' sp. BCH	Taylor's Mistake, Christchurch, South I, NZ	HQ687504
'Bangia' sp. BFK	Frank Kitts Lagoon, Wellington, North I, NZ	HQ687505
'Bangia' sp. BGA	Gentle Annie, Westland, South I, NZ	HQ687506
'Bangia' sp. BMW	Makawhio, North I, NZ	HQ687508
'Bangia' sp. BNS	Bawley Point, N. of Bateman's Bay, NSW, Australia	HQ687509
'Bangia' sp. BPL	Maketu, Bay of Plenty, North I, NZ	HQ687510
'Bangia' sp. BRM	Kaka Point, Otago, South I, NZ	HQ687511
'Bangia' sp. BWP	Woodpecker Bay, Paparoa, Wesland, South I, NZ	EU570051
'Bangia' sp. CH620	Supseom, Jejudo, Korea	HQ728203
'Bangia' sp. MA	Woods Hole, MA, USA	AF043369
'Bangia' sp. NthBC Can	Triple Island, BC, Canada	AF043372
'Bangia' sp. OR	Lincoln City, OR, USA	AF043367
'Bangia' sp. SB Bf 1	Solana Beach, CA, USA	EU289019
'Bangia' sp. TX	Port Aransas, TX, USA	AF043377
'Bangia' vermicularis	Golden Gate, San Francisco Bay, CA, USA	EU289022
'Bangia' sp. OUCPT-01	Putian, Fujian, China	KP747609.1

Table 6. Physical and chemical characteristics of BE1AMT1s and BE1Rh, BE1NRT2 and BE1DUR3s

Name	Amino acids numbers	Molecular weight	Isoelectric point	Grand average of hydropathicity (GRAVY)	Total number of atoms	Transmembrane helices (TMs)	Accession number
BE1AMT1.1	490	51,368	4.85	0.666	7,250	11	MN337339
BE1AMT1.3	616	63,672	5.08	0.501	8,934	11	MN337340
BE1AMT1.4	567	59,556	5.53	0.405	8,349	11	MN337341
BE1AMT1.5	463	47,578	7.15	0.536	6,676	11	MN337342
BE1AMT1.6	576	62,359	5.51	0.504	8,772	11	MN337343
BE1Rh	458	49,842	5.08	0.414	6,986	12	MN337344
BE1NRT2	479	51,646	8.52	0.551	7,318	12	MN337336
BE1DUR3.1	753	79,651	5.4	0.609	11,269	15	MN337337
BE1DUR3.2	680	71,231	5.4	0.771	10,176	15	MN337338

Table 7. Land plant and algal NRTs used for the phylogenetic analysis

Species	Gene symbol/Annotation	Accession No.	Division	AAs
Arabidopsis thaliana	*NRT2.1*	AEE28241.1	Streptophyta	530
Arabidopsis thaliana	*NRT1.1*	AEE28838.1	Streptophyta	590
Arabidopsis thaliana	nitrate transporter	ABX61048.1	Streptophyta	576
Arabidopsis thaliana	*NRT2.6*	AEE77987.1	Streptophyta	542
Arabidopsis thaliana	*NRT2.4*	AED97375.1	Streptophyta	527
Arabidopsis thaliana	*NRT2.3*	AED97376.1	Streptophyta	539
Arabidopsis thaliana	*NRT2.2*	AEE28242.1	Streptophyta	522
Arabidopsis thaliana	*NRT1.8*	AEE84489.1	Streptophyta	589
Arabidopsis thaliana	*NRT1.7*	AEE34993.1	Streptophyta	620
Arabidopsis thaliana	*NRT1.5*	AEE31488.1	Streptophyta	576
Arabidopsis thaliana	*NRT1.4*	Q9SZY4.1	Streptophyta	577
Arabidopsis thaliana	*NRT1.3*	Q9LYD5.1	Streptophyta	481
Arabidopsis thaliana	*NRT1.2*	NP_564978	Streptophyta	585
Arabidopsis thaliana	*NRT2.5*	OAP19210.1	Streptophyta	502
Arabidopsis thaliana	*NRT1.6*	AEE30777.1	Streptophyta	576
'Bangia' sp ESS1	*NRT2*	MN337336	Rhodophyta	480
Chlamydomonas reinhardtii	high affinity nitrate transporter	XP_001696788.1	Chlorophyta	527
Chlamydomonas reinhardtii	nitrate transporter	XP_001694496.1	Chlorophyta	628
Chondrus crispus	nitrate transporter	XP_005716155.1	Rhodophyta	501
Cyanidioschyzon merolae	nitrate transporter	XP_005535838.1	Rhodophyta	568
Cylindrotheca fusiformis	nitrate transporter	AAD49572.1	Rhodophyta	482
Ectocarpus siliculosus	Nitrate high affinity transporter	CBJ31728.1	Heterokontophyta	457
Emiliania huxleyi	putative nitrate transporter	XP_005791440.1	Heterokontophyta	513
Galdieria sulphuraria	MFS transporter, nitrate/nitrite transport	XP_005704380.1	Rhodophyta	622
Gracilariopsis chorda	High affinity nitrate transporter 2.5	PXF49156.1	Rhodophyta	488
Oryza sativa	high affinity nitrate transporter	BAA33382.1	Streptophyta	533
Oryza sativa	nitrate transporter	AAF07875.1	Streptophyta	584
Oryza sativa	*NRT2.1*	XP_015623638.1	Streptophyta	533
Oryza sativa	*NRT2.2*	XP_015623596.1	Streptophyta	533
Oryza sativa	nitrate transporter	AAT85061.1	Streptophyta	587
Oryza sativa	*NRT1.2*	AAP70034.1	Streptophyta	593
Oryza sativa	putative nitrate transporter	AAK15441.1	Streptophyta	594
Phaeodactylum tricornutum	nitrate transmembrane transporter	EEC50797.1	Heterokontophyta	471
Physcomitrella patens	nitrate transporter	BAD00101.1	Streptophyta	517
Physcomitrella patens	nitrate transporter	BAE45929.1	Streptophyta	517
Physcomitrella patens	nitrate transporter	BAE45928.1	Streptophyta	548

Physcomitrella patens	nitrate transporter	BAE45927.1	Streptophyta	549
Physcomitrella patens	nitrate transporter	BAE45926.1	Streptophyta	547
Physcomitrella patens	nitrate transporter	BAE45925.1	Streptophyta	548
Physcomitrella patens	nitrate transporter	BAD00099.2	Streptophyta	549
Porphyra umbilicalis	*NRT2*	OSX68812.1	Rhodophyta	478
Porphyridium_purpureum	nitrate transporter	contig_3397.13	Rhodophyta	561
Porphyridium_purpureum	nitrate transporter	contig_2324.2	Rhodophyta	521
Pyropia yezoensis	*NRT2*	BAG70346.1	Rhodophyta	479
Volvox carteri f. nagariensis	nitrate transporter	EFJ43757.1	Chlorophyta	494

Table 8. Land plant and algal DUR3s used for the phylogenetic analysis

Species	Gene symbol/Annotation	Accession No.	Division	AAs
Arabidopsis thaliana	*DUR3*	OAO92264.1	Streptophyta	704
Asparagus officinalis	*DUR3*	XP_020248790.1	Streptophyta	712
'Bangia' sp ESS1	*DUR3.1*	MN337337	Rhodophyta	753
'Bangia' sp ESS1	*DUR3.2*	MN337338	Rhodophyta	680
Cajanus cajan	DUR3	XP_020236197.1	Streptophyta	713
Chlamydomonas reinhardtii	urea active transporter	XP_001702309.1	Chlorophyta	721
Chlamydomonas reinhardtii	urea active transporter	XP_001702308.1	Chlorophyta	653
Chlamydomonas reinhardtii	urea active transporter	XP_001691580.1	Chlorophyta	571
Chondrus crispus	urea active transporter-like 2	XP_005712214.1	Rhodophyta	669
Chondrus crispus	urea active transporter-like 1	XP_005716890.1	Rhodophyta	675
Ectocarpus siliculosus	urea/Na+ high-affinity symporter	CBJ28389.1	Heterokontophyta	668
Glycine max	*DUR3*	XP_003523904.1	Streptophyta	714
Glycine soja	putative urea active transporter 1	KHN42868.1	Streptophyta	714
Gracilariopsis chorda	*DUR3*	PXF47435.1	Rhodophyta	675
Gracilariopsis chorda	*DUR3*	PXF45390.1	Rhodophyta	675
Oryza sativa Japonica Group	urea active transporter	BAF27350.1	Streptophyta	721
Physcomitrella patens	urea active transporter	PNR40740.1	Streptophyta	678
Physcomitrella patens	urea active transporter	PNR62548.1	Streptophyta	713
Porphyra umbilicalis	urea active transporter	OSX77454.1	Rhodophyta	687
Porphyra umbilicalis	urea active transporter	OSX71042.1	Rhodophyta	673
Porphyra umbilicalis	urea active transporter	OSX69523.1	Rhodophyta	479
Pyropia yezoensis	*DUR3.3*	BAU04114.1	Rhodophyta	679
Pyropia yezoensis	*DUR3.2*	BAU04116.1	Rhodophyta	680
Pyropia yezoensis	*DUR3.1*	BAG70347.1	Rhodophyta	740
Rosa chinensis	*DUR3*	XP_024171130.1	Streptophyta	709
Selaginella moellendorffii	*DUR3*	XP_024532970.1	Streptophyta	684
Solanum lycopersicum	*DUR3*	XP_004245999.1	Streptophyta	710
Triticum urartu	putative urea active transporter 1	EMS63712.1	Streptophyta	594
Vigna angularis	*DUR3*	XP_017426137.1	Streptophyta	714
Volvox carteri f. nagariensis	urea active transporter	EFJ41618.1	Chlorophyta	821
Volvox carteri f. nagariensis	urea active transporter	XP_002957275.1	Chlorophyta	645
Zea mays subsp. mays	*DUR3*	AIT11841.1	Streptophyta	731

Table 9. Experimental conditions

Factor	Treatment	Duration
Desiccation	percentage of initial weight	75%
		50%
		25%
		25%→seawater
		1h
Nutrient-deficiency	ESS_2-less	0 d
		1 d
		2 d
		3 d
		4 d
		5 d
		6 d
		7 d
High salinity	25 mM	1 d
	25 mM	2 d
	25 mM	3 d
	50 mM	1 d
	50 mM	2 d
	50 mM	3 d
	100 mM	1 d
	100 mM	2 d
	100 mM	3 d
Temperature changes	5℃	1 d
	5℃	2 d
	5℃	3 d
	30℃	1 d
	30℃	2 d
	30℃	3 d

Table 10. Sequences of the primers used for qRT-PCR in this study

Gene name	Gene ID / Reference	Gene function description	Primer sequence	Amplicon length (bp)	Efficiency (%)	Correlation coefficient (R^2)
18S rRNA	Wang et al., 2011	small subunit ribosomal RNA	ACAGGACTTGGGCTCTATTTTG AGATGCTTTCGCAGTGGTTCG	135	99	0.9932
GAPDH	Wang et. al., 2011	glyceraldehyde 3-phosphate dehydrogenase	CTGGTGAGGCACTTTGGAA AAGGAGGAGGACTGATGGG	102	105	0.9915
actin	CL1634.Contig3	actin	TCAACCCCAAGGCCAACC TCACGCCGTCCCCAGAAT	150	98	0.9930
α-tubulin	CL70.Contig4	alpha tubulin	ACTCGGTCACATCAACGTTCA TATCTGCCGCCGCTCTCT	131	99	0.9925
EF1	Unigene64554	enlongation factor 1	ATCTCGTTGTAGCGGGACTC AAGCAGCTGATCGTTGGC	86	101	0.9933
60S rRNA	Unigene3570	large subnit ribosomal protein	CCACGTTGTCCATTTACGC CACCTCCTCCAAGTTCGG	98	102	0.9940
BE1Des12	Cao et al., 2017	delta12-fatty-acid desaturase	CACCCAGAGGCAAACCC ATGGACGGGCAGTAGGG	180	96	0.9911

Table 11. Primers sequences of '*Bangia*' sp. ESS1 nitrogen transporters used for qRT-PCR

Primer name	Sequence (5'-3')	Product size (bp)
Q-BE1AMT1.1-F	GCGGAGCAAGAACACGAAGA	94
Q-BE1AMT1.1-R	GGCAAAGGCATACCCAAACAG	
Q-BE1AMT1.3-F	TGGCAACGAGGGAAATGG	85
Q-BE1AMT1.3-R	GAAGAAGAATGCGAGGGAGTG	
Q-BE1AMT1.4-F	GCGGGCAAAAAAACACCAAGA	96
Q-BE1AMT1.4-R	GGGCAAACGCATTCCCAAAC	
Q-BE1AMT1.5-F	CATTTACCAGCTCCCATTCCC	199
Q-BE1AMT1.5-R	CCATAGCCCAACCACCCATACT	
Q-BE1AMT1.6-F	CCCCACCATAAACCCCTT	111
Q-BE1AMT1.6-R	TGCTGCCCCGTTACCATC	
Q-BE1Rh-F	CCTACTTTTTCCTTGTCTTTCA	102
Q-BE1Rh-R	CACCATTATCTACCGCTTTATC	
Q-BE1NRT2-F	CACTTTGCGTGGTCGTCCTT	108
Q-BE1NRT2-R	CGCCGAGTCATCGTTCAGC	
Q-BE1DUR3.1-F	AGGAAGGGGTCAAGGCTGTT	182
Q-BE1DUR3.1-R	CGCATTCGGGTTGGGTGTA	
Q-BE1DUR3.2-F	GCGTTTGGGATCTCCTTTGG	128
Q-BE1DUR3.2-R	GCGGTGAGCCCCGTCTTG	

Table 12. Expression stability analysis of six reference genes using NormFinder

Desiccation		Nutrient deficiency		Salinity		Temperature		Total	
Ranking [a]	SV [b]	Ranking	SV	Ranking	SV	Ranking	SV	Ranking	SV
α-tubulin	0.397	GAPDH	0.137	GAPDH	0.132	60S	0.164	GAPDH	0.392
EF1	0.505	actin	0.217	60S	0.319	actin	0.279	α-tubulin	0.551
actin	0.617	60S	0.511	actin	0.324	GAPDH	0.390	EF1	0.604
GAPDH	0.705	18S	0.705	EF1	0.494	EF1	0.503	actin	0.809
18S [c]	1.073	EF1	0.750	18S	0.679	α-tubulin	0.548	18S	0.962
60S [d]	1.112	α-tubulin	1.143	α-tubulin	1.000	18S	0.862	60S	0.876

a: Ranking indicates the stability of gene expression from the most stable to the least stable.

b: SV represents stability value.

c: 18S represents 18S rRNA.

d: 60S represents 60S rRNA.

Table 13. Expression stability ranking results from geNorm and NormFinder software

Ranking [a]	Desiccation		Nutrient deficiency		Salinity		Temperature		Total	
	geNorm	NormFinder	geNorm	NormFinder	geNorm	NormFinder	geNorm	NormFinder	geNorm	NormFinder
1	EF1	α-tubulin	60S	GAPDH	60S	GAPDH	60S	60S	EF1	GAPDH
2	α-tubulin	EF1	actin	actin	actin	60S	actin	actin	α-tubulin	α-tubulin
3	GAPDH	actin	GAPDH	60S	GAPDH	actin	GAPDH	GAPDH	GAPDH	EF1
4	actin	GAPDH	18S	18S	18S	EF1	EF1	EF1	actin	actin
5	18S [b]	18S	EF1	EF1	EF1	18S	α-tubulin	α-tubulin	18S	18S
6	60S [c]	60S	α-tubulin	α-tubulin	α-tubulin	α-tubulin	18S	18S	60S	60S

a: Ranking indicates the stability of gene expression from the most stable to the least stable.

b: 18S represents 18S rRNA.

c: 60S represents 60S rRNA.

Figures

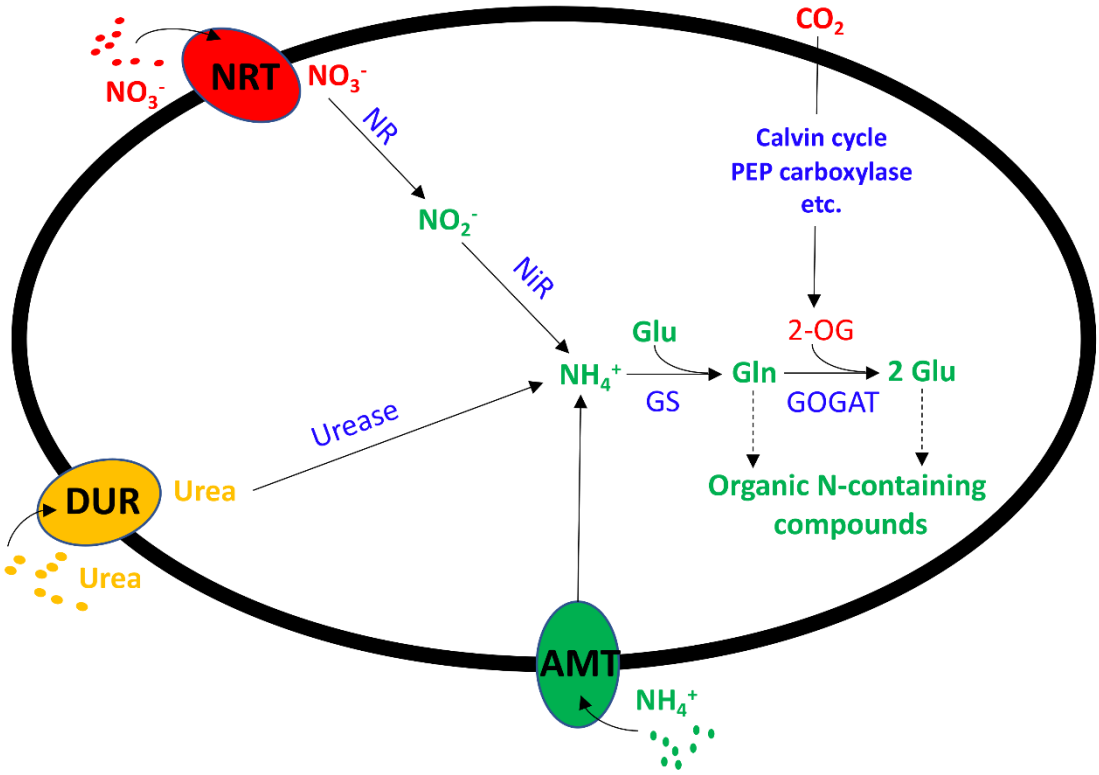

Figure 1


PyAMT1
PyAMT1.2
PyAMT1.3
PyAMT1.4
PyAMT1.5
PyAMT1.6
PyRh
Consensus

Figure 2

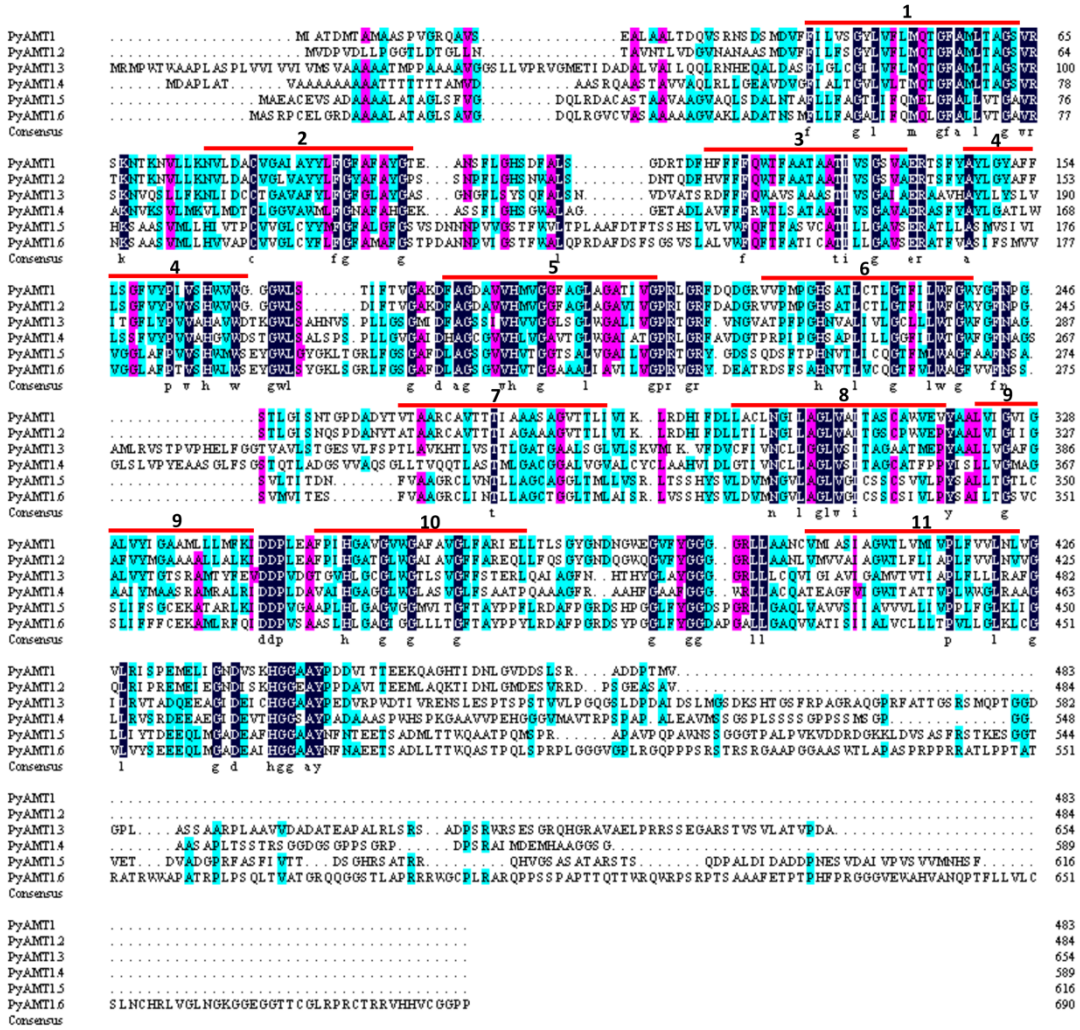

Figure 3

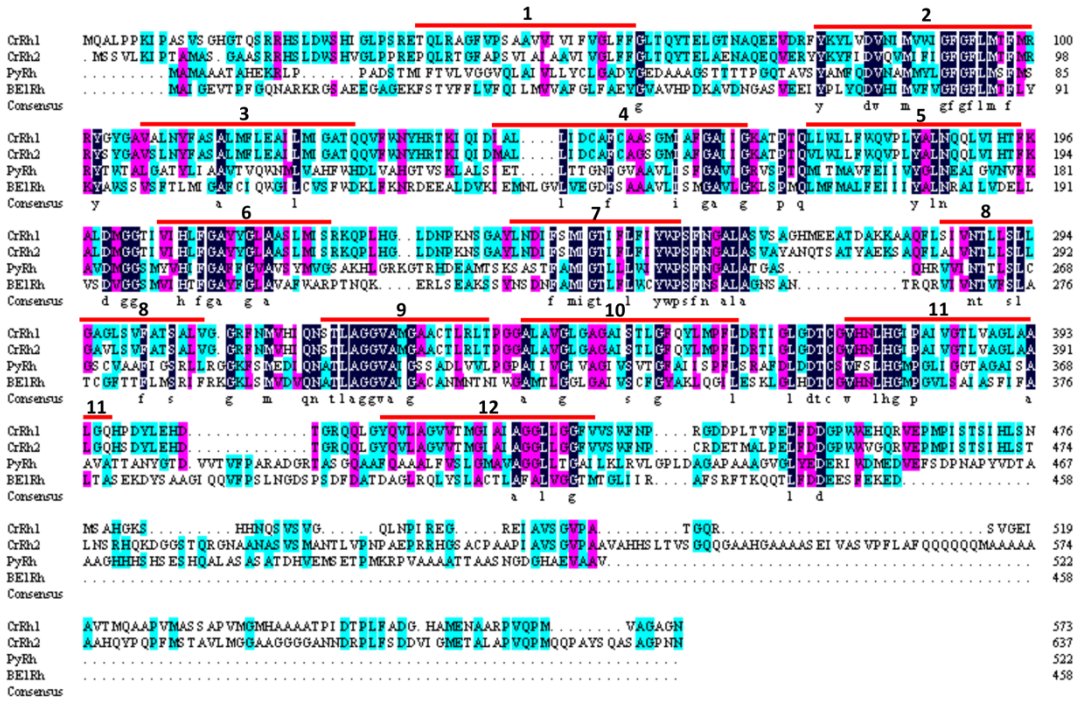

Figure 4

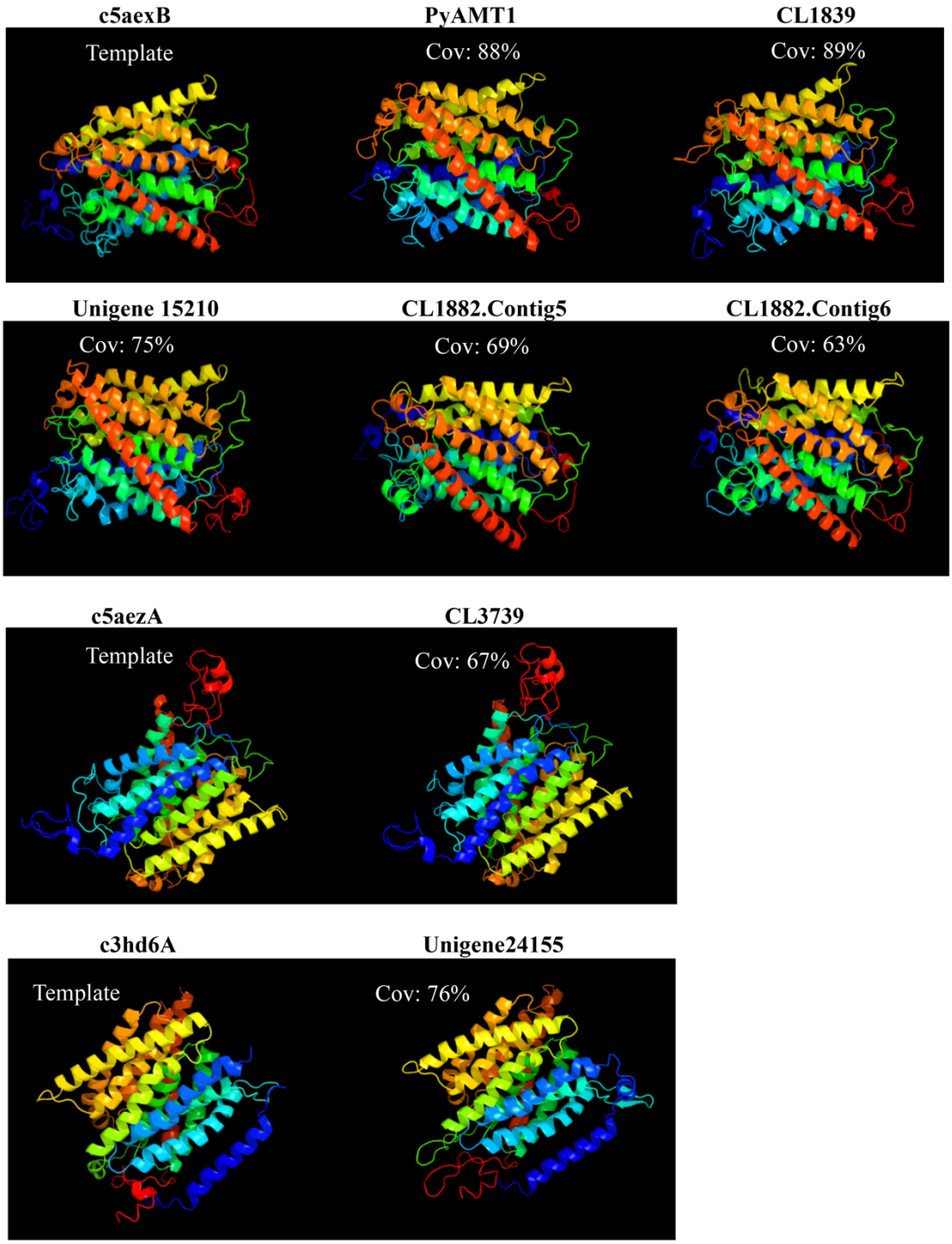
c5aexB
Template
PyAMT1
Cov: 88%
CL1839
Cov: 89%
Unigene 15210
Cov: 75%
CL1882.Contig5
Cov: 69%
CL1882.Contig6
Cov: 63%
c5aezA
Template
CL3739
Cov: 67%
c3hd6A
Template
Unigene24155
Cov: 76%

Figure 5

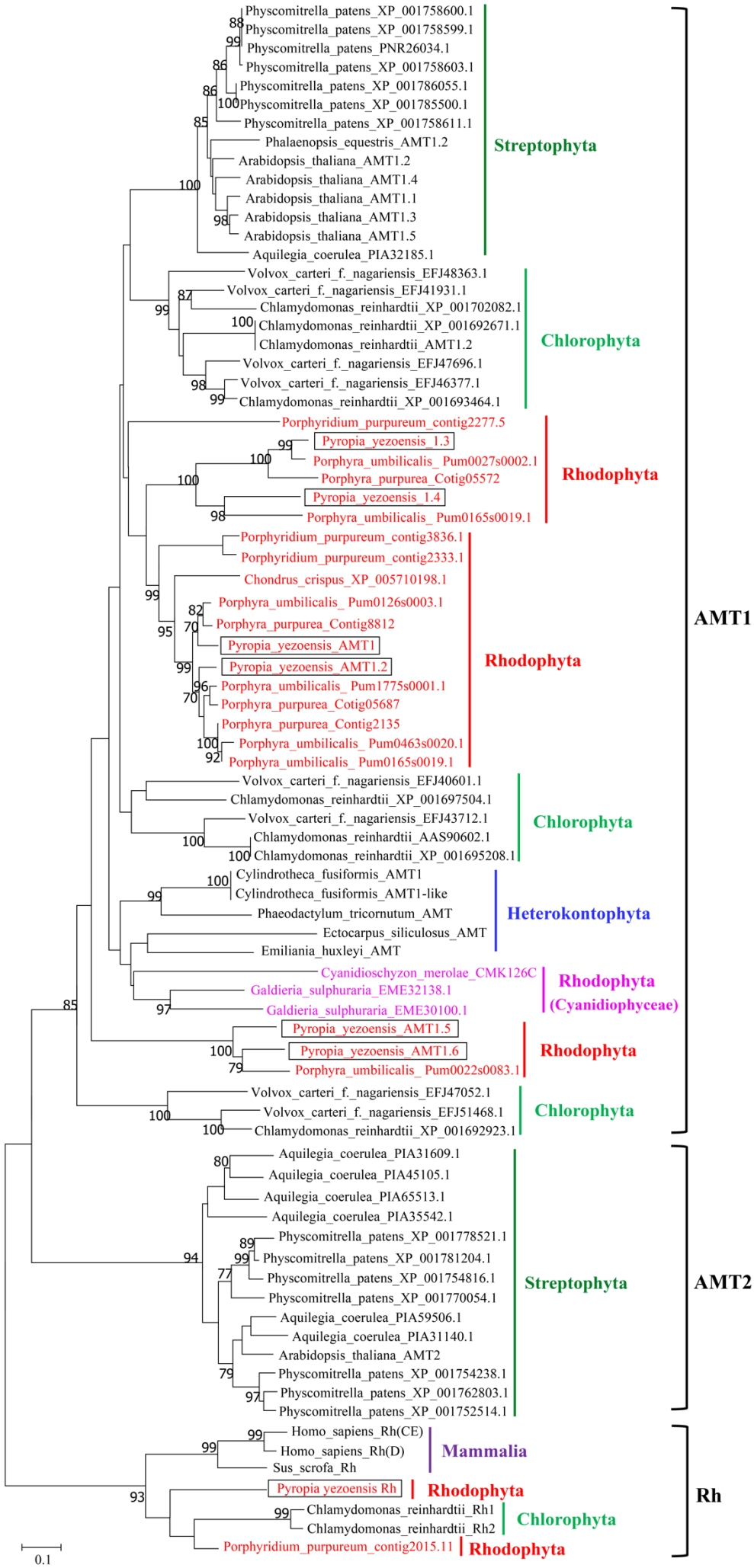
Physcomitrella_patens_XP_001758600.1
Physcomitrella_patens_XP_001758599.1
Physcomitrella_patens_PNR26034.1
Physcomitrella_patens_XP_001758603.1
Physcomitrella_patens_XP_001786055.1
Physcomitrella_patens_XP_001785500.1
Physcomitrella_patens_XP_001758611.1
Phalaenopsis_equestris_AMT1.2
Arabidopsis_thaliana_AMT1.2
Arabidopsis_thaliana_AMT1.4
Arabidopsis_thaliana_AMT1.1
Arabidopsis_thaliana_AMT1.3
Arabidopsis_thaliana_AMT1.5
Aquilegia_coerulea_PIA32185.1
Streptophyta
Volvox_carteri_f._nagariensis_EFJ48363.1
Volvox_carteri_f._nagariensis_EFJ41931.1
Chlamydomonas_reinhardtii_XP_001702082.1
Chlamydomonas_reinhardtii_XP_001692671.1
Chlamydomonas_reinhardtii_AMT1.2
Volvox_carteri_f._nagariensis_EFJ47696.1
Volvox_carteri_f._nagariensis_EFJ46377.1
Chlamydomonas_reinhardtii_XP_001693464.1
Chlorophyta
Porphyridium_purpureum_contig2277.5
Pyropia_yezoensis_1.3
Porphyra_umbilicalis_ Pum0027s0002.1
Porphyra_purpurea_Cotig05572
Pyropia_yezoensis_1.4
Porphyra_umbilicalis_ Pum0165s0019.1
Rhodophyta
Porphyridium_purpureum_contig3836.1
Porphyridium_purpureum_contig2333.1
Chondrus_crispus_XP_005710198.1
Porphyra_umbilicalis_ Pum0126s0003.1
Porphyra_purpurea_Contig8812
Pyropia_yezoensis_AMT1
Pyropia_yezoensis_AMT1.2
Porphyra_umbilicalis_ Pum1775s0001.1
Porphyra_purpurea_Cotig05687
Porphyra_purpurea_Contig2135
Porphyra_umbilicalis_ Pum0463s0020.1
Porphyra_umbilicalis_ Pum0165s0019.1
Rhodophyta
Volvox_carteri_f._nagariensis_EFJ40601.1
Chlamydomonas_reinhardtii_XP_001697504.1
Volvox_carteri_f._nagariensis_EFJ43712.1
Chlamydomonas_reinhardtii_AAS90602.1
Chlamydomonas_reinhardtii_XP_001695208.1
Chlorophyta
Cylindrotheca_fusiformis_AMT1
Cylindrotheca_fusiformis_AMT1-like
Phaeodactylum_tricornutum_AMT
Ectocarpus_siliculosus_AMT
Emiliania_huxleyi_AMT
Heterokontophyta
Cyanidioschyzon_merolae_CMK126C
Galdieria_sulphuraria_EME32138.1
Galdieria_sulphuraria_EME30100.1
Rhodophyta
(Cyanidiophyceae)
Pyropia_yezoensis_AMT1.5
Pyropia_yezoensis_AMT1.6
Porphyra_umbilicalis_ Pum0022s0083.1
Rhodophyta
Volvox_carteri_f._nagariensis_EFJ47052.1
Volvox_carteri_f._nagariensis_EFJ51468.1
Chlamydomonas_reinhardtii_XP_001692923.1
Chlorophyta
AMT1
Aquilegia_coerulea_PIA31609.1
Aquilegia_coerulea_PIA45105.1
Aquilegia_coerulea_PIA65513.1
Aquilegia_coerulea_PIA35542.1
Physcomitrella_patens_XP_001778521.1
Physcomitrella_patens_XP_001781204.1
Physcomitrella_patens_XP_001754816.1
Physcomitrella_patens_XP_001770054.1
Aquilegia_coerulea_PIA59506.1
Aquilegia_coerulea_PIA31140.1
Arabidopsis_thaliana_AMT2
Physcomitrella_patens_XP_001754238.1
Physcomitrella_patens_XP_001762803.1
Physcomitrella_patens_XP_001752514.1
Streptophyta
AMT2
Homo_sapiens_Rh(CE)
Homo_sapiens_Rh(D)
Sus_scrofa_Rh
Mammalia
Pyropia yezoensis Rh
Rhodophyta
Chlamydomonas_reinhardtii_Rh1
Chlamydomonas_reinhardtii_Rh2
Chlorophyta
Porphyridium_purpureum_contig2015.11
Rhodophyta
Rh
0.1

Figure 6

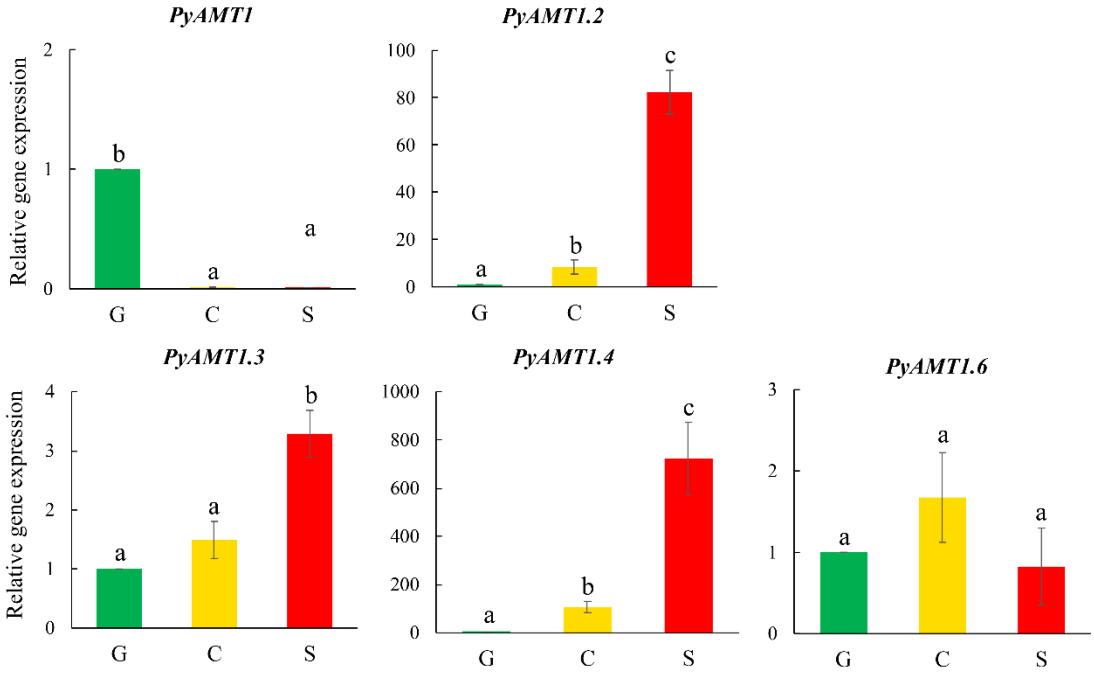
PyAMT1
PyAMT1.2
PyAMT1.3
PyAMT1.4
PyAMT1.6
Relative gene expression
G
C
S

Figure 7

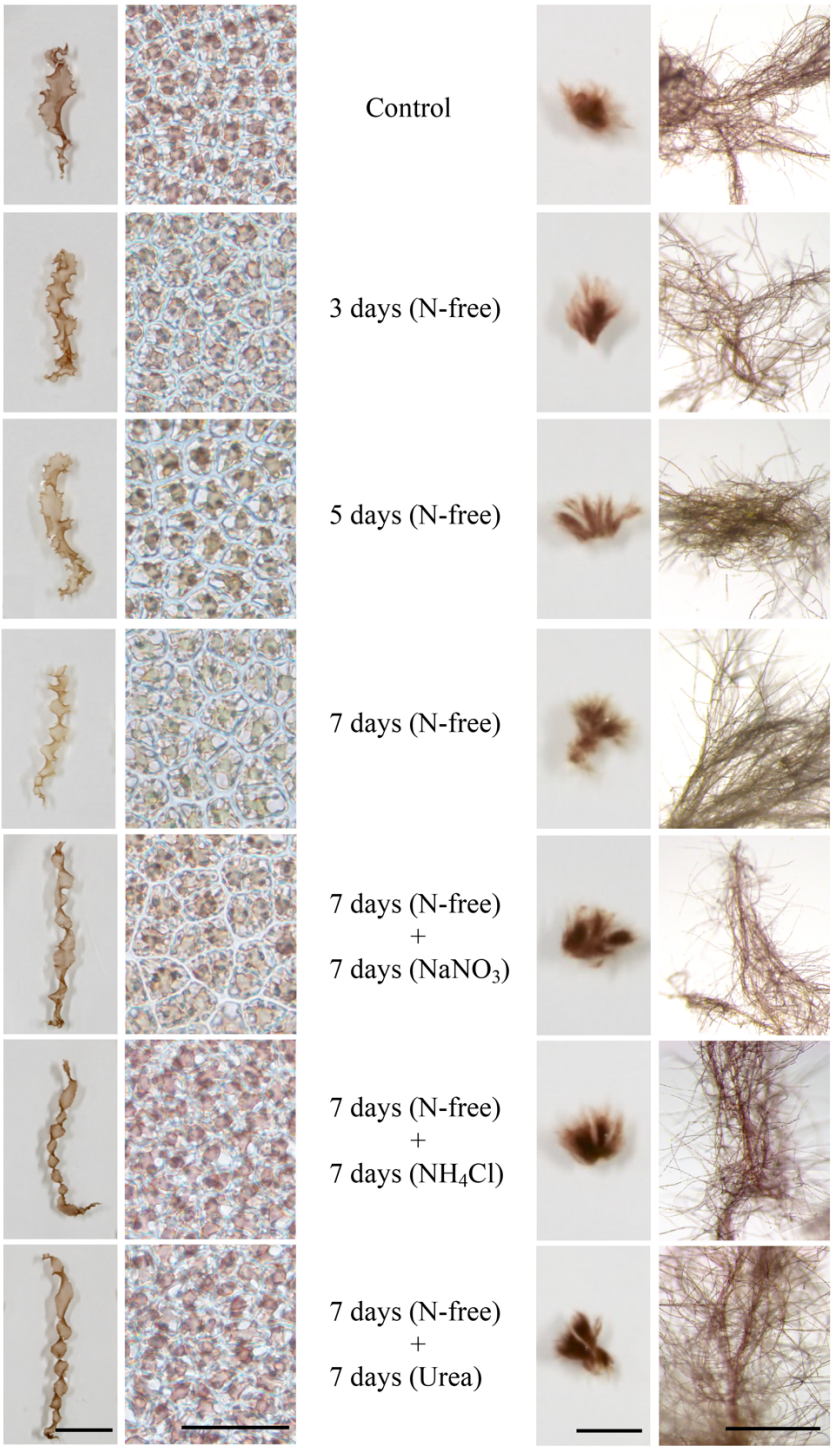
Control
3 days (N-free)
5 days (N-free)
7 days (N-free)
7 days (N-free)
+
7 days ($NaNO_3$)
7 days (N-free)
+
7 days (NH_4Cl)
7 days (N-free)
+
7 days (Urea)

Figure 8

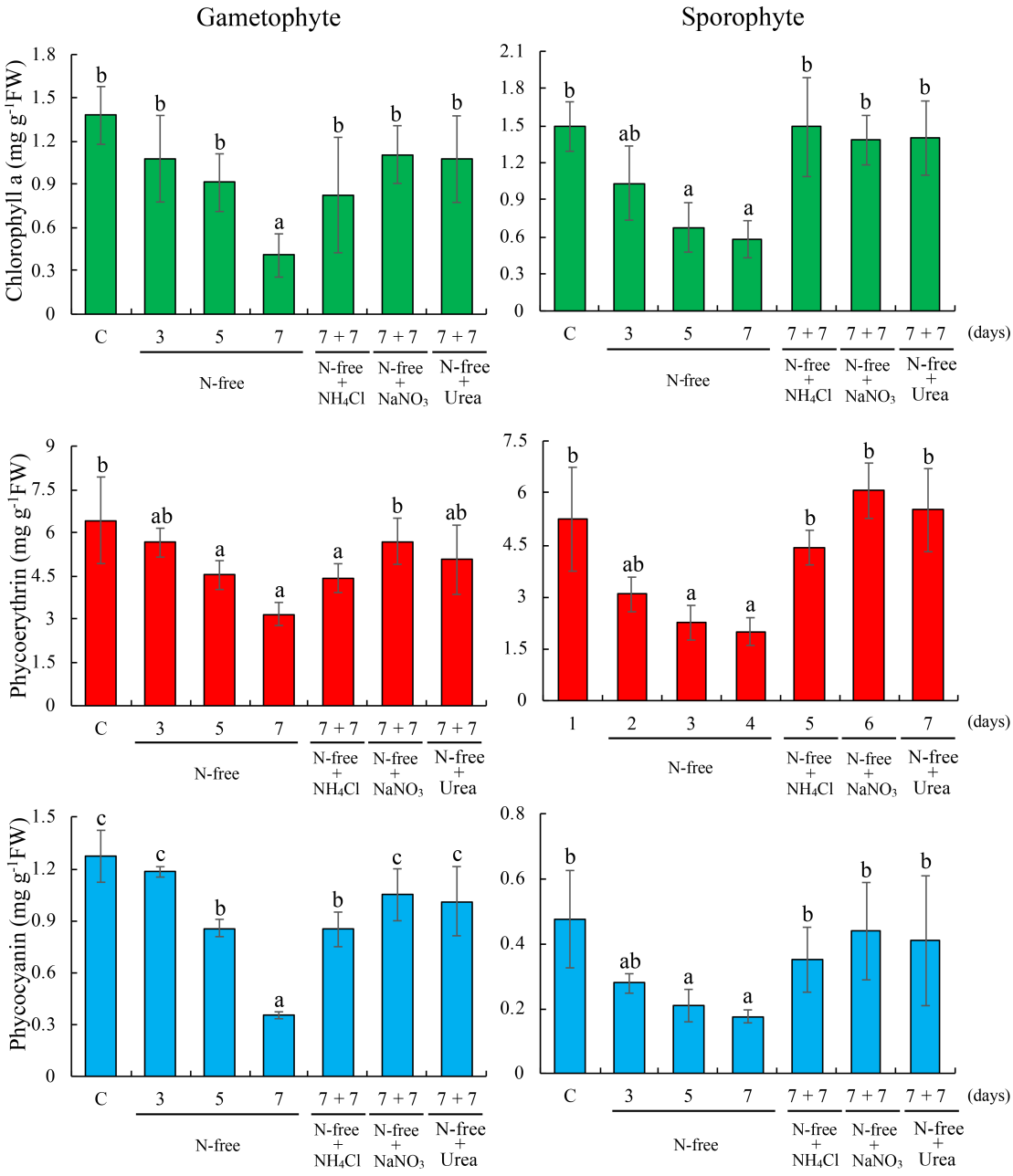
Gametophyte
Sporophyte
Chlorophyll a (mg g-1FW)
Phycoerythrin (mg g-1FW)
Phycocyanin (mg g-1FW)
C
3
5
7
7 + 7
N-free
N-free + NH4Cl
N-free + NaNO3
N-free + Urea
1
2
4
6
(days)

Figure 9

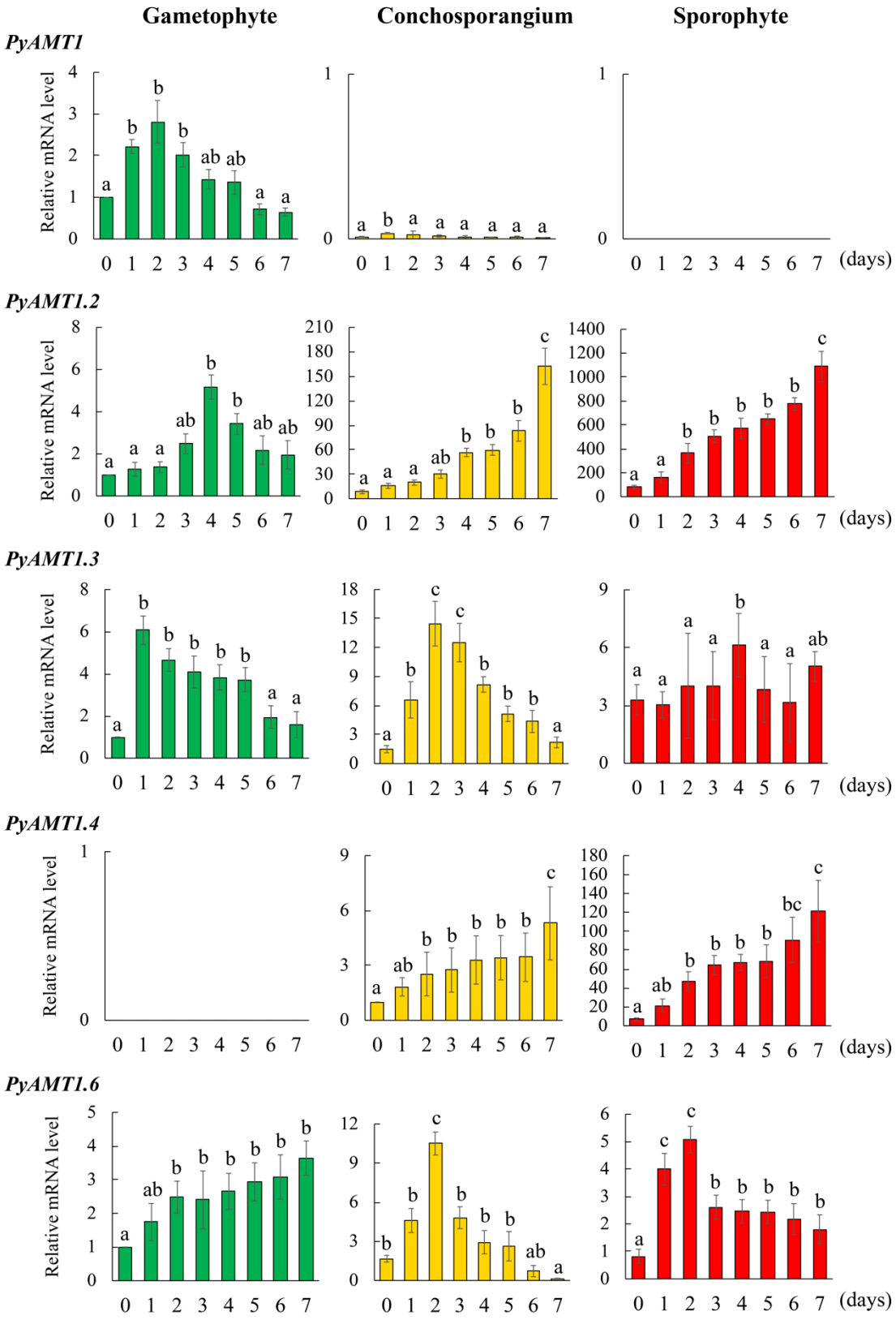
Gametophyte
Conchosporangium
Sporophyte
PyAMT1
PyAMT1.2
PyAMT1.3
PyAMT1.4
PyAMT1.6
Relative mRNA level
(days)

Figure 10

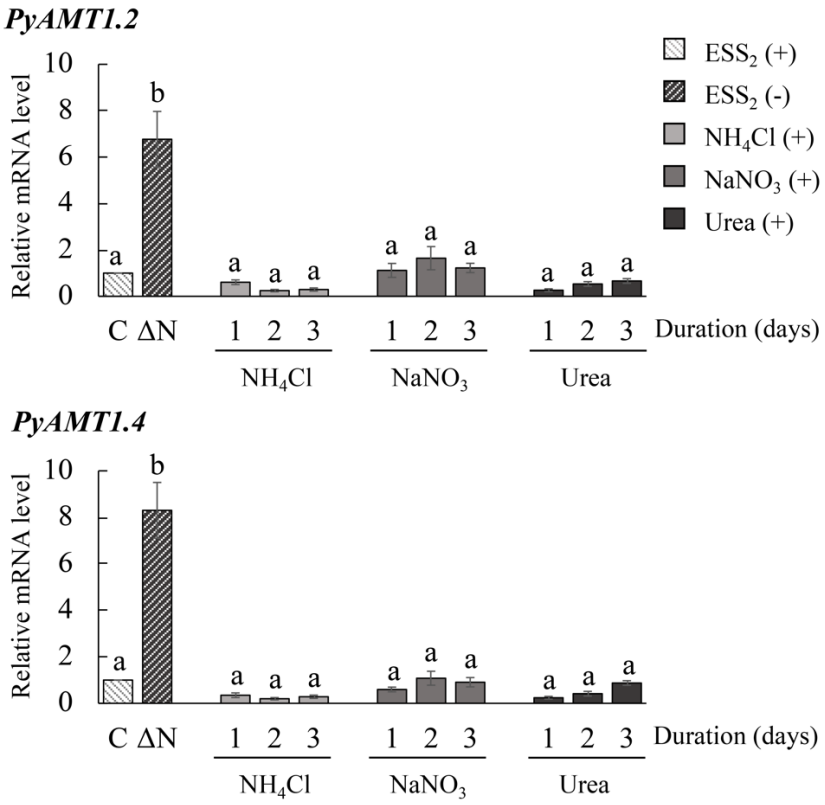
PyAMT1.2
Relative mRNA level
10
8
6
4
2
0
a
b
a a a
a a a
a a a
ESS2 (+)
ESS2 (-)
NH4Cl (+)
NaNO3 (+)
Urea (+)
C ΔN
1 2 3
1 2 3
1 2 3
Duration (days)
NH4Cl
NaNO3
Urea
PyAMT1.4
Relative mRNA level
10
8
6
4
2
0
a
b
a a a
a a a
a a a
C ΔN
1 2 3
1 2 3
1 2 3
Duration (days)
NH4Cl
NaNO3
Urea

Figure 11

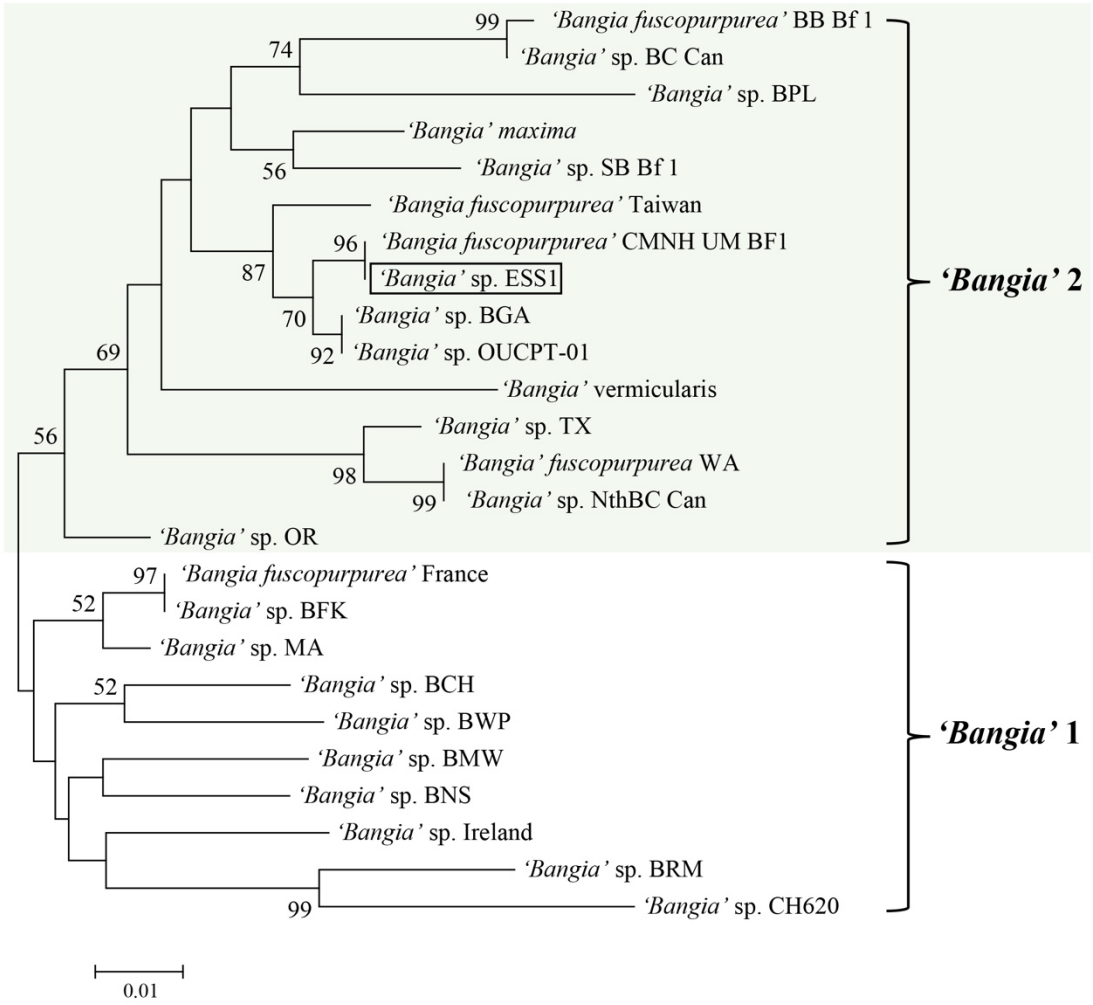
99
'Bangia fuscopurpurea' BB Bf 1
74
'Bangia' sp. BC Can
'Bangia' sp. BPL
'Bangia' maxima
56
'Bangia' sp. SB Bf 1
'Bangia fuscopurpurea' Taiwan
96
'Bangia fuscopurpurea' CMNH UM BF1
87
'Bangia' sp. ESS1
70
'Bangia' sp. BGA
92
'Bangia' sp. OUCPT-01
69
'Bangia' vermicularis
56
'Bangia' sp. TX
98
'Bangia' fuscopurpurea WA
99
'Bangia' sp. NthBC Can
'Bangia' sp. OR
'Bangia' 2
97
'Bangia fuscopurpurea' France
52
'Bangia' sp. BFK
'Bangia' sp. MA
52
'Bangia' sp. BCH
'Bangia' sp. BWP
'Bangia' sp. BMW
'Bangia' sp. BNS
'Bangia' sp. Ireland
'Bangia' sp. BRM
99
'Bangia' sp. CH620
'Bangia' 1
0.01

Figure 12

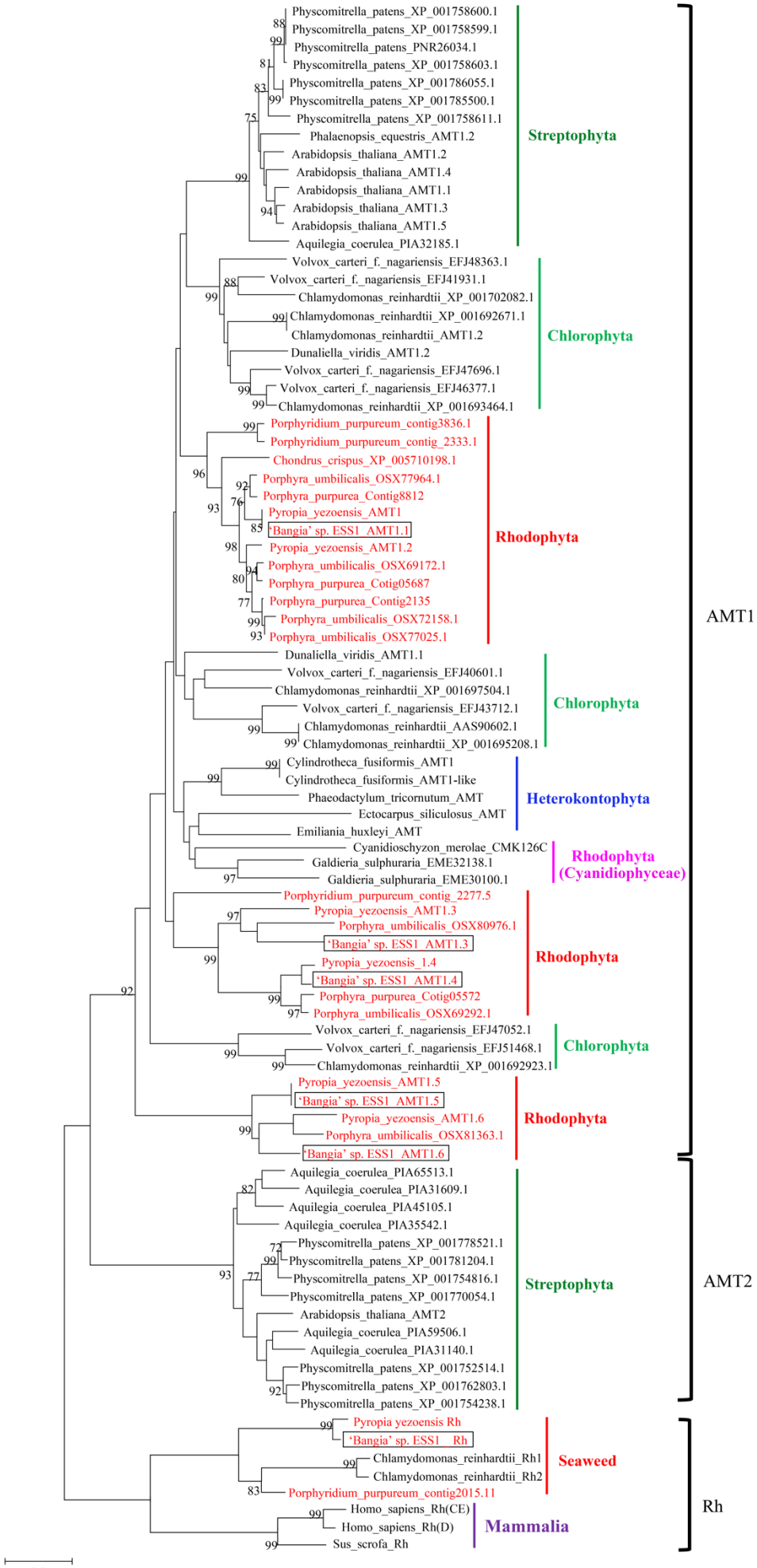
Physcomitrella_patens_XP_001758600.1
Physcomitrella_patens_XP_001758599.1
Physcomitrella_patens_PNR26034.1
Physcomitrella_patens_XP_001758603.1
Physcomitrella_patens_XP_001786055.1
Physcomitrella_patens_XP_001785500.1
Physcomitrella_patens_XP_001758611.1
Phalaenopsis_equestris_AMT1.2
Arabidopsis_thaliana_AMT1.2
Arabidopsis_thaliana_AMT1.4
Arabidopsis_thaliana_AMT1.1
Arabidopsis_thaliana_AMT1.3
Arabidopsis_thaliana_AMT1.5
Aquilegia_coerulea_PIA32185.1
Streptophyta
Volvox_carteri_f._nagariensis_EFJ48363.1
Volvox_carteri_f._nagariensis_EFJ41931.1
Chlamydomonas_reinhardtii_XP_001702082.1
Chlamydomonas_reinhardtii_XP_001692671.1
Chlamydomonas_reinhardtii_AMT1.2
Dunaliella_viridis_AMT1.2
Volvox_carteri_f._nagariensis_EFJ47696.1
Volvox_carteri_f._nagariensis_EFJ46377.1
Chlamydomonas_reinhardtii_XP_001693464.1
Chlorophyta
Porphyridium_purpureum_contig3836.1
Porphyridium_purpureum_contig_2333.1
Chondrus_crispus_XP_005710198.1
Porphyra_umbilicalis_OSX77964.1
Porphyra_purpurea_Contig8812
Pyropia_yezoensis_AMT1
'Bangia' sp. ESS1_AMT1.1
Pyropia_yezoensis_AMT1.2
Porphyra_umbilicalis_OSX69172.1
Porphyra_purpurea_Cotig05687
Porphyra_purpurea_Contig2135
Porphyra_umbilicalis_OSX72158.1
Porphyra_umbilicalis_OSX77025.1
Rhodophyta
Dunaliella_viridis_AMT1.1
Volvox_carteri_f._nagariensis_EFJ40601.1
Chlamydomonas_reinhardtii_XP_001697504.1
Volvox_carteri_f._nagariensis_EFJ43712.1
Chlamydomonas_reinhardtii_AAS90602.1
Chlamydomonas_reinhardtii_XP_001695208.1
Chlorophyta
Cylindrotheca_fusiformis_AMT1
Cylindrotheca_fusiformis_AMT1-like
Phaeodactylum_tricornutum_AMT
Ectocarpus_siliculosus_AMT
Emiliania_huxleyi_AMT
Heterokontophyta
Cyanidioschyzon_merolae_CMK126C
Galdieria_sulphuraria_EME32138.1
Galdieria_sulphuraria_EME30100.1
Rhodophyta
(Cyanidiophyceae)
Porphyridium_purpureum_contig_2277.5
Pyropia_yezoensis_AMT1.3
Porphyra_umbilicalis_OSX80976.1
'Bangia' sp. ESS1_AMT1.3
Pyropia_yezoensis_1.4
'Bangia' sp. ESS1_AMT1.4
Porphyra_purpurea_Cotig05572
Porphyra_umbilicalis_OSX69292.1
Rhodophyta
Volvox_carteri_f._nagariensis_EFJ47052.1
Volvox_carteri_f._nagariensis_EFJ51468.1
Chlamydomonas_reinhardtii_XP_001692923.1
Chlorophyta
Pyropia_yezoensis_AMT1.5
'Bangia' sp. ESS1_AMT1.5
Pyropia_yezoensis_AMT1.6
Porphyra_umbilicalis_OSX81363.1
'Bangia' sp. ESS1_AMT1.6
Rhodophyta
AMT1
Aquilegia_coerulea_PIA65513.1
Aquilegia_coerulea_PIA31609.1
Aquilegia_coerulea_PIA45105.1
Aquilegia_coerulea_PIA35542.1
Physcomitrella_patens_XP_001778521.1
Physcomitrella_patens_XP_001781204.1
Physcomitrella_patens_XP_001754816.1
Physcomitrella_patens_XP_001770054.1
Arabidopsis_thaliana_AMT2
Aquilegia_coerulea_PIA59506.1
Aquilegia_coerulea_PIA31140.1
Physcomitrella_patens_XP_001752514.1
Physcomitrella_patens_XP_001762803.1
Physcomitrella_patens_XP_001754238.1
Streptophyta
AMT2
Pyropia yezoensis Rh
'Bangia' sp. ESS1__Rh
Chlamydomonas_reinhardtii_Rh1
Chlamydomonas_reinhardtii_Rh2
Porphyridium_purpureum_contig2015.11
Seaweed
Homo_sapiens_Rh(CE)
Homo_sapiens_Rh(D)
Sus_scrofa_Rh
Mammalia
Rh
0.2

Figure 13

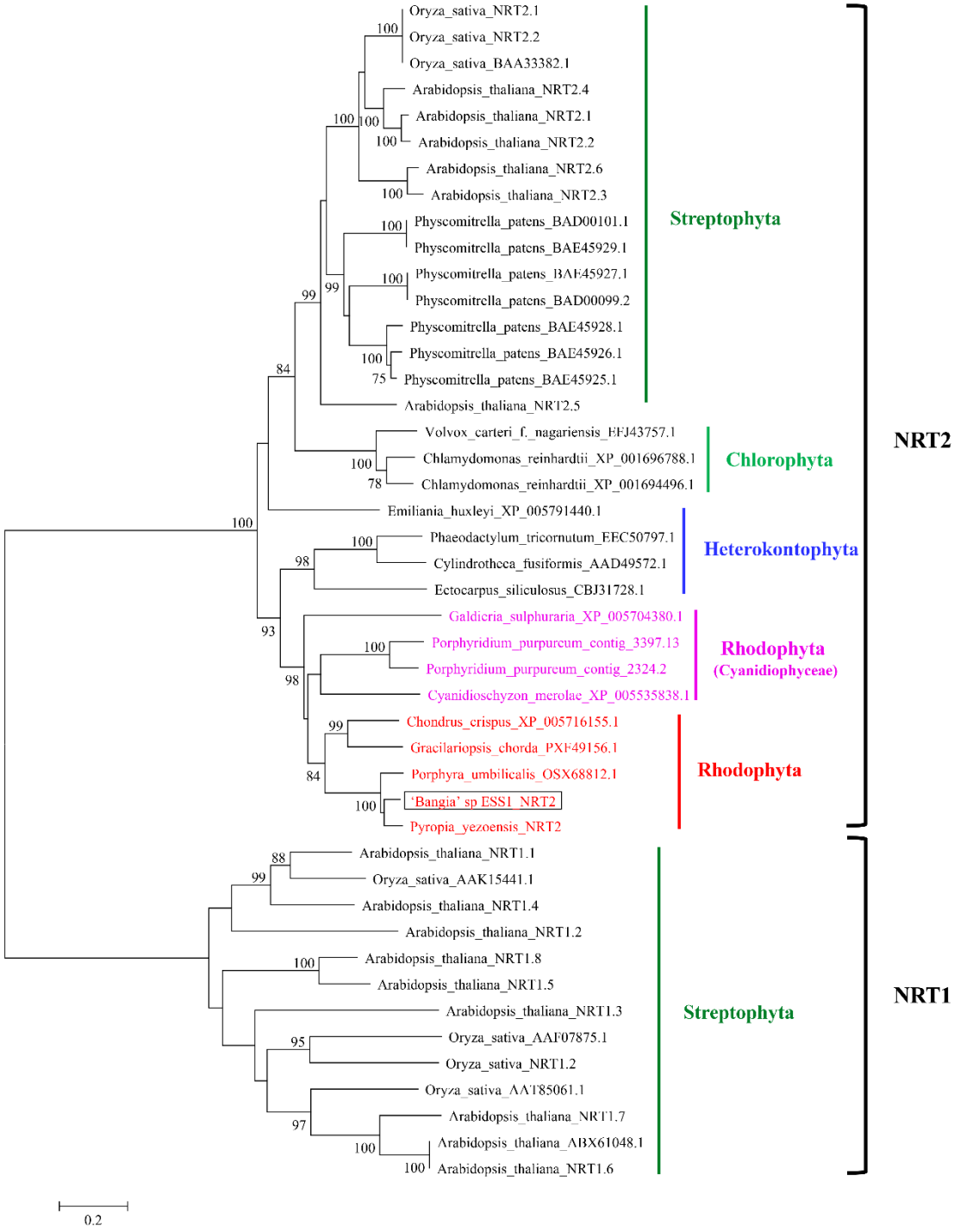
Oryza_sativa_NRT2.1
Oryza_sativa_NRT2.2
Oryza_sativa_BAA33382.1
Arabidopsis_thaliana_NRT2.4
Arabidopsis_thaliana_NRT2.1
Arabidopsis_thaliana_NRT2.2
Arabidopsis_thaliana_NRT2.6
Arabidopsis_thaliana_NRT2.3
Physcomitrella_patens_BAD00101.1
Physcomitrella_patens_BAE45929.1
Physcomitrella_patens_BAE45927.1
Physcomitrella_patens_BAD00099.2
Physcomitrella_patens_BAE45928.1
Physcomitrella_patens_BAE45926.1
Physcomitrella_patens_BAE45925.1
Arabidopsis_thaliana_NRT2.5
Streptophyta
Volvox_carteri_f._nagariensis_EFJ43757.1
Chlamydomonas_reinhardtii_XP_001696788.1
Chlamydomonas_reinhardtii_XP_001694496.1
Chlorophyta
Emiliania_huxleyi_XP_005791440.1
Phaeodactylum_tricornutum_EEC50797.1
Cylindrotheca_fusiformis_AAD49572.1
Ectocarpus_siliculosus_CBJ31728.1
Heterokontophyta
Galdieria_sulphuraria_XP_005704380.1
Porphyridium_purpureum_contig_3397.13
Porphyridium_purpureum_contig_2324.2
Cyanidioschyzon_merolae_XP_005535838.1
Rhodophyta
(Cyanidiophyceae)
Chondrus_crispus_XP_005716155.1
Gracilariopsis_chorda_PXF49156.1
Porphyra_umbilicalis_OSX68812.1
'Bangia' sp ESS1_NRT2
Pyropia_yezoensis_NRT2
Rhodophyta
NRT2
Arabidopsis_thaliana_NRT1.1
Oryza_sativa_AAK15441.1
Arabidopsis_thaliana_NRT1.4
Arabidopsis_thaliana_NRT1.2
Arabidopsis_thaliana_NRT1.8
Arabidopsis_thaliana_NRT1.5
Arabidopsis_thaliana_NRT1.3
Oryza_sativa_AAF07875.1
Oryza_sativa_NRT1.2
Oryza_sativa_AAT85061.1
Arabidopsis_thaliana_NRT1.7
Arabidopsis_thaliana_ABX61048.1
Arabidopsis_thaliana_NRT1.6
Streptophyta
NRT1
0.2

Figure 14

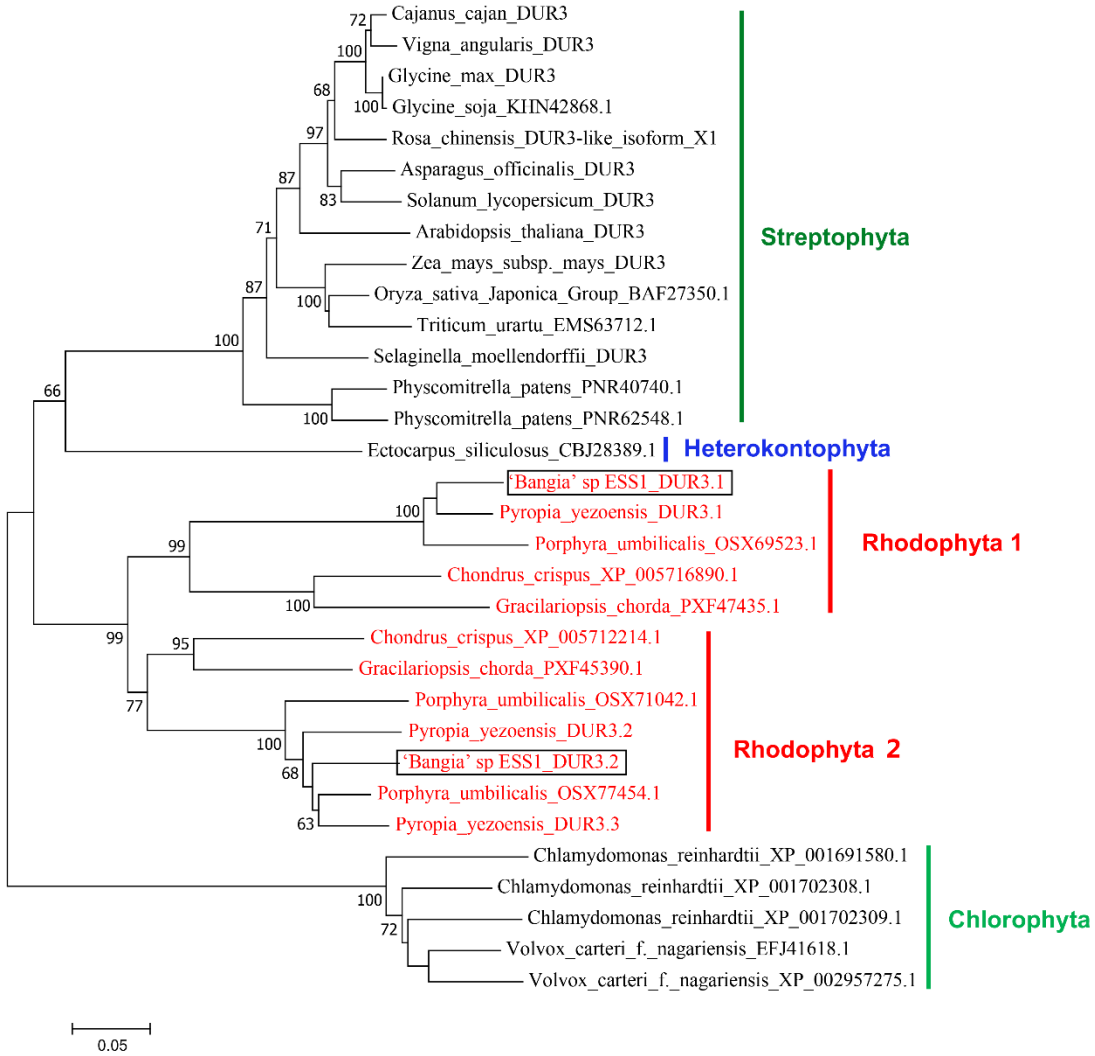
Cajanus_cajan_DUR3
Vigna_angularis_DUR3
Glycine_max_DUR3
Glycine_soja_KHN42868.1
Rosa_chinensis_DUR3-like_isoform_X1
Asparagus_officinalis_DUR3
Solanum_lycopersicum_DUR3
Arabidopsis_thaliana_DUR3
Zea_mays_subsp._mays_DUR3
Oryza_sativa_Japonica_Group_BAF27350.1
Triticum_urartu_EMS63712.1
Selaginella_moellendorffii_DUR3
Physcomitrella_patens_PNR40740.1
Physcomitrella_patens_PNR62548.1
Streptophyta
Ectocarpus_siliculosus_CBJ28389.1
Heterokontophyta
'Bangia' sp ESS1_DUR3.1
Pyropia_yezoensis_DUR3.1
Porphyra_umbilicalis_OSX69523.1
Chondrus_crispus_XP_005716890.1
Gracilariopsis_chorda_PXF47435.1
Rhodophyta 1
Chondrus_crispus_XP_005712214.1
Gracilariopsis_chorda_PXF45390.1
Porphyra_umbilicalis_OSX71042.1
Pyropia_yezoensis_DUR3.2
'Bangia' sp ESS1_DUR3.2
Porphyra_umbilicalis_OSX77454.1
Pyropia_yezoensis_DUR3.3
Rhodophyta 2
Chlamydomonas_reinhardtii_XP_001691580.1
Chlamydomonas_reinhardtii_XP_001702308.1
Chlamydomonas_reinhardtii_XP_001702309.1
Volvox_carteri_f._nagariensis_EFJ41618.1
Volvox_carteri_f._nagariensis_XP_002957275.1
Chlorophyta
0.05

Figure 15


PyAMT1.1
BE1AMT1.1
BE1AMT1.3
BE1AMT1.4
BE1AMT1.5
BE1AMT1.6
BE1Rh
Consensus

Figure 16

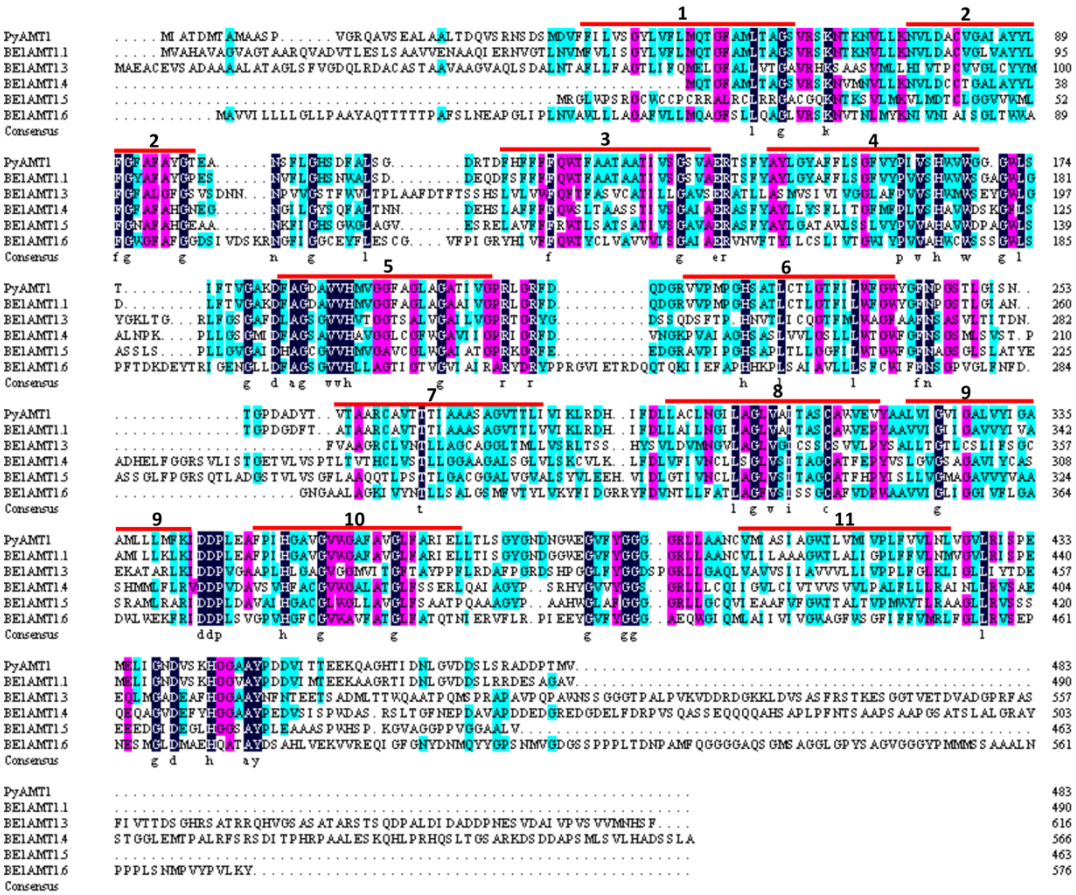

Figure 17

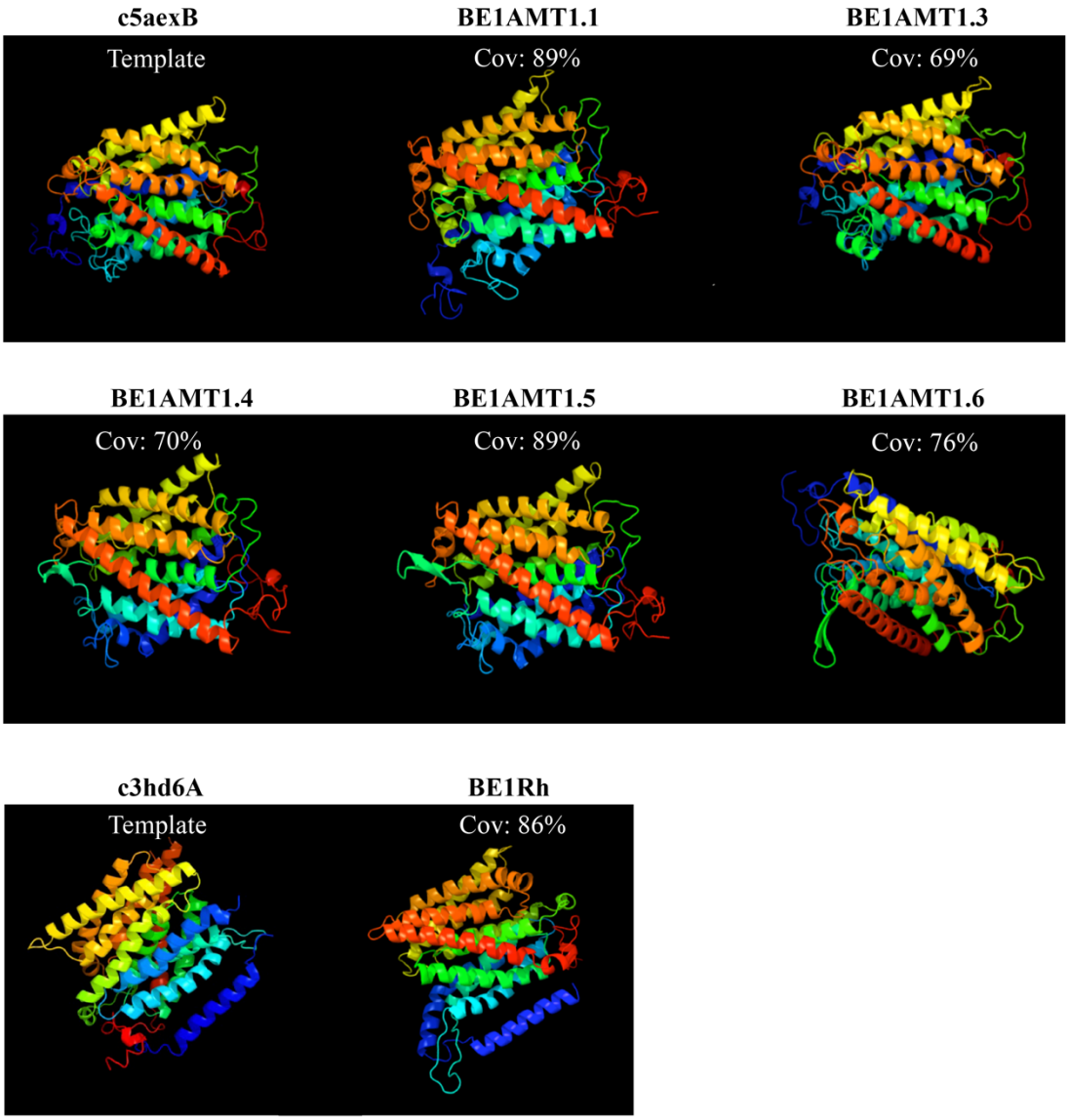
c5aexB
Template
BE1AMT1.1
Cov: 89%
BE1AMT1.3
Cov: 69%
BE1AMT1.4
Cov: 70%
BE1AMT1.5
Cov: 89%
BE1AMT1.6
Cov: 76%
c3hd6A
Template
BE1Rh
Cov: 86%

Figure 18

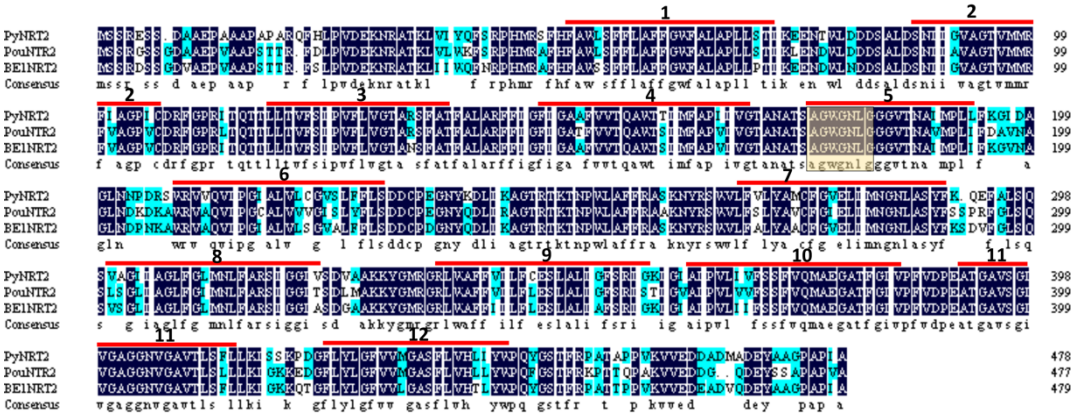

Figure 19

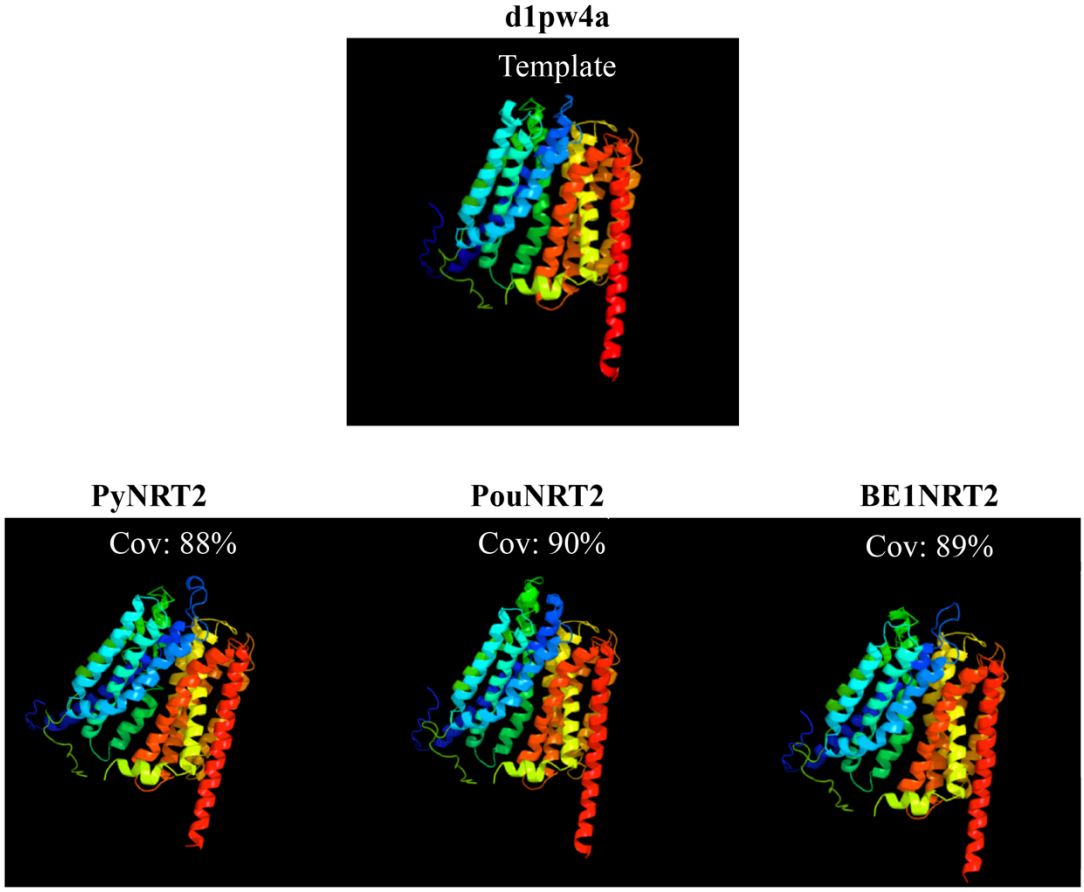

Figure 20

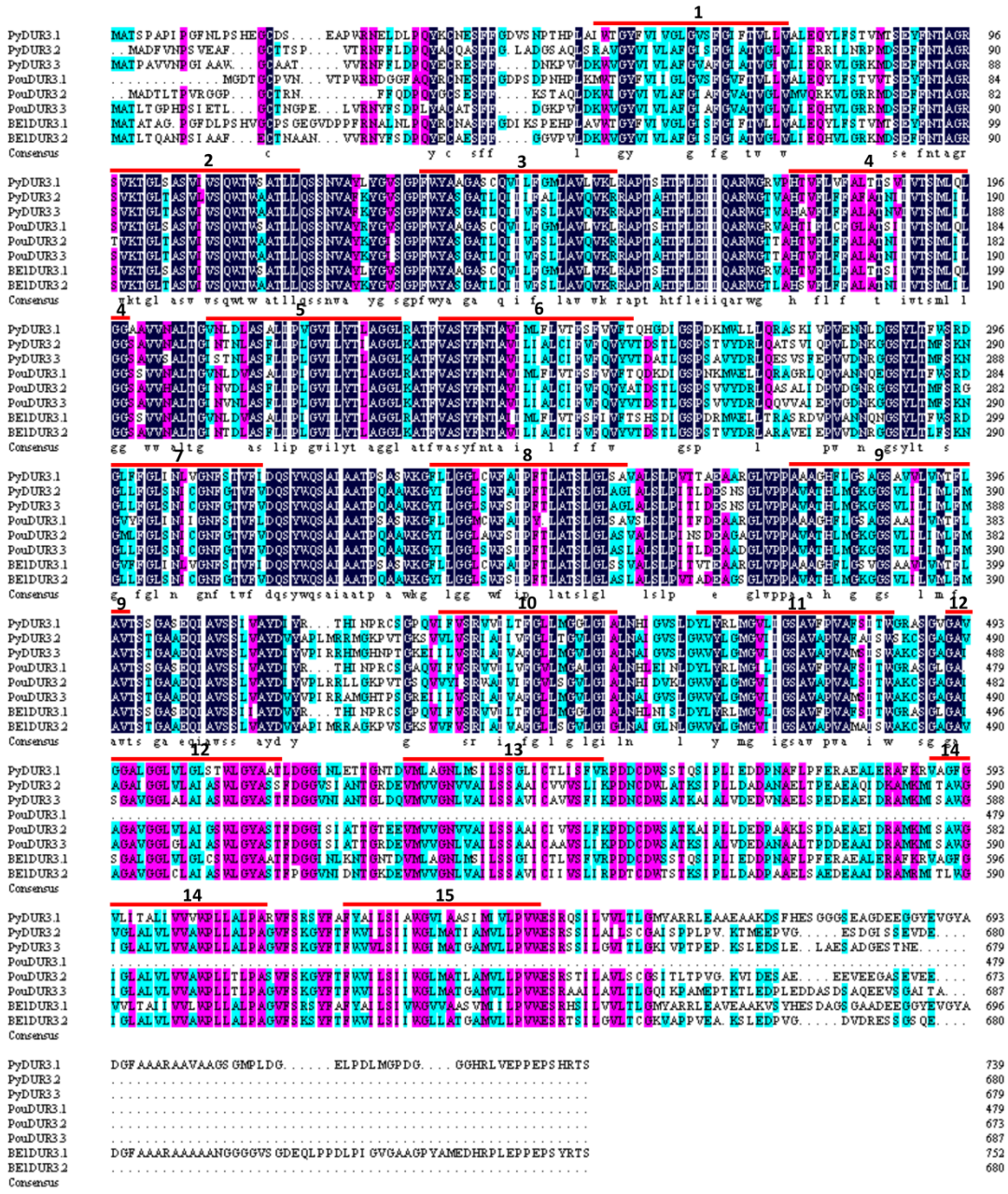

Figure 21

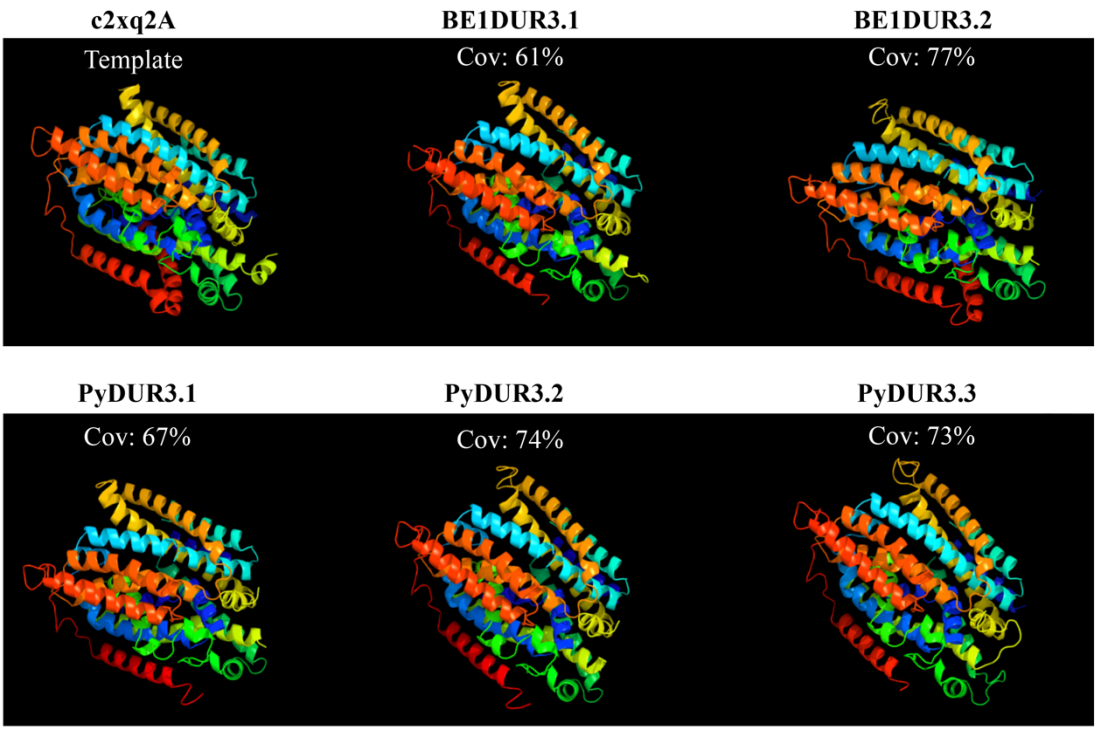
c2xq2A
Template
BE1DUR3.1
Cov: 61%
BE1DUR3.2
Cov: 77%
PyDUR3.1
Cov: 67%
PyDUR3.2
Cov: 74%
PyDUR3.3
Cov: 73%

Figure 22

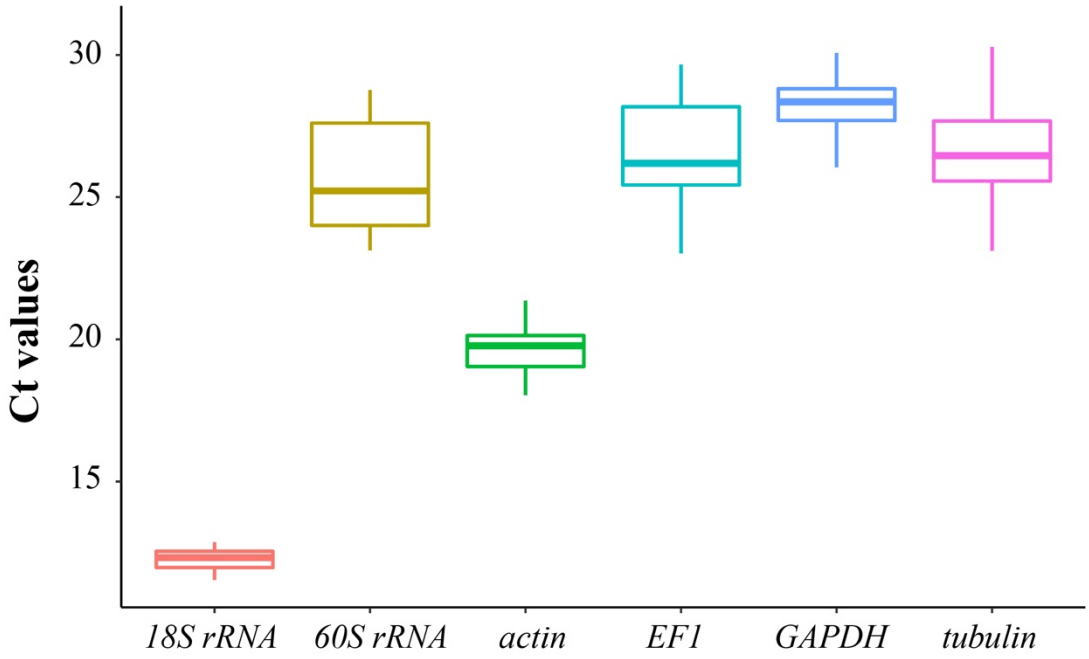
Ct values
30
25
20
15
18S rRNA
60S rRNA
actin
EF1
GAPDH
tubulin

Figure 23

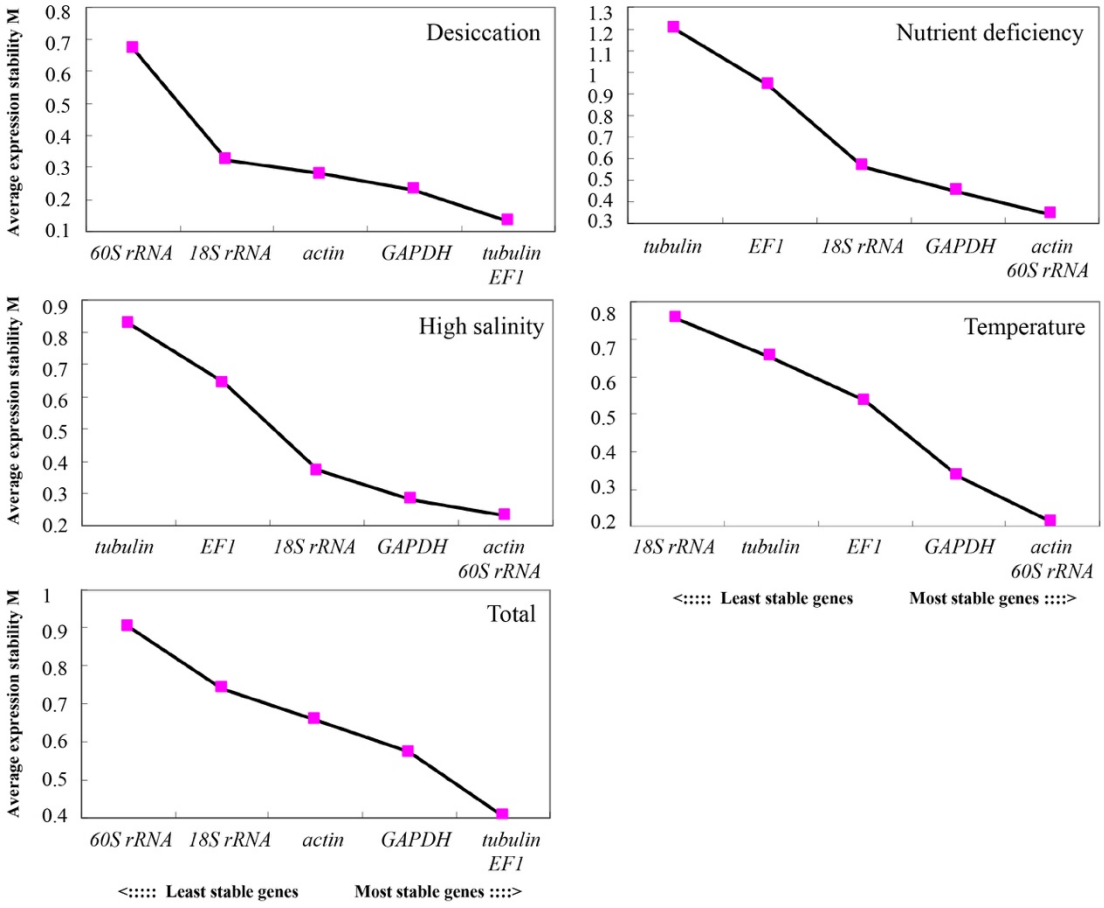
Desiccation
Nutrient deficiency
High salinity
Temperature
Total
Average expression stability M
60S rRNA
18S rRNA
actin
GAPDH
tubulin
EF1
<::::: Least stable genes
Most stable genes ::::>

Figure 24

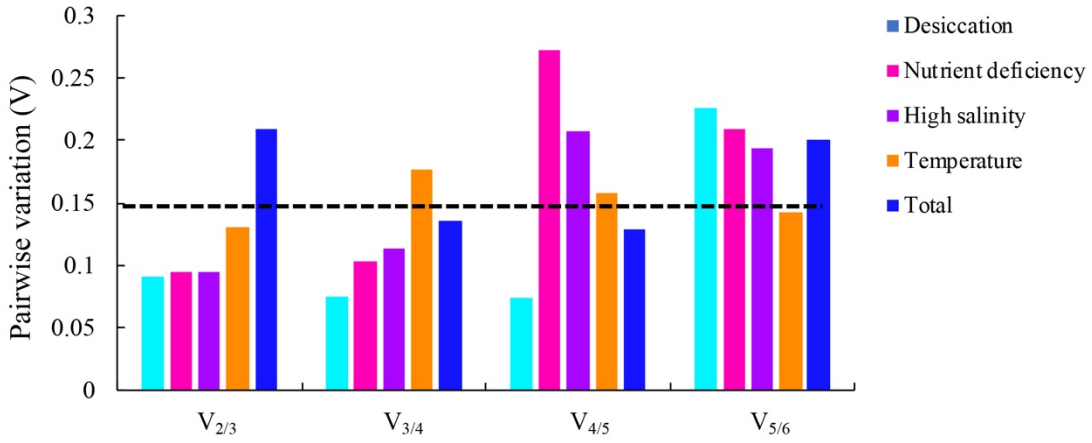
Pairwise variation (V)
0.3
0.25
0.2
0.15
0.1
0.05
0
V2/3
V3/4
V4/5
V5/6
Desiccation
Nutrient deficiency
High salinity
Temperature
Total

Figure 25

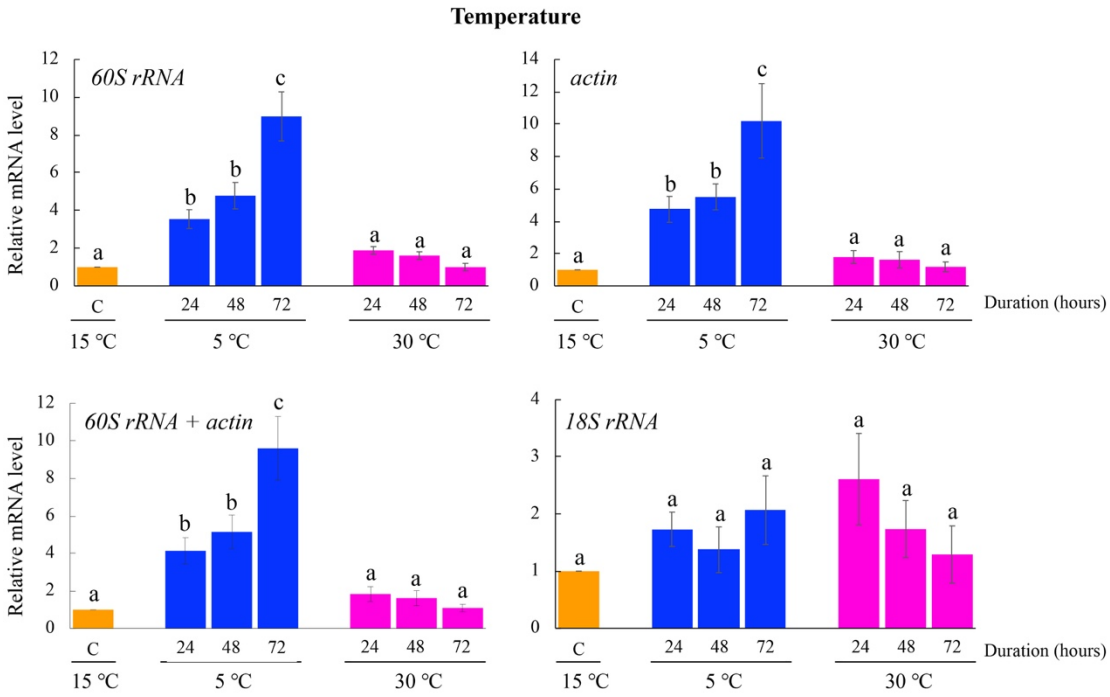
Temperature
60S rRNA
actin
60S rRNA + actin
18S rRNA
Relative mRNA level
Duration (hours)
C
24
48
72
15 ℃
5 ℃
30 ℃

Figure 26

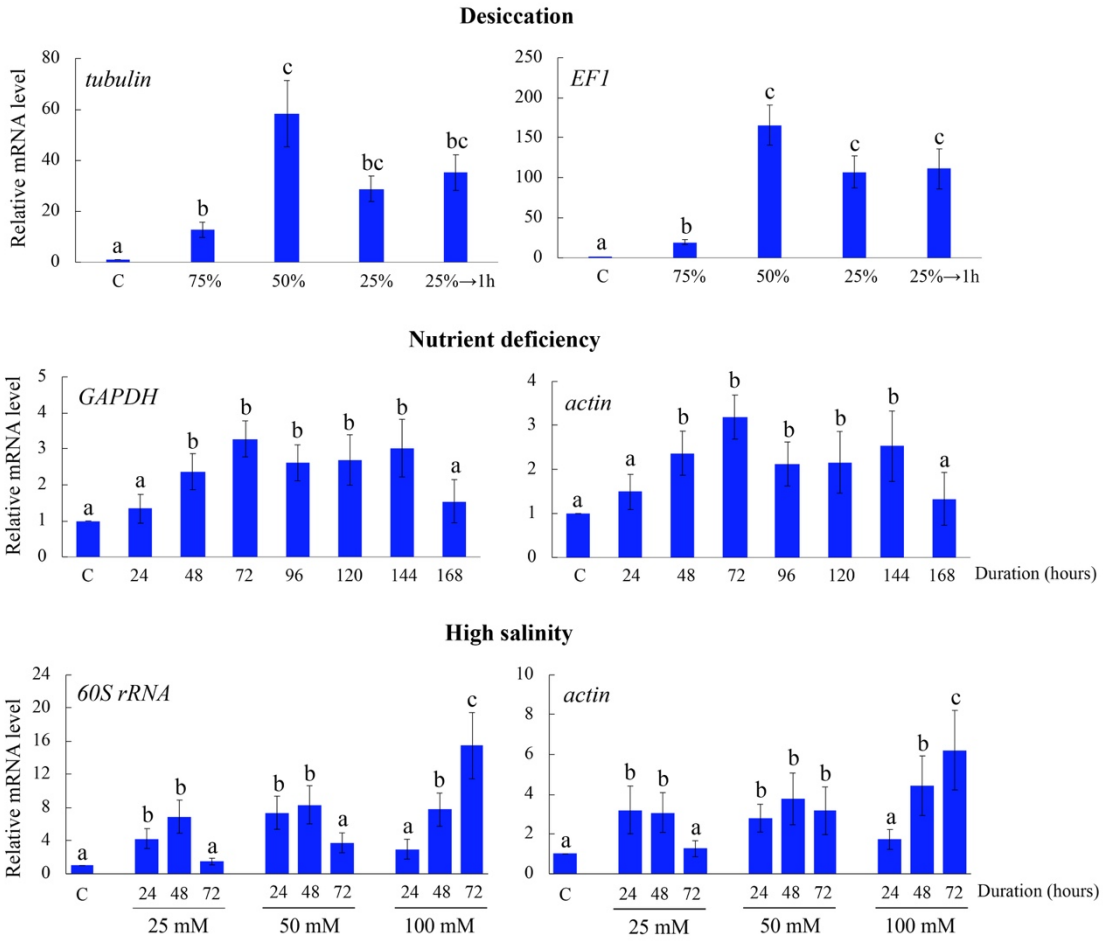
Desiccation
tubulin
EF1
Relative mRNA level
C
75%
50%
25%
25%→1h
Nutrient deficiency
GAPDH
actin
Duration (hours)
High salinity
60S rRNA
actin
25 mM
50 mM
100 mM

Figure 27

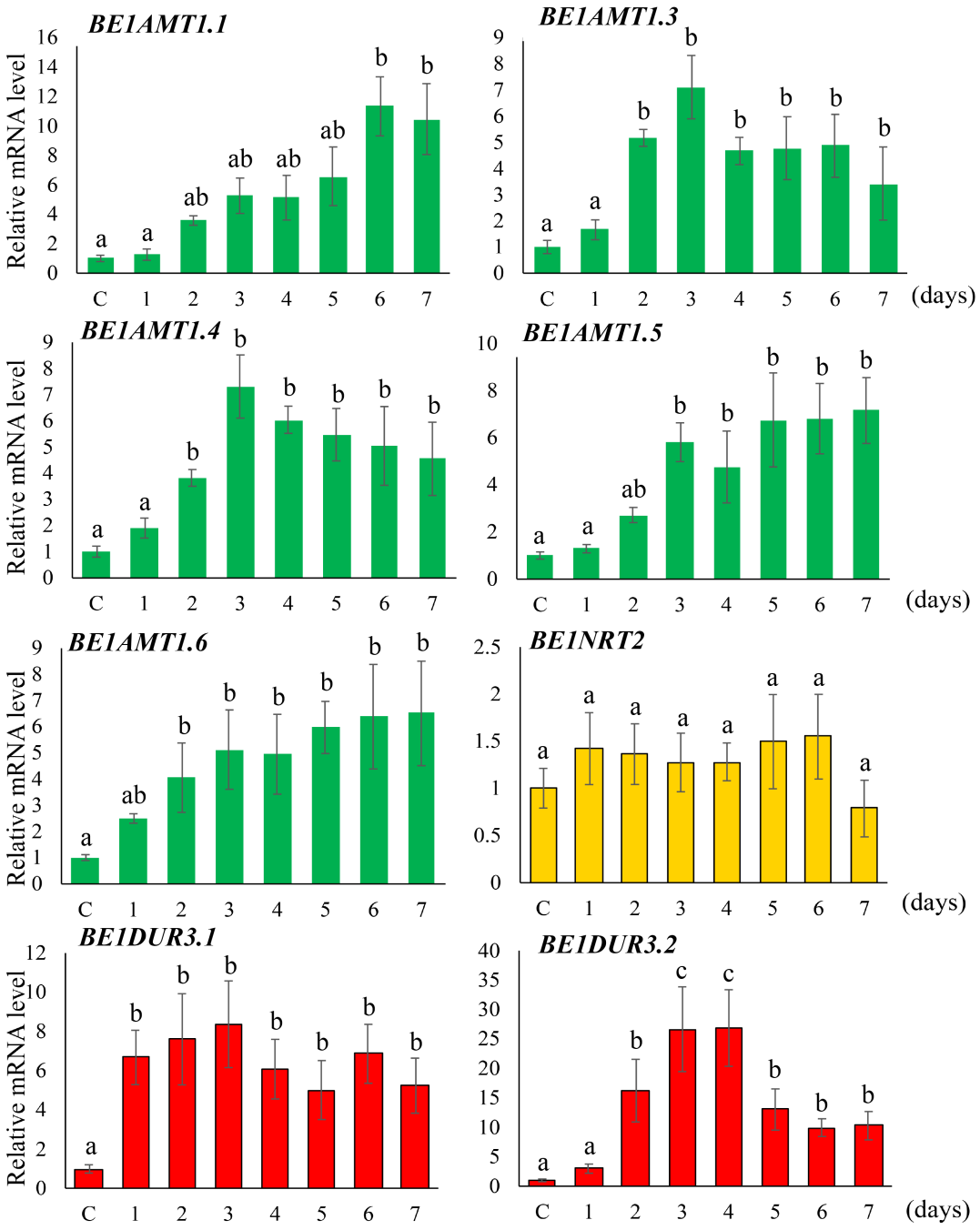
BE1AMT1.1
BE1AMT1.3
BE1AMT1.4
BE1AMT1.5
BE1AMT1.6
BE1NRT2
BE1DUR3.1
BE1DUR3.2
Relative mRNA level
C 1 2 3 4 5 6 7
(days)

Figure 28